POLITECNICO DI TORINO

Automotive Engineering

Master Thesis

Brake Pedal Feeling:
Target Setting Techniques

Advisor:

Prof. Massimiliana Carello

Candidate:

Luigi Vigna

March 2018


POLITECNICO DI TORINO
1906

Summary

1. Introduction

The automotive industry has often been criticized for the environmental impact of their products and because of the apparent lack of disruptive changes in the passenger vehicle since the end of the Second World War. This is a common belief, although the continuous innovation and challenges faced by the carmakers have become year by year more ambitious, showing that, in reality, there is probably no industry with the same research and development efforts as the automotive one. It is also true that the spread of passenger vehicles is continuously increasing and, even if the European and American markets have probably been saturated, the motorization process of emerging countries is supporting and increasing the demand for new vehicles.

Being the passenger vehicle mainly a consumer good, the correct use of the vehicle is demanded to the final customer, whose preparation is assessed during the driving license test, but it is not sufficient to understand which are the technical and physical limits of a vehicle, with possible risks of misuse. This is very different with respect to the railway or aeronautic transportation, where the train operator and the airplane pilot are highly-skilled professionals and their use of the mean of transportation is thoroughly regulated, leaving little freedom to possible misuses. For this reason, the automotive industry has the responsibility to design their vehicles considering also that the final users will improperly use them, adopting the necessary countermeasures to reduce the consequences of their errors. This is particularly true in the safety field, as the accident and mortality rate related to road transportation is much higher with respect to the ones caused by the other means of transport.

To reduce the impact of road accidents, the European Union is working on the road infrastructure and on the automotive transportation regulations, with the target of periodically halve the number of road fatalities, leading the development of safer vehicles in the automotive field.

From an environmental point of view the situation is similar, with the high concentration of vehicles in the most urbanized areas that contributes to the air pollution and to the generation of greenhouse gases that contribute to the global warming. The recent scandals related to the presence of defeat devices that disabled the exhaust gases aftertreatment in some vehicles, is making more stringent the assessment of the environmental impact of each vehicle, ensuring that the achievements obtained by the pollution reduction technology are consistent between the homologation tests and the real use of the vehicle. As the pollutant reduction is reaching its limit, the most challenging targets will be the ones related to the CO_2 emissions, which are directly related to the fuel consumption: the limit of 95 g/km from 2021 as a fleet average of all the vehicles sold in the European Union is demonstrating to be a very demanding target, requiring a complete rethinking of the vehicle and orient the design of each component having in mind its contribution to the total environmental impact of the vehicle.

For both the safety and environmental issues, the braking system is a core element of the vehicle, which is undergoing a strong evolution to face the new requirements, together with the development of the rest of the vehicle and infrastructure.

From a safety point of view, the targets of reduction of road fatalities are impossible to achieve if the contribution of the human error is not reduced, therefore the braking system is becoming an active component able to assist the driver and autonomously intervene when the stability of the vehicle is compromised or when the driver is not reacting to a sudden obstacle, avoiding possible collisions or limiting the consequences of an accident by reducing the relative speed at the moment of the impact.

On the other side, the environmental constraints require an increase of the powertrain efficiency and a reduction of the resistance to motion of the whole vehicle: the design of the braking system must take into account of the reduction of the drag torque that a conventional braking system typically generates. Also, the innovations in the powertrains, with the use of hybrid or purely electric prime movers, had opened the possibilities to recover part of the kinetic energy during the braking, bringing a significant contribution to the emissions reduction, but also requiring a higher engineering effort to integrate the regenerative braking with the conventional braking system, without making noticeable to the driver which one of them is contributing to the vehicle deceleration. Another impact of the new powertrains is that the intermittent or no use of an internal combustion engine is reducing the availability of a convenient source of vacuum pressure, which has been used for decades to feed the brake booster, reducing the effort required by the driver for the application of the brake pedal.

All these changes require a complete redesign of some components of the braking system, opening the possibilities to new ways of interaction between the driver and the vehicle brakes: it is now already possible to decelerate a vehicle without the driver's intervention, therefore it is possible that the future trend will lead, with the necessary safety back-up solutions, to decupling the brake pedal from the rest of the braking system, bringing the brake-by-wire in a similar manner to what happened with the accelerator pedal and is starting to happen with the steering system, with the drive-by-wire and steer-by-wire solutions.

For these reasons, the brake pedal feeling is being investigated, as it will probably be no longer influenced by the components of the braking system, but by an artificial feedback system that will have to, in any case, provide a feeling to the driver that gives him confidence about the braking ability of the vehicle.

The objective of this thesis is, therefore, to analyze which components influence the brake pedal feeling of today's vehicles and to identify which are the objective parameters related to the pedal feeling that are measurable during the experimental testing of a vehicle. Using the results obtained from a group of tested vehicles, an investigation on the subjective evaluation of the

brake pedal feeling will be performed, searching for possible correlations between the objective parameters analyzed and the subjective evaluations, trying to understand possible trends and benchmarks in the set-up of the brake pedal feeling of future vehicles. In the end, it will be proposed a method for identifying, from experimental tests, the main design parameters of a braking system that influence the brake pedal feeling of a vehicle.

The thesis has been developed during a six-month experience in Fiat Chrysler Automobiles, at the Balocco Proving Ground, the test facility used by the carmaker to assess and develop the comfort, vehicle dynamics and reliability of their vehicles. The information and experimental data provided during this experience, in particular by Andrea Franco, Lorenzo Ceccarini, Pier Salvo Fiducia and Antonello Donzelli, have given a fundamental contribution to this work.

2. The Braking System

The braking system is a set of devices installed in a vehicle which allow the operator to [1]:

- Stop the vehicle in the shortest possible distance;
- Modulate its speed in any driving condition;
- Maintain the vehicle stationary on a slope, even if the driver is not present.

This is typically achieved by exploiting the mechanical friction between rotating and static elements within the wheels, that transform the kinetic energy of the vehicle into heat, which is absorbed and dissipated by the braking elements during their operation.

To accomplish the above-mentioned tasks, the braking system must be able:

- to generate braking moments large enough to fully exploit the adherence at the tire – ground contact of all the wheels;
- to maintain moderate braking moments for a long time, such as to keep constant the vehicle speed when it is running on a downhill;
- to provide a reliable mechanism to ensure that the vehicle will not move when it is parked.

As the functions of the braking system are strictly related to the vehicle safety, government institutions, such as the European Union, require a minimum level of performance and reliability to be ensured by the vehicle manufacturer before granting the type approval necessary to commercialize a new vehicle. In the United States the requirements are similar, as it is in progress a harmonization of the homologation rules.

For today's standards, the performance requirements mandated by the homologation rules are not particularly stringent, and almost every carmaker has much higher self-imposed performance targets to achieve; also, most automotive magazines include braking assessments that are more demanding than the homologation rules. For most today's passenger vehicles, it is possible to state that the braking performance is more limited by the tires friction coefficient than by the brakes themselves.

On the other side, the safety requirements mandated by the legislations impose a particular design of the braking system, so that three independent systems must be present:

- Service brake system
- Secondary brake system;
- Parking brake.

The service brake system is the one normally used to moderate the vehicle speed and to safely stop the vehicle motion in any condition: it must be possible to operate it without leaving the hands from the steering wheel; therefore, a brake pedal is the common solution.

The secondary brake system must accomplish the same tasks of the service brakes, although it is possible a reduced performance, in case of failure of the service brakes.

The parking brake must be able to hold stationary a vehicle, not only when it is left unattended, but also when it is parked on a slope. The braking force of the parking brake must be provided by a mechanical system, without the use of hydraulic systems.

These requirements also expect minimum performance levels to be achieved in case of failure of critical components of the braking system, such as the brake booster or a connection hose for one of the wheels. For this reason, every vehicle uses a split hydraulic system, in order to not to completely loose the braking force in case of a fluid loss in one point of the system.

For what concerns the pedal feeling, there is not a specific requirement from a homologation point of view, although it is required a monotonic function between the force applied to the brake pedal and the deceleration of the vehicle: as the pedal force increases, the vehicle deceleration must increase. There are also limits on the minimum and maximum force to be applied on the brake pedal to pass the braking tests: the deceleration levels prescribed in each homologation maneuver must be obtained with a pedal effort between 6,5 and 50 daN.

In the following paragraphs, a description of each component of the braking system will allow to understand its function and its possible influence on the pedal feeling.

2.1 Brake Pedal

The brake pedal is the interface between the driver and the rest of the braking system. Its function is to provide an ergonomic surface that allows the driver to securely and firmly apply his force and to transfer it, amplified, to the input rod of the brake booster. In most vehicles it is hinged in its upper part (1) to a structure shared with the other pedals, while the contact surface (3) with the driver's foot is at the bottom. Between the two extremities, there is a second hinge (2) that performs the connection between the beam of the pedal (4) and the input rod (5) of the brake booster.

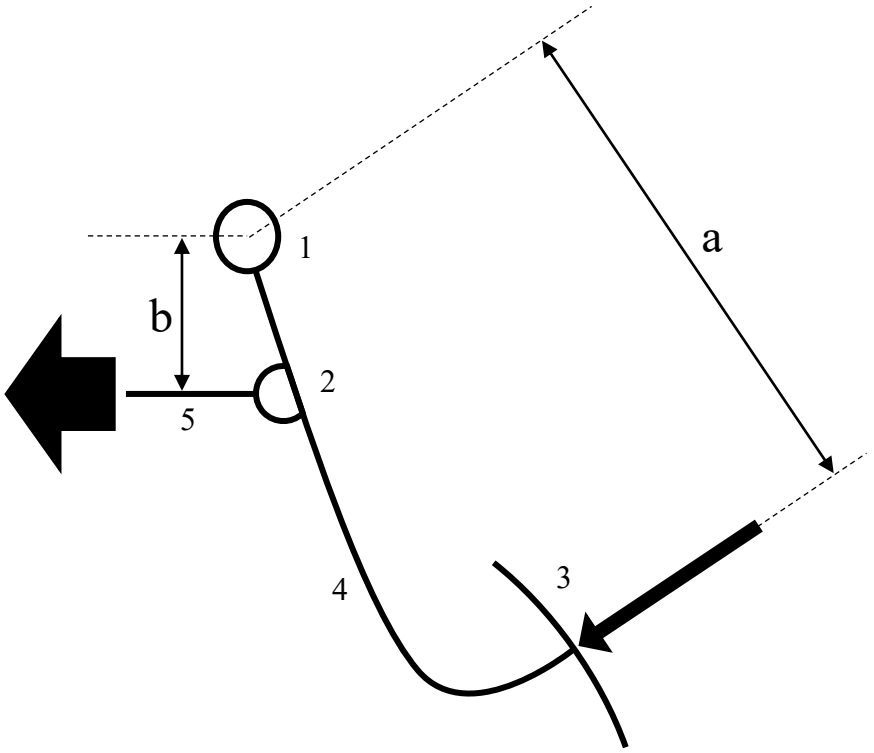

Figure 1. Brake pedal and its lever arms.

This configuration, with the resistive load placed in between of the fulcrum and the point of application of the driver's force, is usually defined as a Class 2 lever and allows the transmission of an output force which is amplified with respect to the force applied by the driver. The amount of this amplification is the pedal ratio and it depends on the geometric arrangement of the hinge, the booster rod connection point and the application point of the driver's force.

Being a the distance between the application force axis and the hinge, and b the distance between the booster rod axis and the hinge, the pedal ratio R_{bp} is easily obtained:

$$R_{bp} = \frac{a}{b} \tag{2.1}$$

Typical values for passenger cars are between 3:1 and 5:1.

The consequence of the force amplification is that the stroke of the brake pedal is increased by the same amount: for this reason, the pedal ratio cannot be too high. On the other side, a very low pedal ratio might require an excessively high force on the pedal in case of failure of the brake booster.

During the rotation of the pedal when it is depressed, the angle between the booster input rod and the beam of the pedal changes; therefore, even assuming that the applied force by the driver remains normal to the pedal surface, the pedal ratio slightly changes as the stroke increases. The amount of this variation depends on the angles among the various components, but can be neglected as a first approximation.

While the pedal ratio defined in the design process typically considers the application force point as the center of the pedal surface, the actual contact point varies among different drivers, because it depends on the shoe size, the length of the upper and lower part of the leg and on the vertical and longitudinal coordinates of the seating position.

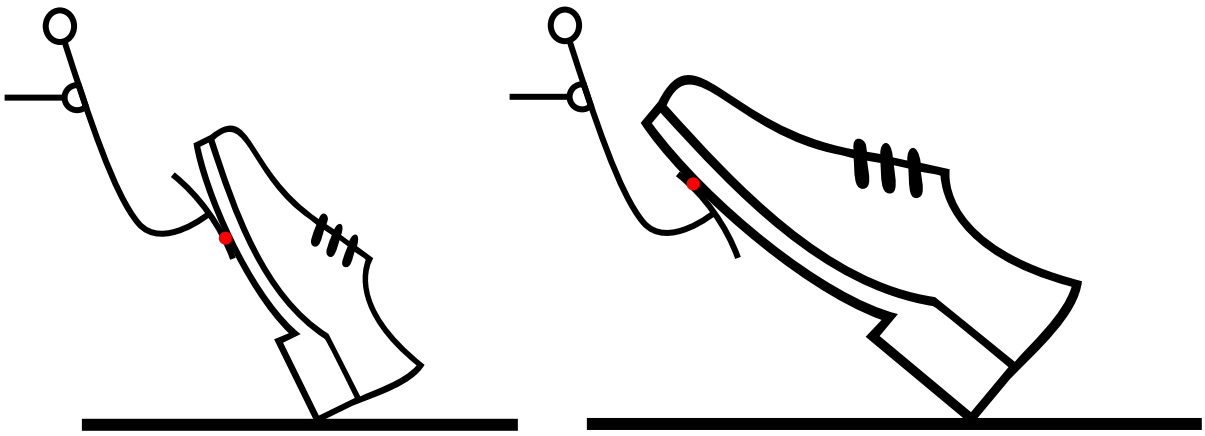

Figure 2. Example of variation of the point of application of the pedal force as a function of the shoe size and seating position.

In the picture, two possible extreme configurations are considered: on the left there is the shoe of a tall driver with small feet, on the right the shoe of a short driver with big feet. Assuming that the tall driver will adjust the seat in a lower and backward position with respect to the one of the short driver, the angles of the legs will also be different. The tall driver will have the legs

well extended and the feet almost vertical in rest conditions, while the short driver will have a more seated position, with the feet more horizontal.

Being the pedal the same for both drivers, the contact point between foot and pedal will be different, affecting the actual length of the lever and the actual pedal ratio. Since the variation of the contact point is unavoidable, it is important to evaluate most of the combinations of shoe sizes and heel positions, to ensure that the associated pedal ratios do not require a pedal effort or a perceived stroke outside the ranges of acceptability.

2.2 Brake Booster

The brake booster is a power device that connects the brake pedal to the tandem master cylinder while it provides an additional force that helps the driver by reducing the effort required to obtain the desired braking force.

In its most common configuration it is a pneumatic device that exploit the pressure difference between its two chambers to produce an output force higher than the input force, modulating its contribution to maintain the proportionality between the input command given by the driver and the force transmitted to the tandem master cylinder.

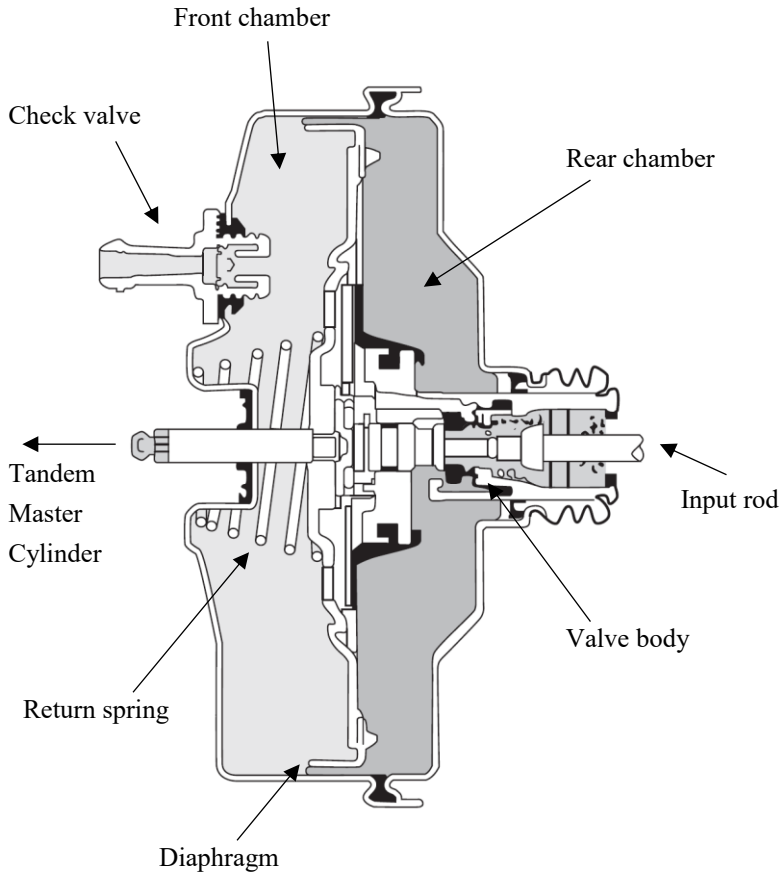

Figure 3. Vacuum Brake Booster internal components.

The two chambers are separated by a flexible diaphragm supported by a stiff plate that holds also the tandem master cylinder rod and transfers to it the force generated by the pressure difference among the two chambers.

The front chamber is connected to a vacuum source through a check valve that allows the suction of the air from the chamber without letting the air to enter in again. The type of vacuum source depends on the powertrain: spark-ignition engines generally modulate the engine power using a throttle valve that restricts the amount of air available for combustion. When the engine is working at low load, the pressure in the intake manifold drops below the atmospheric level, allowing the extraction of air from the front chamber of the brake booster. In compression-ignition engines it is not necessary to limit the amount of air admitted to the engine; therefore, a mechanical pump driven by the engine camshaft is used to generate the vacuum pressure. Electric vehicles and hybrid vehicles that can move in pure electric mode use an electric pump to provide the vacuum to the brake booster.

The rear chamber pressure depends on the input force received by the brake pedal. At rest, it is under vacuum at the same pressure of the front chamber; when the brake pedal is lightly depressed, the rear chamber has a pressure that is intermediate between the front chamber pressure and the atmospheric one; when the pedal is fully depressed, the rear chamber is at atmospheric pressure. The increased pressure at the rear chamber with respect to the front one generates a thrust on the diaphragm plate that is transferred to the tandem master cylinder rod, increasing the force received by the brake pedal.

The pressure regulation and the closed-loop feedback that regulates the pressure, as a function of the pedal force, is made possible by a valve assembly located between the input rod and the diaphragm plate, composed by a Communication valve and an Admission valve. The Communication valve creates a connection between the front and the rear chambers, equalizing their pressures, while the Admission valve connects the rear chamber to the external environment at ambient pressure.

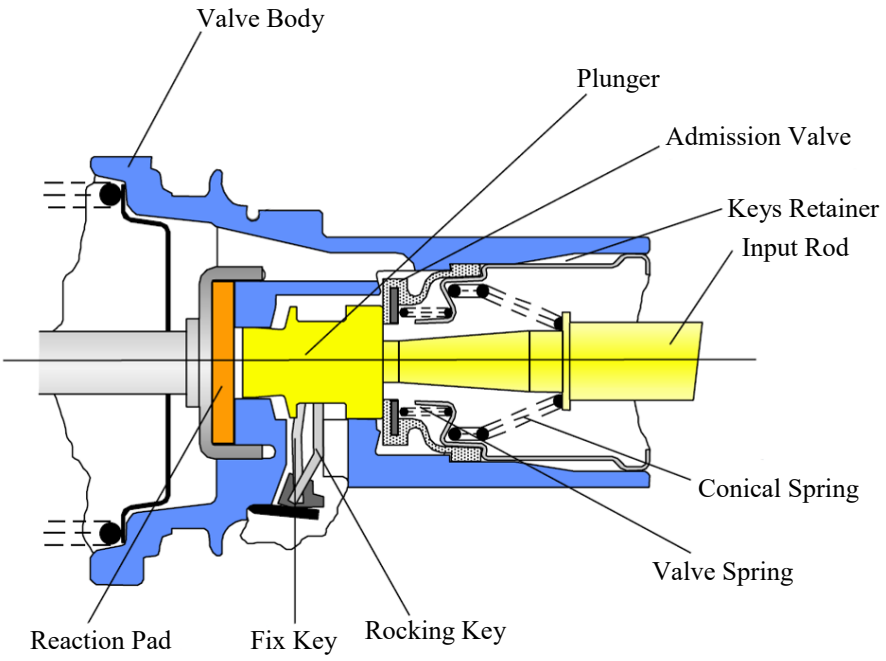

Figure 4. Section view of the internal components of the valve body in the brake booster.

When the brake pedal is gradually depressed from the rest condition up to the maximum force, the valves in the brake booster assume different configurations, described in the following phases.

2.2.1 Phase 1 – Rest condition

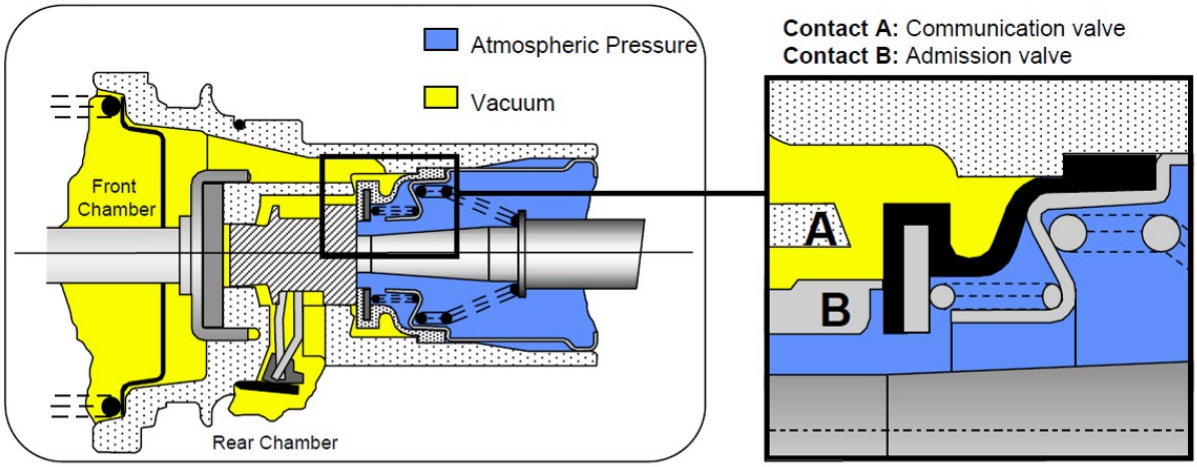

Figure 5. Brake booster valves configuration in rest conditions.

At rest conditions, the brake pedal is not exerting any force on the brake booster and the front and rear chamber are at the same vacuum pressure thanks to the opening of the Communication valve. The Admission valve is closed, sealing the rear chamber from the external environment.

2.2.2 Phase 2 – Crack point

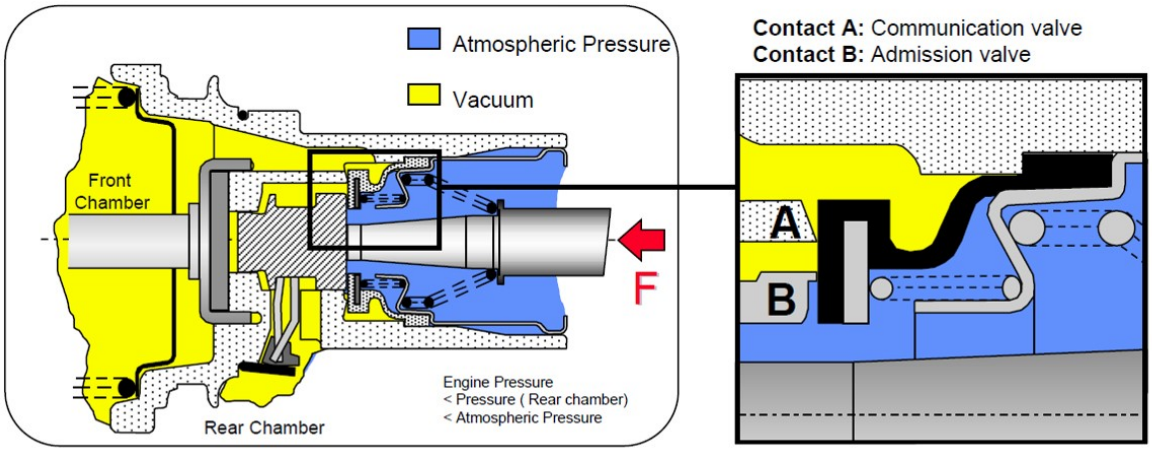

Figure 6. Brake booster valves configuration at the crack point.

When the pedal force reaches a certain value, determined by the preload of the valve springs, the plunger is moved forward with respect to the valve body, closing the Communication valve. Note that the output force is still zero, because there is no contact between the plunger and the reaction disc and the pressure between the two chambers is still the same.

2.2.3 Phase 3 – Jump-in

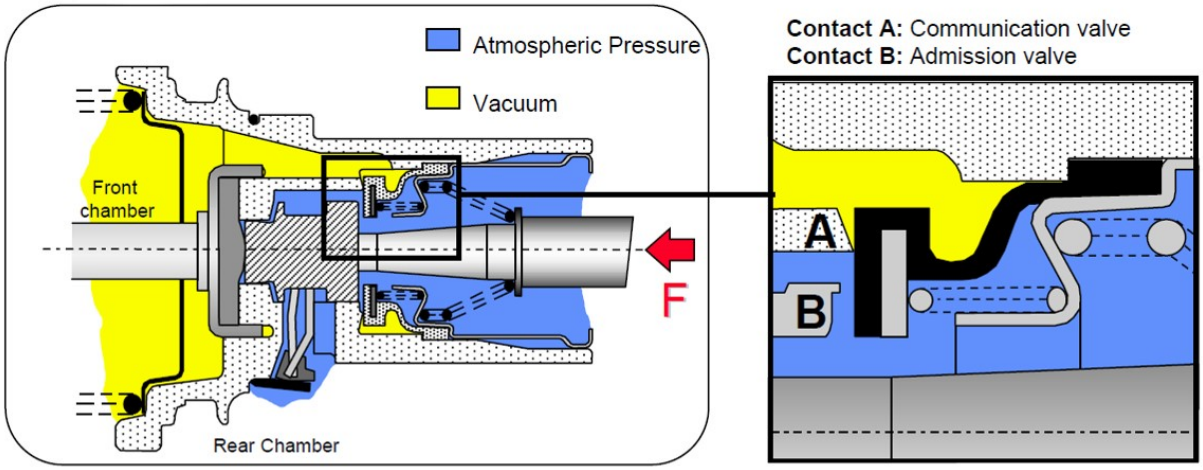

Figure 7. Brake booster valves configuration during the Jump-in phase.

From the crack point condition, a very small increment in the pedal force causes the admission valve to open, suddenly increasing the rear chamber pressure: the force generated by the pressure difference causes the piston assembly to move forward and to squeeze the reaction pad until it touches the plunger. At this point, the relative motion between the plunger and the sleeve causes the closing of the Admission valve. Even if the input force has not increased significantly in this phase, the output force makes a step, passing from zero to a value defined as Jump-in Force. The amount of the final Jump-in force value depends on the gap between the plunger and the reaction pad: the higher the gap, the higher the Jump-in force. It is also possible to make

the output force increase less steep by giving a convex shape to the central part of the reaction pad, obtaining a more gradual transition between this phase and the following one.

2.2.4 Phase 4 – Braking (Boost)

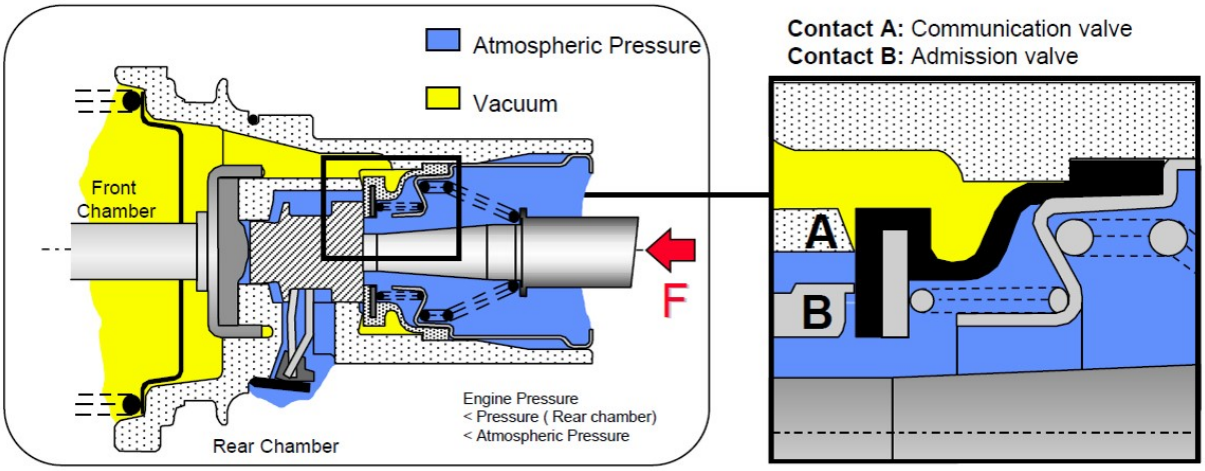

Figure 8. Brake booster valves configuration at equilibrium during braking.

After the Jump-in phase, the brake booster works in a closed-loop way, with the input force, thanks to the continuous contact with the reaction pad, whose mechanical characteristics makes it similar to a hydraulic fluid. An increment of the pedal force causes the plunger to compress the central part of the reaction pad which, for the volume conservation law, causes a slight backwards motion of the sleeve, opening again the Admission valve until the pressure increase moves the sleeve and the piston assembly forward enough to compress the outer ring of the reaction pad and close the Admission valve.

The quasi-fluid behavior of the reaction pad allows a uniform pressure distribution between the contact surface of the plunger and the contact surface of the sleeve. For this reason, the ratio between the output force increment and the input force increment in this phase, named as Boost Ratio, is determined by the contact surface areas of the plunger and of the sleeve:

$$F_{out} = F_{in}\frac{S}{s} \tag{2.2}$$

where: S is the contact surface between the sleeve and the reaction pad, s is the contact surface between the plunger and the reaction pad, F_{in} is the input force and F_{out} is the output force.

2.2.5 Phase 5 – Saturation

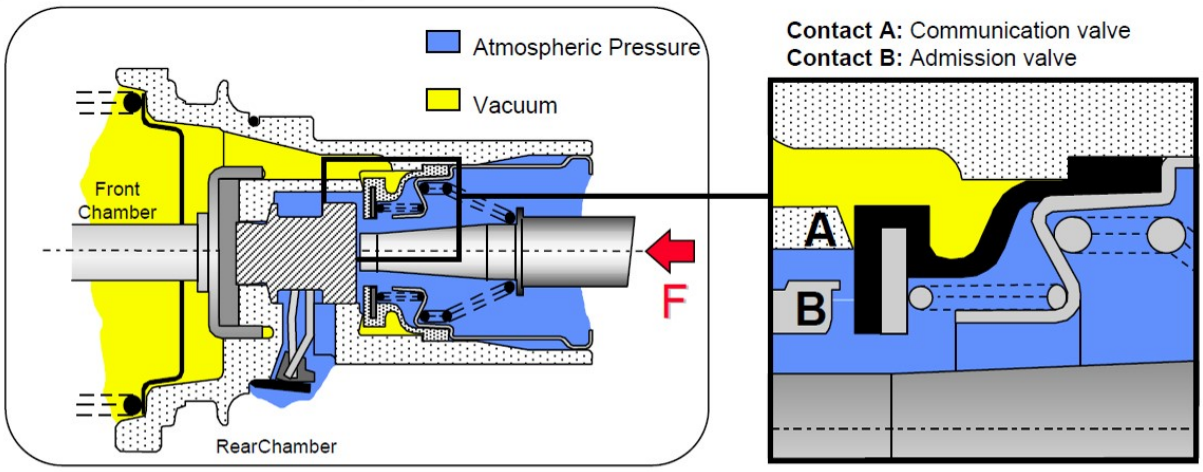

Figure 9. Brake booster valves configuration in the saturation phase.

At a certain point the increment of the input force has caused the rear chamber to achieve the ambient pressure: the brake booster has reached its maximum force and any further increment of the input force is directly transmitted at the output, without amplification.

2.2.6 Phase 6 – Brake release

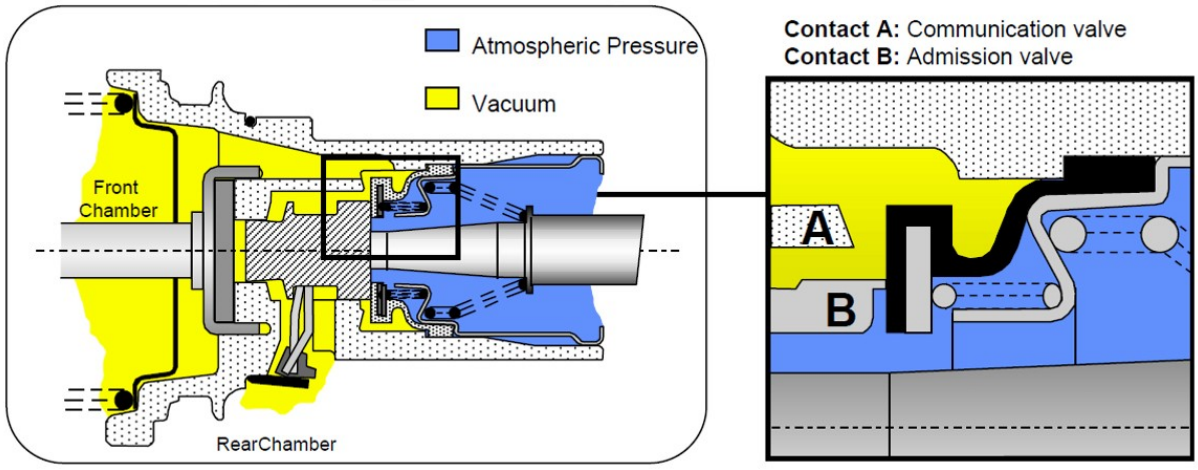

Figure 10. Brake booster valves configuration when the brake is being released.

When the force on the brake pedal is reduced, the retraction of the plunger with respect to the sleeve causes the opening of the Communication valve, reducing the pressure difference between front and rear chambers and, consequently, the booster force, until the reaction pad reaches again an equilibrium position or until the brake pedal is fully released.

The various phases are indicated on Figure 11, which shows the output force vs. the input force.

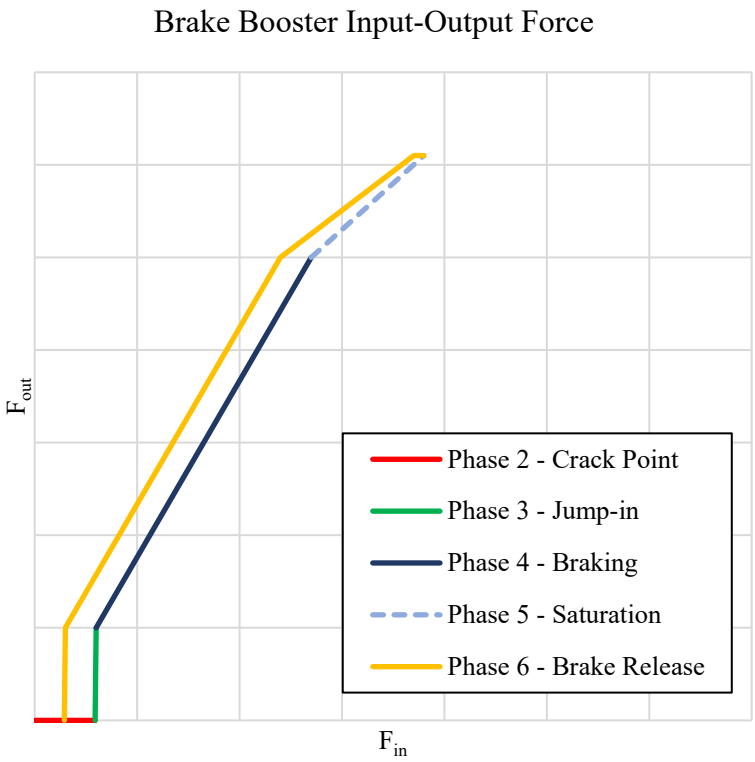

Figure 11. Brake booster output force vs. input force during a complete brake application and release.

The slope ratio between the curve representing Phase 4 and the curve representing Phase 5 is equivalent to the boost ratio of the brake booster. The point in which the transition between the Braking curve and the Saturation curve occurs is named Knee-point.

It is interesting to analyze how the behavior of the brake booster changes if the boost ratio or its maximum force are modified. The graphs shown in Figures Figure 12 andFigure 13 are theoretical, to highlight the differences of each parameter variation.

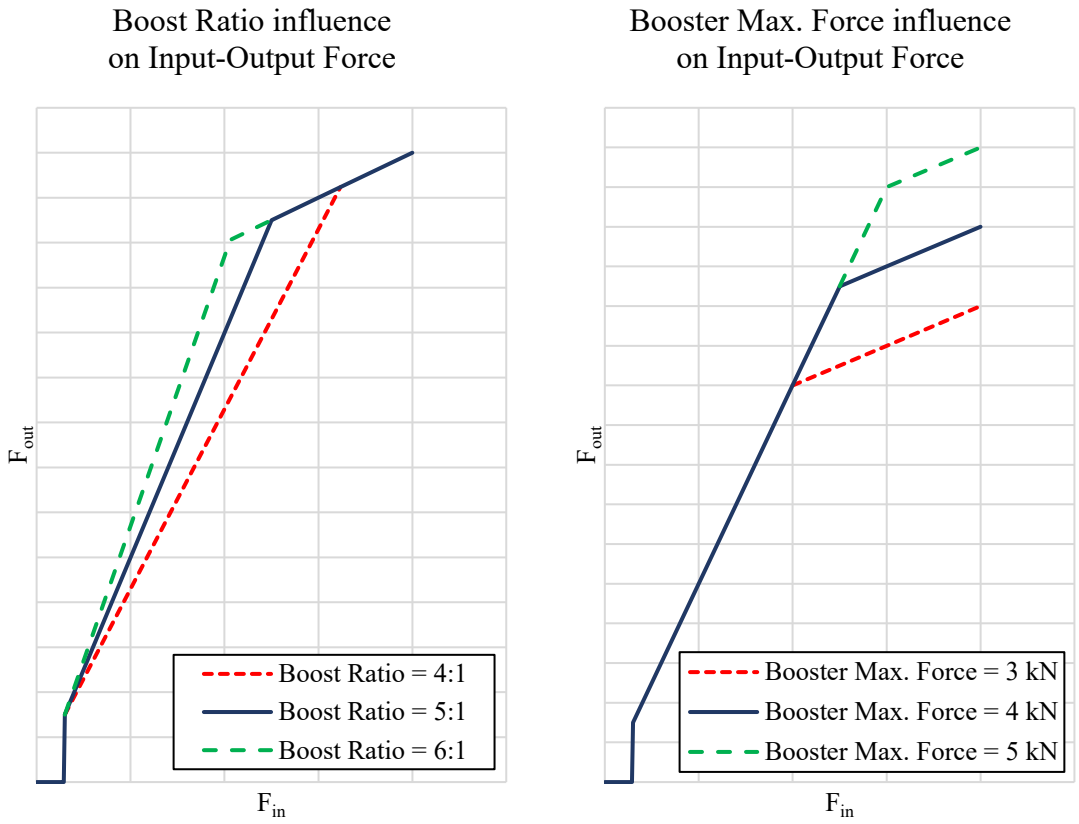

Figure 12. Brake booster output force vs. input force with different boost ratios (left) and different booster maximum forces (right).

Looking at Figure 12 on the left, it is visible that a change in the boost ratio influences the slope of the curve in the closed-loop braking phase. The knee-point is modified too, because the output force is the sum of the input force and of the booster contribution, therefore, the higher the boost ratio, the lower the input and output forces at which the booster reaches its maximum assistance. It is worth to note that, once the saturation has been reached, the working condition is the same regardless of the boost ratio.

When the maximum booster force is changed, as in Figure 12 on the right, the only variation is the position of the knee point along the closed-loop braking line. The booster maximum force F_{max} depends on the surface area of the booster piston A, and on the maximum pressure difference among the two chambers Δp_{max}:

$$F_{max} = A\,\Delta p_{max} \tag{2.3}$$

While the piston surface area is a constructional parameter, the maximum pressure difference depends both on the vacuum level achieved in the front chamber and on the ambient pressure at the rear chamber. If the vacuum obtained is weak and/or the ambient pressure is low, such as at high altitude, the pressure difference and the maximum booster force can be halved with respect to more ideal conditions.

Other constructional parameters that influence the relationship between the input and the output force are the gap between the plunger and the reaction pad, when the booster is at rest conditions, and the stiffness of the conical spring in the valve assembly.

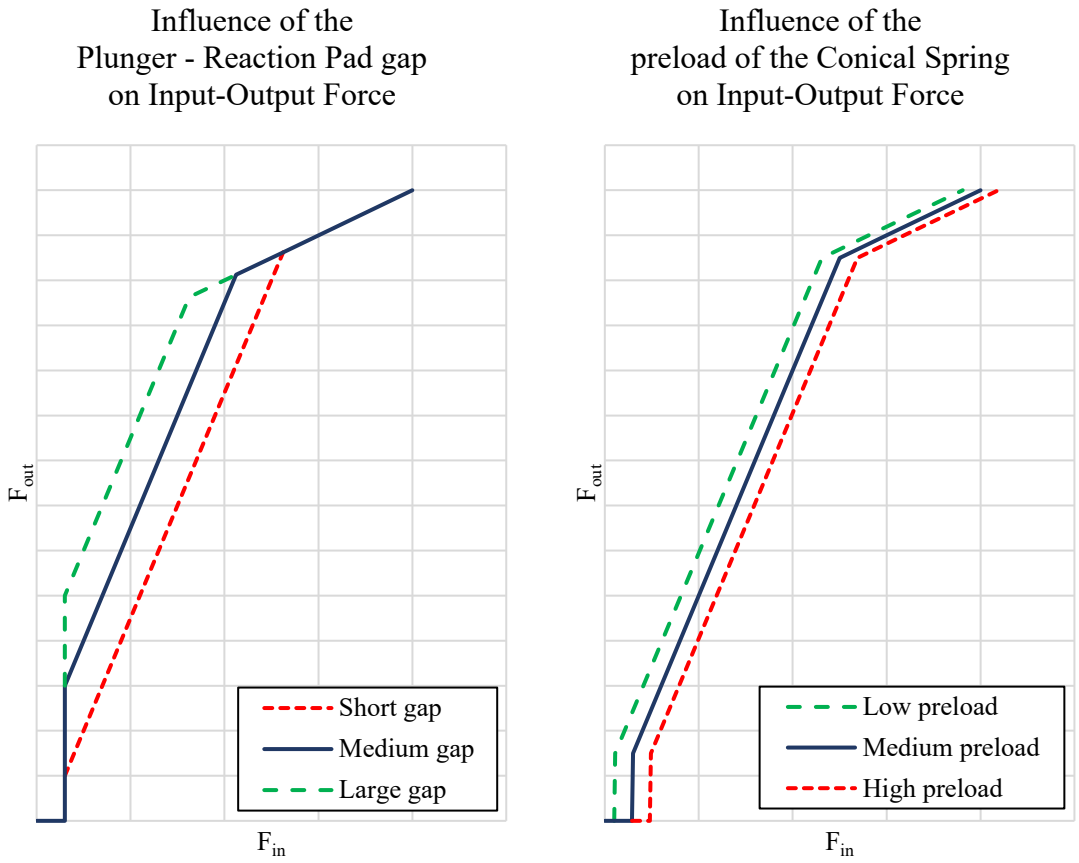

Figure 13. Brake booster output force vs. input force. Influence of the gap between plunger and reaction pad (left) and of the preload of the conical spring (right) on the booster behavior.

As it was mentioned during the description of the Jump-in phase, the amount of the gap between the plunger and the reaction pad determines the initial increase of the pressure in the rear chamber. It is visible in Figure 13 on the left, that the larger the gap, the higher the pressure rise before the reaction pad starts to contact the plunger, closing the Admission valve and returning a force feedback to the input shaft. The boost ratio remains the same, as well as the behavior of the brake booster when it has been saturated. The maximum booster force is unchanged too, moving the knee point along the saturation line as a function of the contribution of the input effort to the total output force.

The stiffness and the preload of the conical spring, on the other side, determines the minimum force to be applied at the input rod to close the communication valve and start to open the admission valve. Being all the other characteristic of the booster unchanged, the result is that the whole curve is offset along the input force axis, as it is possible to see in Figure 13 on the right.

2.3 Tandem Master Cylinder

The Tandem Master Cylinder (TMC) is the component that transforms the force received by the brake booster into fluid pressure to the brake lines. Another function performed by the TMC is the splitting of the braking system into two independent circuits, satisfying the redundancy requirements mandated by the vehicle regulations.

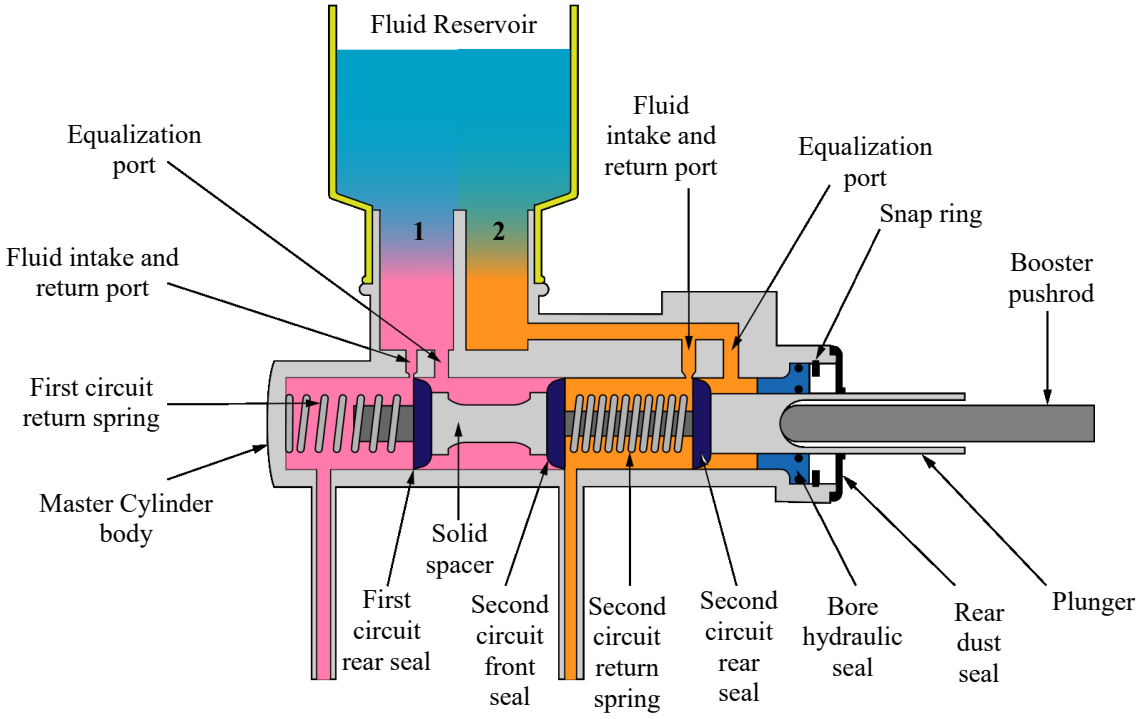

Figure 14. Schematic representation of a Tandem Master Cylinder and description of its internal components.

In Figure 14 is represented the TMC in rest conditions, it is visible the common reservoir that feeds both circuits with the brake fluid through the intake and return ports. To prevent the total loss of brake fluid in case of failure of one of the two circuits, a separator at the bottom of the reservoir allows to save a minimum quantity on brake fluid for the correct operation of the working circuit.

When the brake system is actuated, the booster pushrod is moved to the left, causing the displacement of the second circuit rear seal. As the fluid intake port of the second circuit is closed, the second circuit is sealed and pressure starts to build up under the effect of the force

of the booster pushrod. Then, the second circuit front seal and the first circuit rear seal, joined by the solid spacer, move forward until the first circuit fluid port is closed too. The solid spacer transmits the force from the second circuit front seal to the first circuit rear seal, equalizing the pressure between the two circuits.

Should the first circuit fail, when the brakes are actuated, the first circuit rear seal moves forward until its end-stop touches the master cylinder body: at this point, the second circuit front seal can generate the necessary resistance to sustain the pressure generation inside it. Similarly, if the second circuit fails, when its rear and front reals come in mechanical contact, the force received by the booster pushrod can be transmitted to the first circuit rear seal, generating the braking pressure in the first circuit. The effect of the failure of one of the two circuits is an increase of the dead stroke during which no pressure is generated in both circuits and, if the working circuit is connected to only part of the braking system, a reduction of the braking effectiveness.

2.4 Brake circuit configurations

As the Tandem Master Cylinder provides a redundant supply of brake fluid pressure, the two output ports are independently connected to the brakes, creating two separate brake circuits. In normal conditions, both circuits provide fluid pressure to the brakes, performing the function of the service brakes. Should one of the two circuits be damaged, such as in case of the rupture of a brake hose, the working circuit functions as a secondary brake.

The two brake circuits can be arranged in five configurations, each one with different advantages and disadvantages, named “I I”, “X”, “H I”, “L L” and “H H”.

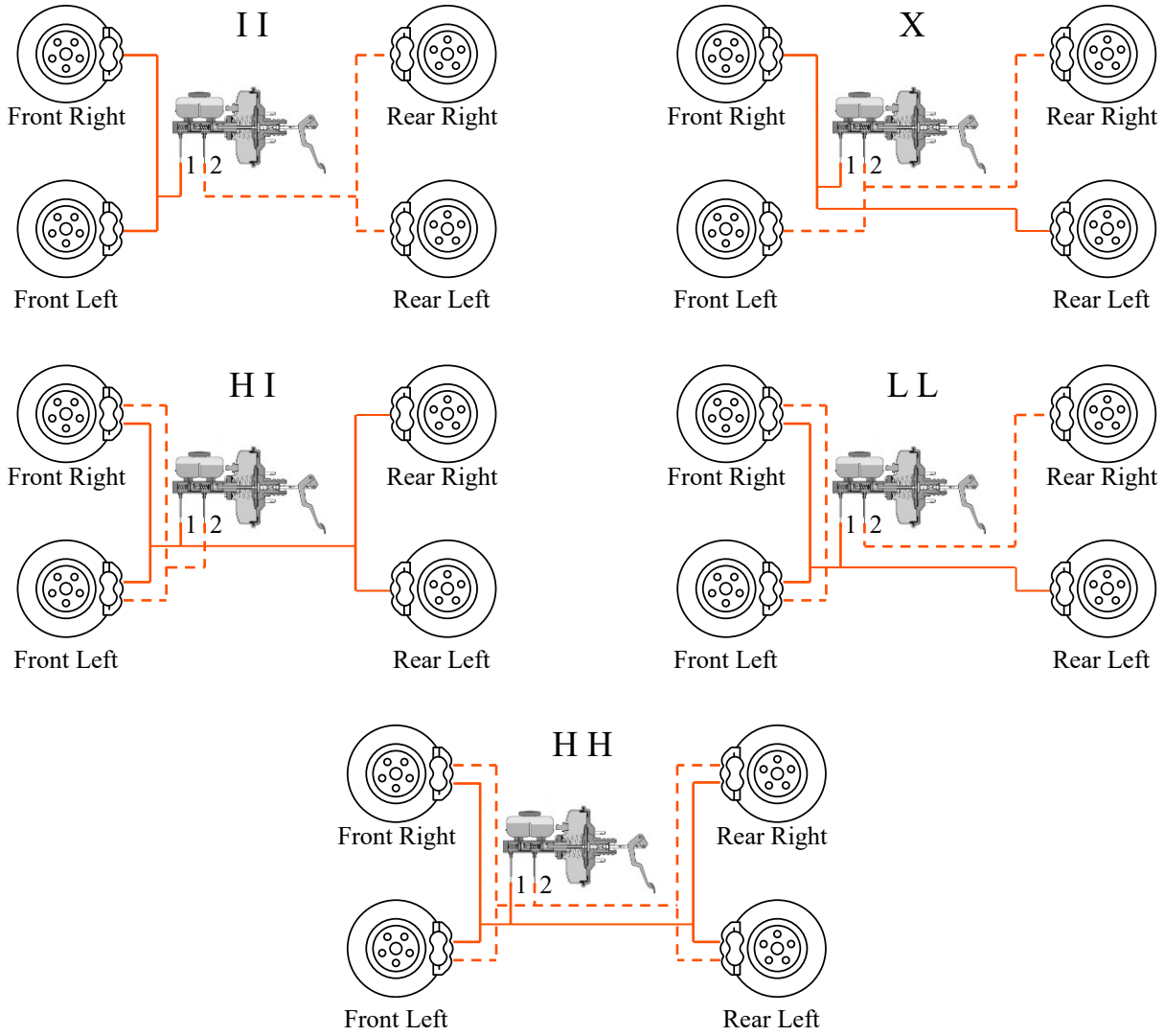

Figure 15. Different configurations of the two circuits of a split-circuit braking system.

The “I I” configuration uses separate circuits for front and rear axles, while in the “X” configuration the two circuits are split in diagonal form: front left and rear right for one circuit and front right and rear left for the other one.

The “H I” configuration feeds all the brakes with one circuit, while the second circuit is used for the front brakes; the “L L” configuration has both circuits connected to front brakes and one of the two rear brakes; the “H H” is the most complete, with the two circuits connected to all the wheels.

The first two configurations – “I I” and “X” – are the most cost-effective and lightweight solutions, because each wheel is connected to only one of the two circuits. The drawback is that the braking performance when one of the circuits fails is severely limited, because the vehicle can rely only on two wheels to decelerate. The front-rear split solution has the further advantage of requiring only one pressure-limiting device for adjusting the brake force distribution among

the two axles, but the stopping distances when the failed circuit is the front one can be very long, with the risk of vehicle instability if the rear wheels start to slip under the effect of the braking forces. The diagonal-split circuit provides higher braking performance with only one circuit, because there is always one front wheel contributing to the deceleration, but the front suspensions must be designed to counteract the torque steer generated by the imbalance of braking force among the wheels of the same axle. Moreover, the adoption of the electronic brake force distribution system has eliminated the need of rear pressure limiting devices, cancelling the cost advantage of the "I I" solution.

The other three solutions – "H I", "L L" and "H H" – guarantee higher braking performance with only one circuit, because the both front wheels always contribute to the vehicle deceleration, ensuring also a more stable behavior. However, the fact that some or all the wheels are connected to both circuits, require a higher number of connections and more complex brake calipers with at least two cylinders, increasing costs and weight.

Moreover, special care is required in addressing possible overheating of the brakes fed by both circuits. Should one of these brakes reach too high temperatures, i.e. because of a continuous contact between the friction lining and the brake rotor, if the brake fluid in both circuits reaches the boiling temperature at the same time, the braking ability of the vehicle is completely lost. In fact, the compressibility of the brake fluid, which is normally very low, increases of various orders of magnitude because of the vapor bubbles generated when the fluid is boiling, causing the sudden increase of the brake pedal stroke without pressure generation at the master cylinder: this phenomenon is called vapor-lock.

Given the features of each configuration and the very low probability of a failure of a brake circuit, the most widely adopted solution is the diagonal-split one, and it will be used as a reference in this thesis for the description of the rest of the braking system and in the experimental analysis of the tested vehicles.

2.5 Drum Brake

The drum brake, as the disk brake, is the ultimate part of the braking system and generates the braking moment at the wheel by pressing together two surfaces in relative motion and exploiting the friction between them. Drum brakes were widely adopted in the past for both front and rear wheels because of their low cost, ease of maintenance and good braking torque with respect to their dimensions. The major drawback is their low cooling effectiveness: being the friction surfaces inside the drum structure, there is no direct airflow to the linings and the internal surface of the drum, impairing the braking performances if it is continuously used.

Nowadays, the drum brake is mainly used in small vehicles at the rear axle, because of the small contribution of the rear axle to the total braking force and the high durability of the friction

linings compared to disc brakes. Moreover, drum brakes allow the implementation of a very effective parking brake with minimum costs, while disc brakes require more expensive and complex solutions, or even a small drum brake coaxial to the disc brake with the only purpose of providing a parking brake.

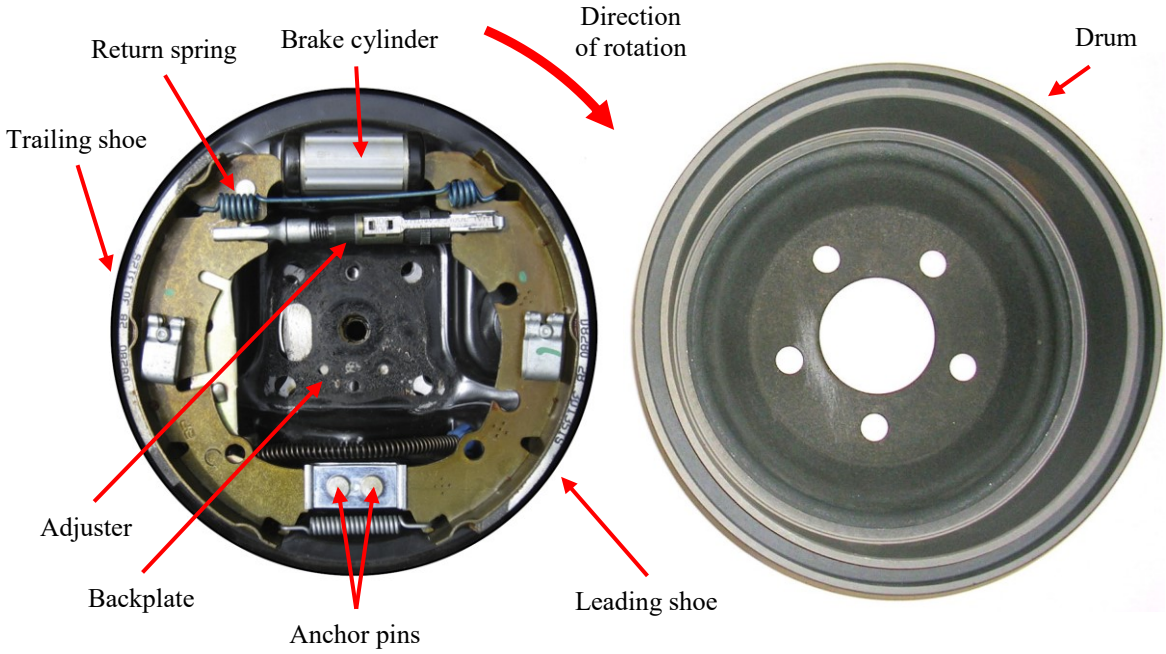

Figure 16. Internal view of a drum brake and its components.

Inside the drum brake there are two shoes that support the friction lining and use the force provided by the brake cylinder to press the linings against the internal surface of the drum. The two shoes are named differently depending on the main direction of rotation: the leading shoe is directed towards the direction of motion of the vehicle, while the trailing shoe is on the opposite side. The brake cylinder is connected to the brake circuit and converts the brake fluid pressure into linear force to both its sides. When the brakes are no longer applied, the shoes and the pistons of the brake cylinder are forced back to their rest positions by one or more return springs. As the linings wear down, their clearance with respect to the drum increases, leading to an unacceptable increase of the pedal stroke during braking. For this reason, an automatic adjuster placed in between of the two shoes senses their travel when the brakes are applied and, if a threshold is reached, it adjust their rest position to maintain an almost constant clearance. Since the friction linings become more compressible when the brakes are at high temperature, a bimetallic strip disables the adjuster mechanism when a certain temperature is reached, to avoid an over-adjustment that could lead to a residual braking torque when the brakes are not applied.

A brief analysis of the forces exchanged between the linings and the drum is useful to understand which are the main parameters that influence the braking torque as a function of the brake pressure.

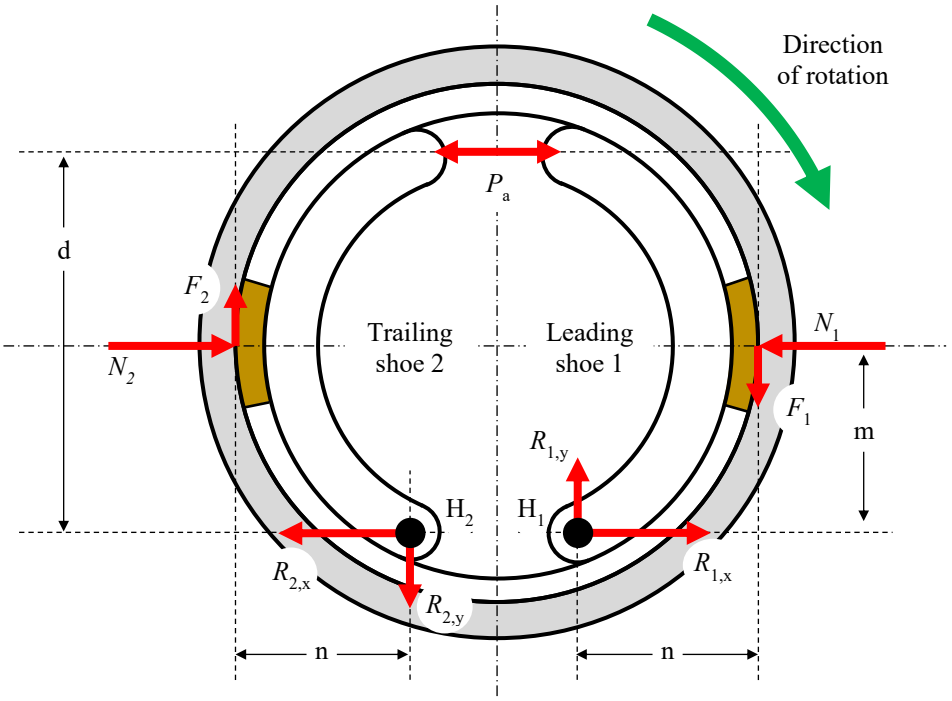

Figure 17. Simplified representation of a drum brake and the internal forces generated during the brake application. [2]

In the example shown in Figure 17, the leading shoe and the trailing shoe are pivoted around the points H_1 and H_2 respectively, and the actuation force P_a is assumed to be the same for both shoes. Being r_e the effective radius of the contact surface between linings and drum constant and equal to the drum inner diameter, the friction force can be considered as tangential to the drum inner circumference and its amount depends on the pressure distribution of the lining against the drum.

The equilibrium of forces applied to the leading shoe is resolved by the following three equations, whose symbols are consistent with the ones in Figure 17:

$$\text{Horizontal forces: } P_a + R_{1,x} - N_1 = 0 \tag{2.4}$$

$$\text{Vertical forces: } R_{1,y} - F_1 = 0 \tag{2.5}$$

$$\text{Moments around } H_1\text{: } P_a d + F_1 n - N_1 m = 0 \tag{2.6}$$

The radial force between the pad of friction material and the drum is:

$$N_1 = P_a d/(m - \mu n) \tag{2.7}$$

where μ is the friction coefficient between the shoe lining and the drum. Considering the friction coefficient as constant, which is an acceptable assumption as a first approximation, and knowing that the friction drag force F_1 is directly proportional to the friction coefficient and to the normal load, it is possible to state:

$$F_1 = \mu N_1 = \mu P_\mathrm{a} \mathrm{d}/(\mathrm{m} - \mu \mathrm{n}) \tag{2.8}$$

Therefore, the relationship between the applied force at the brake cylinder P_a and the obtained drag force F_1 by the leading shoe is:

$$F_1/P_\mathrm{a} = \mu \mathrm{d}/(\mathrm{m} - \mu \mathrm{n}) \tag{2.9}$$

Repeating the calculations for the trailing shoe, the result is:

$$F_2/P_\mathrm{a} = \mu \mathrm{d}/(\mathrm{m} + \mu \mathrm{n}) \tag{2.10}$$

It is possible to see that the friction force is non-linear with respect to the force applied by the brake cylinder and that it is different between the two shoes, with the leading shoe providing a higher contribution to the total braking force.

Being the total friction force the sum of F_1 and F_2 and considering that they are tangential to the inner circumference of the drum whose radius is $\mathrm{r_e}$, the total braking torque τ that will be transferred to the wheel is given by:

$$\tau = (F_1 + F_2)\, \mathrm{r_e} \tag{2.11}$$

Therefore:

$$\tau = \mathrm{r_e} \frac{2\mu P_\mathrm{a} \mathrm{d}}{1 - \left(\frac{\mu \mathrm{n}}{\mathrm{m}}\right)^2} \tag{2.12}$$

On a real drum brake the surface of the two linings is much larger and it is not immediate to determine the pressure distribution and the resultant of the normal forces, making an accurate design of the brake much more complex than how it has been described here. Moreover, actual brakes also use a sliding pivot for the shoes, to allow a better matching between the lining surfaces and the drum, adding more degrees of freedom to the model. However, the equations used are still useful to understand how the geometry of the drum brake influences the braking performance.

2.6 Disc Brake

As for the drum brake, the disc brake transforms the brake circuit pressure into braking moment by pressing together two surfaces in relative motion, but its characteristics make the disc brake

more suitable for the automotive application: even if it is generally heavier and more expensive than the drum brake, the cooling performance of the disc brake is much better. For this reason, disc brakes are used on almost all vehicles at the front axle, while on the rear axle it is widely adopted on vehicles of segments C and above. For small vehicles, the drum brake is still a convenient solution, even if some manufacturers prefer the disc brake even in this segment, using the higher perceived quality of a vehicle equipped with four disc brakes as a selling point.

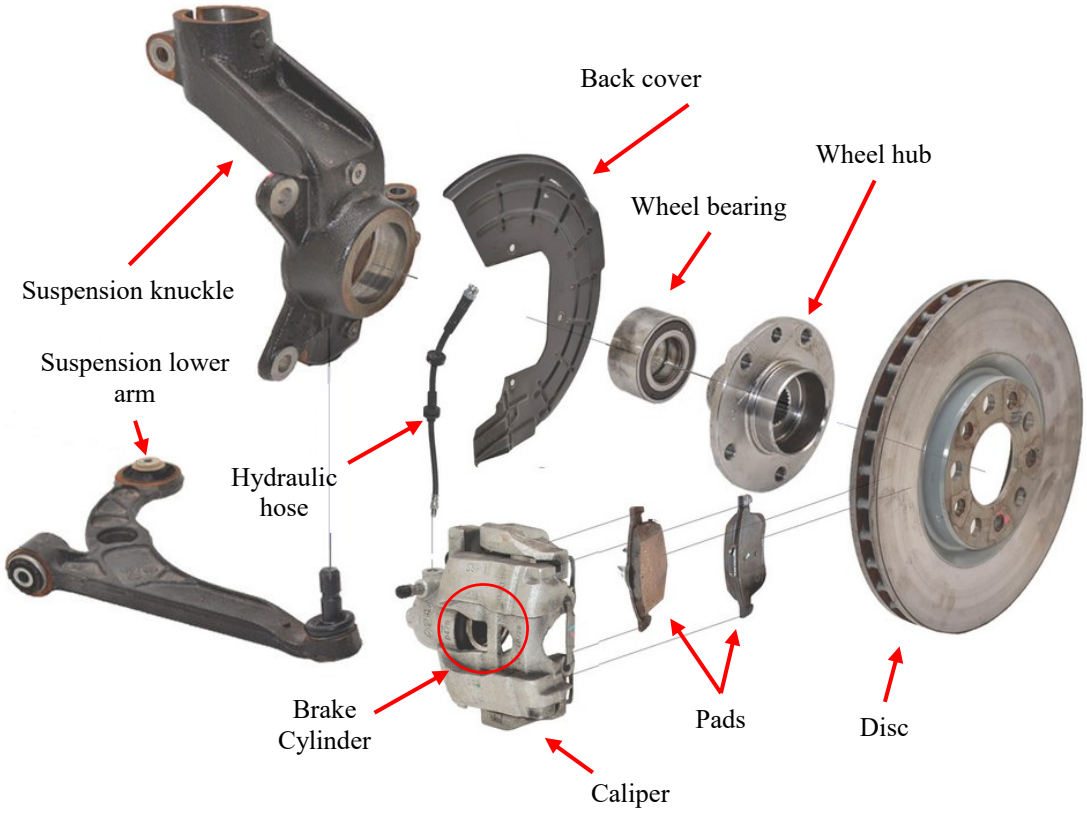

Figure 18. Disassembled view of a disk brake and of the supporting suspension components.

The main components of the disc brake are the disc rotor, the brake caliper and the brake pads. A piston inside a cylinder housing of the caliper uses the brake fluid pressure to press the pads against the two sides of the disc, generating the friction force that gives rise to the braking moment.

The thermal capacity of the disc rotor is lower with respect to the one of the drum, but the direct exposure of the disc to the wheel airflow allows a higher cooling rate when the vehicle is in motion. A significant improvement in the cooling ability of the disc rotor is by using a vented disc, which is made by two discs kept together by thin vanes (as the disc in figure Figure 18), doubling the surfaces that dissipates the heat. Moreover, if the vanes are suitably arranged, the wheel rotation will increase the airflow through the disc, further improving the cooling performance. Some high-performance discs also have a cross-drilled or slotted braking surface,

to be more abrasive on brake pad and provide an escape to the gases that are generated on the lining surface at high temperatures, increasing the friction coefficient.

The brake pad is made by a stiff backplate that distributes the force received by the brake piston to the pad surface, by the friction lining material and by a thin underlayer in between of them. The role of the underlayer is to reduce the heat transfer to the backplate (and, eventually, to the brake fluid through), improve the acoustic comfort and the bond strength to the backplate. Behind the backplate it is glued the shim, a sheet of harmonic steel with one or more rubber layers to further reduce the noise generation. The geometry of the friction material also includes chamfers and slots to improve the acoustic comfort.

The brake caliper holds the pads and includes the hydraulic cylinder with its piston to convert the brake fluid pressure into normal force at the pad. Two main types of calipers can be distinguished: fixed and floating. The fixed caliper is rigidly mounted to the suspension knuckle and has two pistons at both sides of the brake disc to press the pads against the rotor: this solution generally provides a better pressure distribution among the pads and allows the installation of pads of greater dimension, but they are more expensive. Moreover, the brake fluid must also reach the external side of the caliper, passing through the caliper bridge, very close to the brake disc, where very high temperatures are developed, increasing the risk of a vapor lock. The floating caliper is the most widely adopted because of its lower cost and uses only one piston in the inner side to compress the pads against the disc: the caliper is free to translate along the disc axis, distributing the pressure on both pads with the translation of the caliper. The drawback of the floating solution is that the pressure distribution among the pads can be uneven and that dirt and wear of the floating system can cause the caliper to stick to the sliding pins, causing noise during braking, worse pressure distribution and an increased drag torque when the brakes are not in use.

The back cover protects the disc and pads from dirt that might generate noise during braking and scratch the friction surfaces, and also shields the suspension components from the heat and dust generated by the brake.

Differently from the drum brake, there are no springs that force the pads and the piston to return to its rest position, although there are metallic clips that maintain the pad parallel to the disc surface when the brakes are not used.

The design of the cylinder includes a seal of squared section that has a certain sticking capability to the piston, exploiting the elastic properties of the seal material to pull back the piston when the brakes are not applied.

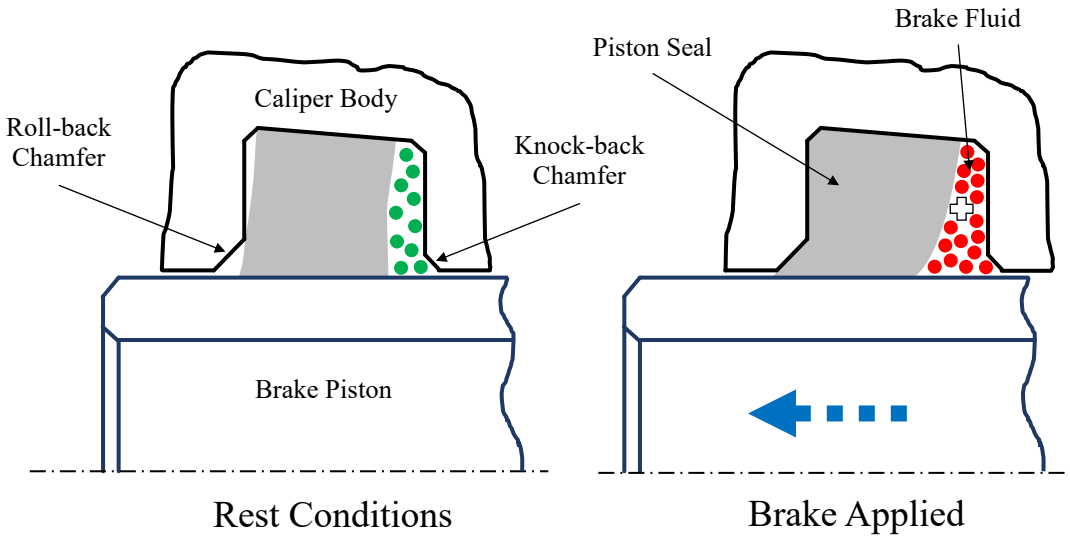

Figure 19. Schematic representation the piston seal deformation before (left) and after (right) the piston displacement in the caliper of a disc brake.

When the piston is pushed outwards per effect of the brake application, the seal remains adherent to the piston until it is totally compressed against the caliper body: only at this point, if the piston moves further, there is a relative motion between the piston and its seal. When the brakes are released, the seal recovers its original shape and pulls back the cylinder: the amount of return travel is determined by the size of the roll-back chamfer. In normal conditions, the relative motion between piston and seal occurs only by the effect of the wear of the brake pad.

Similarly, the compliance of the wheel hub might slightly influence the position of the brake disc when the wheel is under high lateral forces, causing the contact between pad and disc even if the brake has not been applied. In this situation, the piston could be retracted by the contact force received by the pad, leading to an excessive pedal stroke the next time the brakes are applied. To prevent this situation, a knock-back chamfer is made in the caliper body, which allows the piston seal to recover the piston retraction in these circumstances.

Although the motion of the piston is governed by the piston seal, it is not possible to pull back the brake pad with the retraction of the piston, therefore, a minimum drag given by the contact of the brake pad with the disc is unavoidable. Caliper manufacturers are developing a special design of the metallic clip that holds the brake pad to the caliper, which includes small springs able to slightly retract the brake pad from the disc, maintaining a small clearance when the brakes are not in use: such design, if it correctly manages the adjustment of the clearance as a function of the pad wear, would eliminate the drag torque of the disc brakes when they are not in use, without significantly affecting the brake pedal stroke.

For the analysis of the influence of disc brake geometry on the generated braking torque, a simple model with one cylinder and two pads is considered.

Starting from the cylinder, the surface area of the piston is easily obtained from the diameter d:

$$A_{cyl} = \frac{\pi d^2}{4} \tag{2.13}$$

and the relationship between the normal force generated by the piston and the fluid pressure p is:

$$F_{cyl} = pA_{cyl} \tag{2.14}$$

Due to the friction, part of the force provided by the piston is spent to overcome the resistances F_r in the displacement of the piston itself and in the displacement of the caliper if it is of the floating type. The net normal force N between pads and disk is then:

$$N = F_{cyl} - F_r \tag{2.15}$$

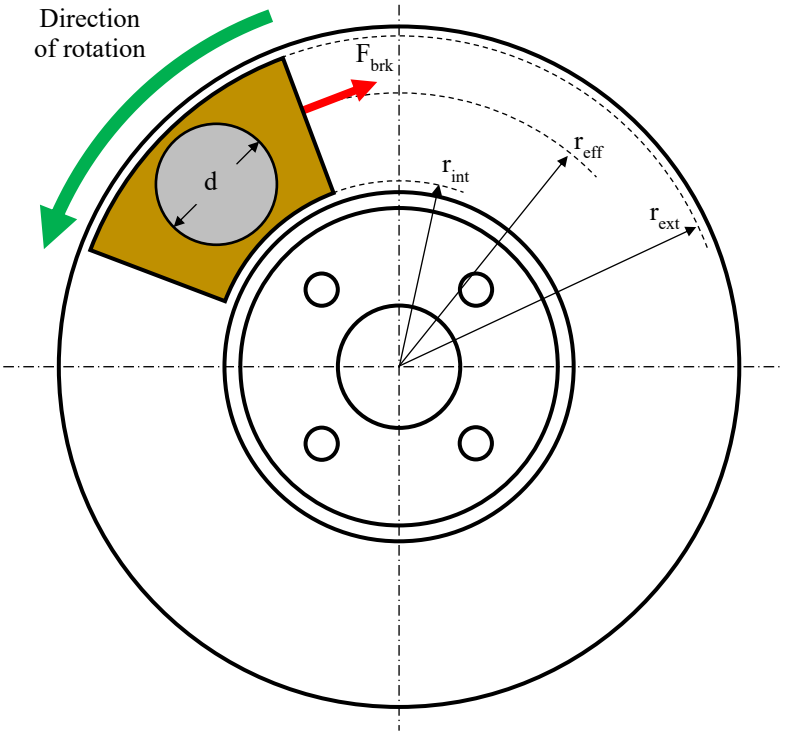

Figure 20. Schematic representation of a disc brake and the internal forces generated during the brake application.

The brake pad is developed along an arc, determined by its outer radius r_{ext} and its inner radius r_{int}. Considering an even pressure distribution, the radius r_{eff} that locates the resultant of the braking force is determined by the formula:

$$R_{eff} = \frac{2}{3}\frac{r_{ext}^3 - r_{int}^3}{r_{ext}^2 - r_{int}^2} \tag{2.16}$$

Being μ the friction coefficient between pads and rotor and knowing that two pads contribute to the braking force, the total braking force F_{brk} is:

$$F_{brk} = 2\mu N \tag{2.17}$$

Therefore, since the braking torque is:

$$\tau = F_{brk} r_{eff} \tag{2.18}$$

the braking torque as a function of the brake fluid pressure is obtained combining equations (2.13), (2.14), (2.15), (2.16), (2.17) and (2.18):

$$\tau = 2\mu\left(p\frac{\pi d^2}{4} - F_r\right)\left(\frac{2}{3}\frac{r_{ext}^3 - r_{int}^3}{r_{ext}^2 - r_{int}^2}\right) \tag{2.19}$$

If the resisting force term F_r is neglected, there is braking torque is directly proportional to the brake fluid pressure. The friction coefficient can be considered as a constant at first approximation, it is generally temperature independent until 300-350 °C, above which it starts to decrease because of fading. It is slightly dependent on the relative velocity between the pads and the rotors, increasing as the vehicle speed is reduced. With respect to the applied pressure, the friction coefficient tends to decrease as the pressure increases.

2.7 Anti-lock Braking System

Once the braking torque has been generated, the transmission to the ground as a longitudinal force is made possible by the vehicle tires. The tire is a semi-tubular composite component, made of several layers of rubber, synthetic polymers, fabric and steel, that is mounted on the circumference of the wheel rim and, with the help of pressurized air in the volume enclosed by the rim and the tire, accomplishes three functions:

- Support the vehicle weight, while providing some cushioning to absorb minor road asperities;
- Exchange with the ground longitudinal forces, providing the vehicle traction and braking ability to accelerate and decelerate the vehicle;
- Exchange with the ground lateral forces, allowing the vehicle to change direction during its motion.

Being a compliant element, the tire deforms while it is performing its functions, changing locally its shape near the tire-ground contact area. While it is a common experience to see the

vertical deformation of the tire sidewall under the vehicle load, in particular if the tire is underinflated, the longitudinal and lateral deformation of the threads under acceleration/braking and cornering forces is less evident. Such deformations imply that the tangential velocity of the tire, computed as the product of its angular velocity times its radius, is slightly different with respect to the ground speed of the vehicle. This difference becomes larger when the tire is tire is exchanging longitudinal forces: under traction forces, the tire spins faster with respect to a wheel in pure rolling conditions, while under braking forces the tire is rotating at a lower speed. Similarly, the generation of lateral forces when the tire is rolling requires an angular difference between the equatorial plane of the wheel and its actual direction of motion.

Focusing on braking forces, the relative difference between the tangential velocity of the tire and its longitudinal speed is referred to as slip ratio σ, computed as:

$$\sigma = 1 - \frac{\omega \mathrm{r}}{V} \tag{2.20}$$

where: ω is the angular velocity of the wheel, r its radius and V the longitudinal speed of the vehicle. In pure rolling conditions, the tangential velocity of the tire is equivalent to the longitudinal speed of the vehicle, therefore the slip ratio is equal to zero. If the wheel is completely locked by the braking torque and is slipping on the ground, the slip ratio is equal to 1. During a normal braking the slip ratio is between 0 and 1, depending on the braking moment and on the friction coefficient at the tire-ground contact.

Remembering that the longitudinal and lateral tire friction coefficients μ_{x} and μ_{y} are defined as the ratio between the longitudinal or lateral force and the vertical load normal to the ground, the influence of the slip ratio on both coefficients on an asphalted ground is shown in Figure 21.

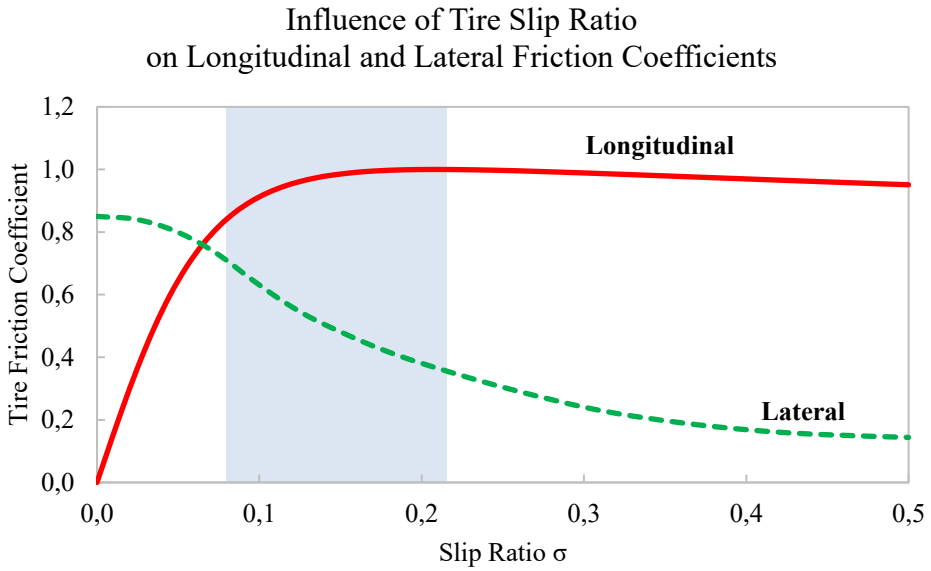

Figure 21. Influence of the tire slip ratio on the longitudinal and lateral friction coefficients. The shaded area represents the slip ratio range of intervention of the ABS system.

In this representation the value of slip ratio is limited up to 0,5: for higher slip ratio values, the lateral friction coefficient tends to zero, while the longitudinal friction coefficient slightly decreases. Considering a different ground, such as wet asphalt, snow or ice, the shape of the curves is similar, but the peak values are lower. Also, the tire compound and its size change the shape and the peak values of the curve, but, as a general rule, it is possible to state that:

- The longitudinal force reaches its maximum with slip ratios between 0,1 – 0,3;
- The lateral force decreases as the slip ratio increases.

This is consistent with the friction ellipse principle, since the available lateral force is reduced as the longitudinal force increases.

For these reasons, to maximize the braking performance and to maintain the lateral support of the tire, it is necessary to modulate the braking torque of the wheels in order to not exceed the slip ratio at which the maximum braking force is achieved. Although it is relatively simple to control the vehicle when the tires are working in their linear region (slip ratio between 0 and 0,05), as the tire reaches its limit it becomes more difficult, because the friction loss after the peak value causes the sudden deceleration of the wheel, further reducing the friction coefficient and eventually coming to a complete wheel lock in fractions of a second. Moreover, differences in the vertical load among the wheels and/or in the road surface grip might cause some wheels to lock while the other ones are still not expressing their maximum braking potential.

To address these issues, an automatic system that modulates the brake pressure at the individual wheels has been developed in 1978 by Bosch, named Anti-lock Braking System (ABS). Many evolutions and equivalent systems from other manufacturers have arrived in the automotive

industry in the years, but the main function remains to control the wheel slip ratio in the range of the shaded area of Figure 21, allowing the driver to control the vehicle trajectory during an emergency braking, achieving both a good lateral tire support and short stopping distances.

With the economies of scale, the system has become more and more adopted and the addition of the ability to autonomously generate the brake pressure without the driver's action on the pedal has greatly extended its functions, making possible to use the brakes to reduce the spinning of the wheels generated by an excessive engine torque (known as Traction Control TC) and to generate a yawing torque to correct an understeering or oversteering condition of the vehicle (known as Electronic Stability Control ESC). Such systems have become mandatory in 2011 to obtain the type approval for European passenger vehicles.

The electro-hydraulic module of the ABS/ESC is located between the tandem master cylinder output and the wheels, and it is designed to keep the separation between the two hydraulic circuits, maintaining the redundancy requirements of conventional braking systems.

To evaluate the vehicle state, the electronic control unit of the ABS/ESC requires individual wheel speed sensors, a pressure transducer at one of the two tandem master cylinder outputs, longitudinal/lateral acceleration sensors, a yaw rate sensor, and a steering angle sensor.

In Figure 22, it is shown a schematic representation of the internal components of the hydraulic unit of the system, to better understand its working principle.

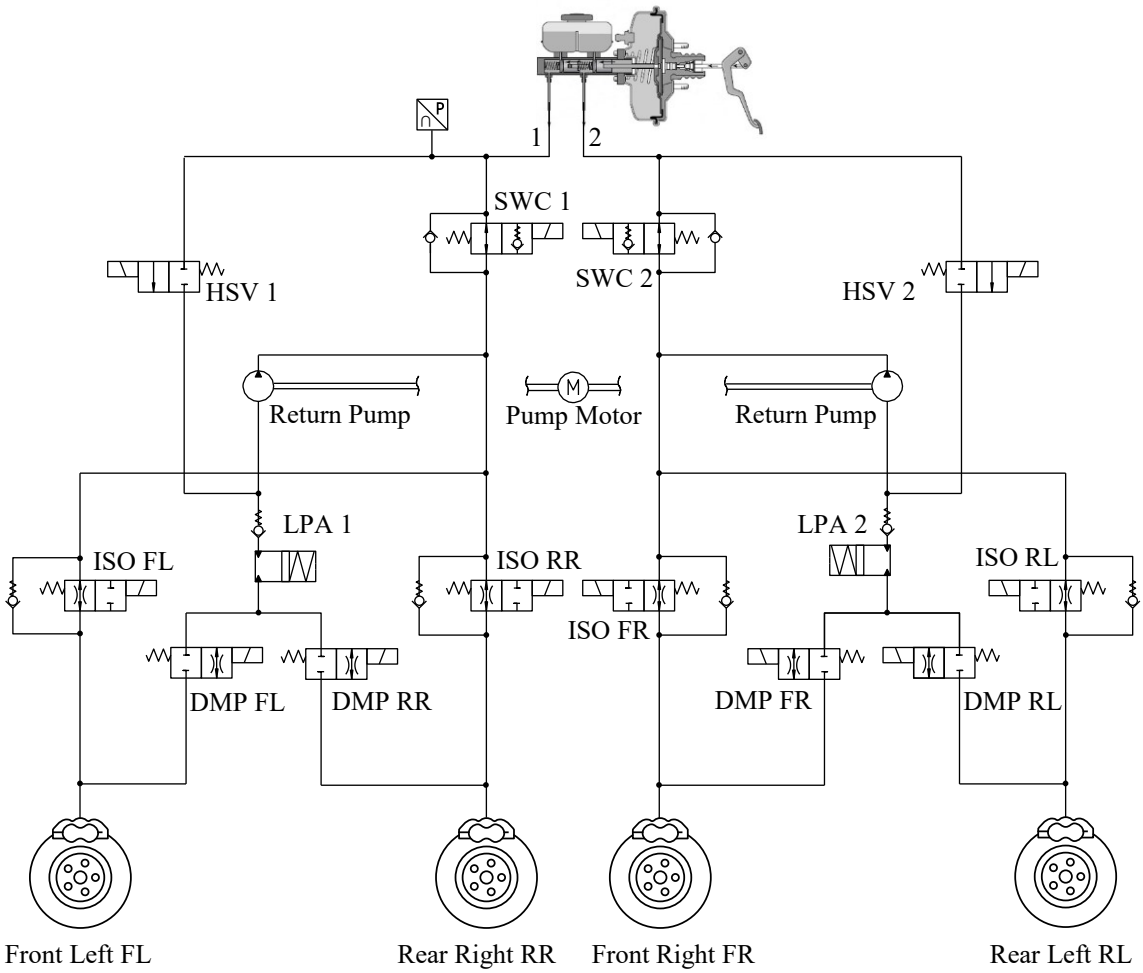

Figure 22. Simplified representation of the hydraulic scheme of an Anti-lock Braking System (ABS) with the additional functions of Traction Control by braking (TC) and Electronic Stability Control (ESC).

Each wheel is connected to the TMC through a normally open isolation valve (ISO) and to a low-pressure accumulator (LPA) through a normally closed dump valve (DMP). A normally open switchover valve (SWC) in each brake circuit (1 and 2) provides the brake fluid to the wheel brakes, while a normally closed high-pressure switch valve (HSV) connects the pump inlet ports to the tandem master cylinder.

In normal braking conditions, when the brake force is not enough to lock the wheels, the system is at idle and all the valves are at their rest positions. As the electronic control unit detects that the slip ratio and/or the angular deceleration of a wheel exceed a predefined threshold, the corresponding isolation valve is activated, preventing a further increase of the braking moment if the force on the brake pedal is increased. If this is not enough and the slip ratio continues to increase, the dump valve is briefly activated, reducing the brake pressure at the wheel and allowing the acceleration of the wheel until the slip ratio is again in the linear region. As soon as the wheel has been stabilized, the isolation valve is gradually opened, to increase the braking pressure until the pressure level at the TMC has been reached, or until a new wheel lock-up occurs.

When the dump valve is energized, the brake fluid discharged from the brake caliper is stored in a small reservoir (the low-pressure accumulator) until the pump of the system (activated as soon as one or more dump valves are energized) brings back the fluid to the high-pressure side of the circuit.

The switchover valves and the high-pressure switching valves are simultaneously activated whenever the system needs to increase the brake pressure beyond the level reached by the driver, or to autonomously brake one or more wheels without the driver's intervention. The activation of these valves puts in communication the pump with the tandem master cylinder, directing the fluid towards the isolation valves of the wheels: the wheel that requires a braking torque will have the isolation valve open, while the other wheels will have them closed. In these conditions, if the driver presses the brake pedal, is not able to transmit its pressure to the brakes, because the pressure level in the circuit is given by the pump. For this reason, the pressure transducer allows to detect the amount of braking force required by the driver and adjust the pressures at the individual wheels during its intervention to provide the required braking force.

An example for a single wheel of a vehicle of the time history of the wheel speed and the modulated brake pressure during an emergency braking maneuver with the ABS activated is shown in Figure 23 for better understanding the behavior of the system.

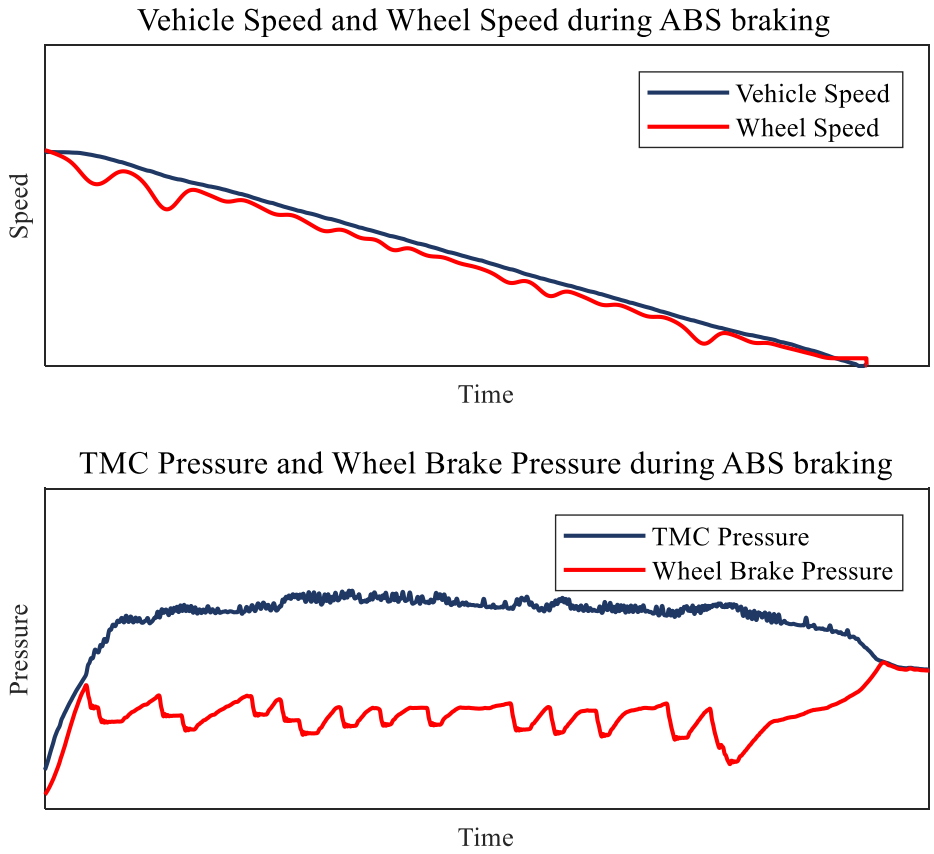

Figure 23. Time evolution of the vehicle speed and of the tangential speed of one of its wheels during an emergency braking maneuver with ABS activated (top). Time evolution of the Tandem Master Cylinder pressure and of the brake pressure at one wheel during the same braking maneuver (bottom).

It is visible how the pressure rises, is held constant or reduced through the proper activation of the ISO and DMP valves, as well as the wheel speed oscillation around the ideal slip ratio value during the whole deceleration. The cycling of the pressure inside the braking system causes a vibration at the brake pedal which is a normal phenomenon that indicates the activation of the system.

Another function required to any braking system, is to properly distribute the braking force among the front and rear axle, according to the loading condition of the vehicle and to the deceleration achieved during the braking maneuver. As it was mentioned during the tire description, the maximum force transmissible at the tire-ground contact depends on the vertical load exerted on the tire, therefore, the weight transfer during the braking of the vehicle must be considered.

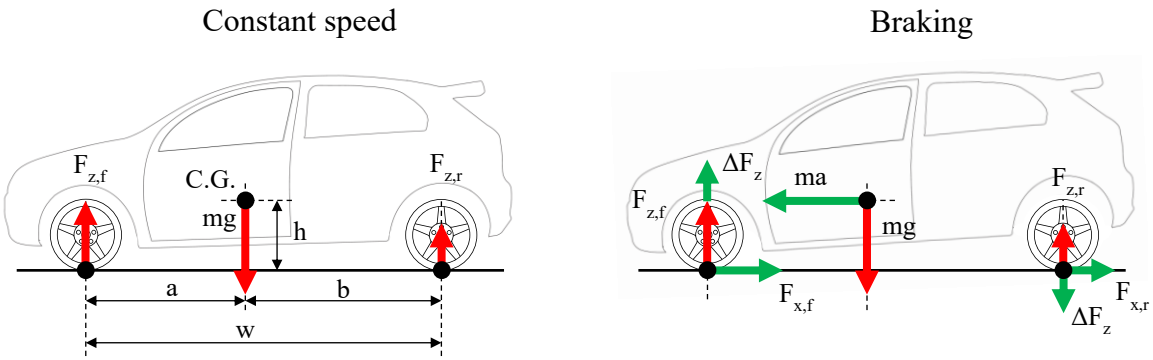

Figure 24. Longitudinal and vertical forces exerted on the wheels of a vehicle at constant speed (left) and during a braking maneuver (right).

When the vehicle is in static conditions, or moving at constant speed, the weight is distributed among the front and the rear axle, according to the position of the center of gravity.

The load at the front axle $F_{z,f}$ and at the rear axle $F_{z,r}$ is determined as:

$$F_{z,f} = mg\frac{b}{w} \tag{2.21}$$

$$F_{z,r} = mg\frac{a}{w} \tag{2.22}$$

being a and b the distances between the center of gravity and the front and rear axles respectively, and w the wheel base of the vehicle, while m is the vehicle mass and g the gravity acceleration.

As the vehicle is decelerated, the moment generated by the distance between the longitudinal forces of the tires and the inertia force of the vehicle causes a transfer of part of the normal force acting on the rear tires to the front ones, by the amount ΔF_z:

$$\Delta F_z = ma\frac{h}{w} \tag{2.23}$$

where: a is the longitudinal acceleration and h is the distance between the vehicle center of gravity and the ground.

As the vehicle is loaded with passengers and luggage, the center of gravity is displaced both longitudinally and vertically, changing both the static and the dynamic load distribution among the axles. As a consequence of this, if the braking force is not adapted to the changed loading conditions, one axle may start to reach the tire limit of friction, while the other is still not fully exploited. Even if the ABS can modulate the brake pressure when one of the wheels starts to lock, it is preferred to have an even exploitation of the tires longitudinal ability, because even at slip-ratios below the threshold of intervention of the ABS, a difference in the slip ratio

between front and rear wheels can affect the lateral friction coefficient of the tires and make a vehicle more prone to oversteer or understeer if its braked while cornering.

For this reason, in Figure 25 an ideal braking curve is considered, where, taking into account the load transfer, the ideal brake force distribution that allows to exploit the same grip coefficient between the front and rear wheels is represented as a function of the vehicle deceleration.

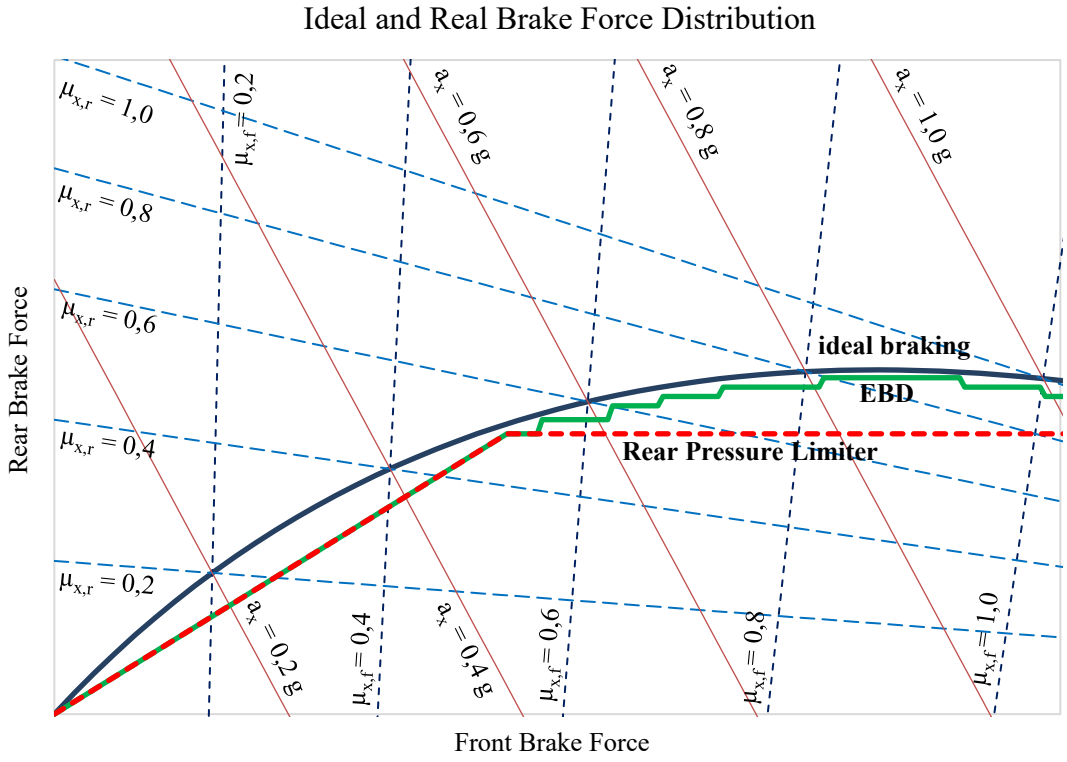

Figure 25. Distribution between front and rear braking forces during a braking maneuver in ideal and real conditions. $\mu_{x,f}$: front wheels friction coefficient. $\mu_{x,r}$: rear wheels friction coefficient. a_x: longitudinal deceleration.

As the vehicle deceleration increases, the relative contribution of the rear tires to the total braking force is reduced, while the front tires increase their braking ability as the deceleration increases. In a braking system without any type of brake force distribution, the proportion of front/rear brake force is fixed, corresponding to a straight line as in the first part of the green and red lines in the graph. It is evident that, in these conditions, the ideal brake force distribution is reached only at one deceleration value, while in other conditions one axle will start to lock before the other one. Since the ideal braking curve exploits the friction coefficient of both tires in the same way, then the limit of adherence is reached, following the ideal brake force distribution, all the wheels reach the maximum braking force at the same time. If the real force distribution is located below the ideal curve, the rear wheels are less exploited and the front wheels will lock first; vice-versa, if the real brake force distribution curve is above the ideal curve, the front brakes are less exploited and the rear wheels will start to lock first.

Considering that a perfect brake force distribution is not possible, it is preferable to have the front wheels to lock first, because it brings to an understeering behavior that is easier to control, since the vehicle will tend to move on a straight line; if the rear wheels lock first, the vehicle becomes instable and more prone to deviate from the trajectory desired by the driver.

As the loading condition of the vehicle increases, the ideal braking curve tends to raise, giving more brake force contribution to the rear axle, as normally the luggage and the rear passengers tend to move back the vehicle center of gravity. For this reason, the braking system is designed to provide a relatively high braking force to the rear axle, in order to better approximate the ideal braking curve at low deceleration values and to provide adequate braking force when the vehicle is fully loaded. As the deceleration increases, if the vehicle is unladen, the rear brake force may become excessive, therefore, a pressure limiting device reduces or totally prevents a further increase of the rear brake pressure, leaving to the front axle a higher contribution at the higher decelerations.

Mechanical pressure limiters can operate at fixed pressure levels or can adjust their point of intervention according to the rear suspension ride height (which is related to the vertical load on the rear axle), or to the vehicle deceleration. The type of pressure limited adopted depends on the difference in vehicle weight between full load conditions and unladen conditions, as well as on the center of gravity height: the device that best approximates the ideal braking curve in all the loading conditions is used.

As the ABS has become more widespread, its ability to continuously measure the relative angular velocity between front and rear wheels can be used to infer which axle is more exploited during the braking, providing a better approximation to the ideal brake-force distribution curve at any loading condition and deceleration. This function is called Electronic Brake-force Distribution EBD and it does not require additional hardware with respect to the one needed for the ABS operation.

It is worth to note that, even if the EBD is able to finely follow the ideal braking curve, as shown by the green line in Figure 25, such stepped adaptation of the rear pressure would generate pressure oscillations in the brake circuit that make the driver feel a pulsating brake pedal as in an emergency braking with the ABS intervention. Since the EBD intervenes much more frequently, even in normal decelerations far from the tire friction limit, such frequent pulsation of the brake pedal is considered unacceptable from a comfort point of view and could mislead the driver in the evaluation of the friction limit available at the tires. For this reason, the EBD strategy is generally defined to mimic the working behavior of a pressure limiter, activating the isolation valves of the rear wheels as their exploitation reaches a certain threshold and maintaining the pressure constant for any increase in the vehicle deceleration. Even adopting this behavior, the EBD is more effective than a mechanical pressure limiter, because the knee

point of the rear brake force can be adapted to the actual tire friction coefficient, without intervening only at a determined pressure or deceleration value. Moreover, if the front wheels reach the friction limit and start to lock, as the ABS starts to cycle, the EBD increases the rear brake pressure until the rear wheels also reach the friction limit, exploiting the maximum longitudinal tire force of all the tires, even if the driver has not applied enough effort on the brake pedal.

3. Experimental Analysis and Objective Measurements

In this chapter, it will be described how the analyzed vehicles have been experimentally assessed, starting from the instrumentation used for the objective measurements and continuing with the initial conditioning of the braking system, which is necessary to break-in the friction surfaces of the braking system of a new vehicle, or when the brake pads and/or rotors are renewed. In the end, the main maneuvers performed during braking tests and the data obtainable from them will be described.

3.1 Measurement Equipment

The validity of and objective analysis strongly depends on the accuracy of the numerical data obtained and on the repeatability of the tests performed. This is true even in the vehicle dynamics testing, where the number of variables to be measured and the harsh environment in which water, dust and vibrations affect the operation of most sensing devices determine a challenge in the development of suitable measurement equipment. In the following paragraphs, a description of the variables involved in a braking maneuver and of the state-of-the-art tools used for their measurement is provided.

3.1.1 Brake Pedal Travel

The brake pedal travel is usually measured with a linear displacement sensor with a sensing range long enough to exceed the complete pedal travel, from rest to the firewall: typical values are between 200 and 300 mm. This kind of linear displacement sensor is a telescopic potentiometer, which is fed by a constant DC voltage and outputs an analog signal whose voltage is linearly dependent on the longitudinal position of the sensor. For this application, it is required to have a 0.1 % accuracy and it is necessary a temperature compensation.

Figure 26. Brake pedal travel sensor (blue) and pedal force transducer (circular pad on the brake pedal).

It is worth to note that the pedal trajectory is an arc of circumference, while the sensor measures only linear displacements: this generates a geometric error in the measurement which is proportional to the sine of the angle between the sensor axis and the normal of the pedal. To minimize this error, it is important to install the sensor so that to be perpendicular to the pedal

when it is in rest position. In this way it is possible to have an accurate measurement, at least for the initial part of the pedal travel.

A typical installation of the sensor is with one end mounted on the lower part of the steering column housing, while the other end is connected to the left side of the brake pedal, at mid-height of the contact surface between foot and pedal. The leftward position avoids interferences in the movement of the driver's right foot between the accelerator pedal and the brake pedal.

For the majority of the brake tests, the accuracy in the measurement of the brake pedal travel given by a properly installed linear displacement sensor is enough, but in other circumstances, such as physical model validation or during the simulation of braking components failure, which require the complete displacement of the brake pedal until it stops against the firewall, the measurement accuracy might be unsatisfactory: in these cases it is possible to correct the error by knowing the geometry of the brake pedal and the installation position of the displacement sensor in the post-process of the acquired data.

3.1.2 Brake Applied Force

The brake pedal force is measured with a force sensor installed on the center of the pedal contact surface. A typical requirement for this sensor application is to provide a measure between 0 and 2000 N with an accuracy of $\pm$0,4 %. Considering that in an emergency braking maneuver the application of the brake pedal is as fast as the driver can, it is important that the sensor is able to withstand impulsive loads and to maintain its accuracy even if applied force is not perfectly centered on the sensor.

Electrically, the sensor is a Wheatstone bridge, in which one of the resistances varies with the applied force. Therefore, the output signal is a voltage which linearly depends on the excitation voltage (the input voltage provided to the sensor) and on the applied force. The resistive nature of the sensor makes it particularly sensitive to temperature variations, therefore the sensor must be designed to provide a temperature compensation and the HVAC system should not provide any airflow to the footwell area, especially when the heater or the air conditioner are used.

3.1.3 Vehicle Speed

The vehicle speed is provided by a GPS (Global Positioning System) receiver: it can be a standalone unit, or be integrated into the Data Acquisition System. Typical requirements for vehicle dynamics are a speed range between 0,1 and 250 km/h with a $\pm$0,1 km/h maximum error and a sample rate of 100 Hz.

The working principle is based on a constellation of satellites orbiting around the planet, each of them is aware of its own position and has an atomic clock for providing an accurate timing signal: this information is periodically broadcasted to the receivers that are in direct line of sight. Assuming a perfect synchronization of the clock of all the satellites, a perfect accuracy

of their position knowledge and that the signals are transmitted at the speed of light, a receiver can triangulate its own position by computing the propagation time of the signals of at least 4 satellites (3 for the position in the three coordinates and 1 for the time information). A higher number of satellites allows to rely on less strict assumptions, increasing the accuracy in the position up to 10-100 m.

A complementary service (WAAS, EGNOS, etc.) made of base stations on Earth and geostationary satellites, is able to augment the accuracy of the GPS system by comparing the position computed by the receivers on the base stations with their actual location, broadcasting additional information which allows to reduce positioning error up to 1-2 m.

It is possible to further improve the position accuracy using the Real Time Kinematic (RTK) positioning, which uses a fixed base station within few kilometers from the mobile receiver to exploit not only the messages transmitted by the satellites, but also the phase of the carrier of their signals, achieving a centimeter level accuracy.

Advanced receivers, such as the ones used in Vehicle Dynamics, can provide accurate velocity measurements by taking advantage of the Doppler effect in the signal transmitted by the satellites and, if available, by the integration of the data provided by the Inertial Measurements Unit in the GPS receiver.

To properly work, the receiver antenna must have direct visibility of the sky, therefore it is usually placed on the top of the roof of the vehicle and measurements should be taken far from tall buildings or other obstacles, which could shadow or reflect the signal.

Figure 27. Roof-mounted GPS antenna and its metallic support.

Moreover, in high dynamic conditions, it must be considered the vehicle pitch and roll, which generate a relative motion between the GPS antenna and the vehicle's center of gravity. For example: during a braking maneuver, the exact moment at which the vehicle stops could be hard to detect, since the rock-back motion of the vehicle body has a velocity component that the GPS antenna detects.

3.1.4 Longitudinal Acceleration

The measurement of longitudinal acceleration is provided by a single axis accelerometer, or by an Inertial Measurement Unit (IMU), which provides longitudinal, lateral and vertical acceleration, together with roll rate, pitch rate and yaw rate. Typical requirements for braking tests are a range of ± 2 g (approx ± 20 m/s^2) and a maximum error of 0,1 %. To decuple the

acceleration measurements from the vehicle body rotations, the accelerometer (or the IMU) must be installed as close as possible to the vehicle center of gravity. Using an IMU it is possible to correct the measurement error due to the offset between the measurement unit and the center of gravity.

Figure 28. Longitudinal acceleration sensor mounted on the fixed part of the front seat slide.

These sensors provide information to the Data Acquisition system using a voltage signal which linearly varies as a function of the measured variable (therefore, for an IMU, six independent voltage signals are transmitted for the accelerations and yaw rates in the three coordinate axes) or using a digital communication protocol, such as CAN Bus.

3.1.5 Vacuum Pressure

The vacuum pressure measure is provided by an absolute pressure sensor with a pressure range between 0 and 2 bar and a maximum error of 0,1 %.

The working principle is similar to the one of the pedal force sensor, in which a strain gauge connected to a Wheatstone bridge varies its electrical resistance as a function of the measured pressure. The output is an analogue voltage signal which depends on the measured pressure and on the excitation voltage provided to the sensor itself. Due to its resistive nature and to the installation position, it is important that the sensor is temperature compensated for the whole range of temperatures reached in the engine compartment.

In the majority of today's vehicles, two sensors are installed for braking tests: one between vacuum chamber of the brake booster and its check valve, the other one between the check valve and the vacuum source. Both sensors must have a connection to the atmosphere which is opened during the initialization of the sensors to have the zero-reference pressure.

If the vehicle uses a vacuum-less brake booster there is no need for these sensors.

3.1.6 Brake Circuit Pressure

The brake circuit pressure is provided by relative pressure sensors with a pressure range between 0 and 200 bar and a maximum error of 0,1 %.

The working principle is similar to the vacuum pressure sensor, while the construction characteristics are necessarily different to withstand the high pressures and for assuring compatibility with the brake fluid.

Brake pressure is measured at the output of the tandem master cylinder and at the wheels. Being virtually all modern passenger vehicles equipped with a diagonal split brake circuit, one

pressure sensor is installed at one of the two output ports of the TMC and at least two wheels of the same side are equipped with the pressure sensor.

In this way it is possible to measure the brake pressure of a front and a rear wheel and, at the same time, the pressure in both lines of the split brake circuit. Performing straight-line brake tests, this configuration is enough to analyze the brake pressures in the whole system, to detect the ABS interventions and the brake force distribution between front and rear wheels.

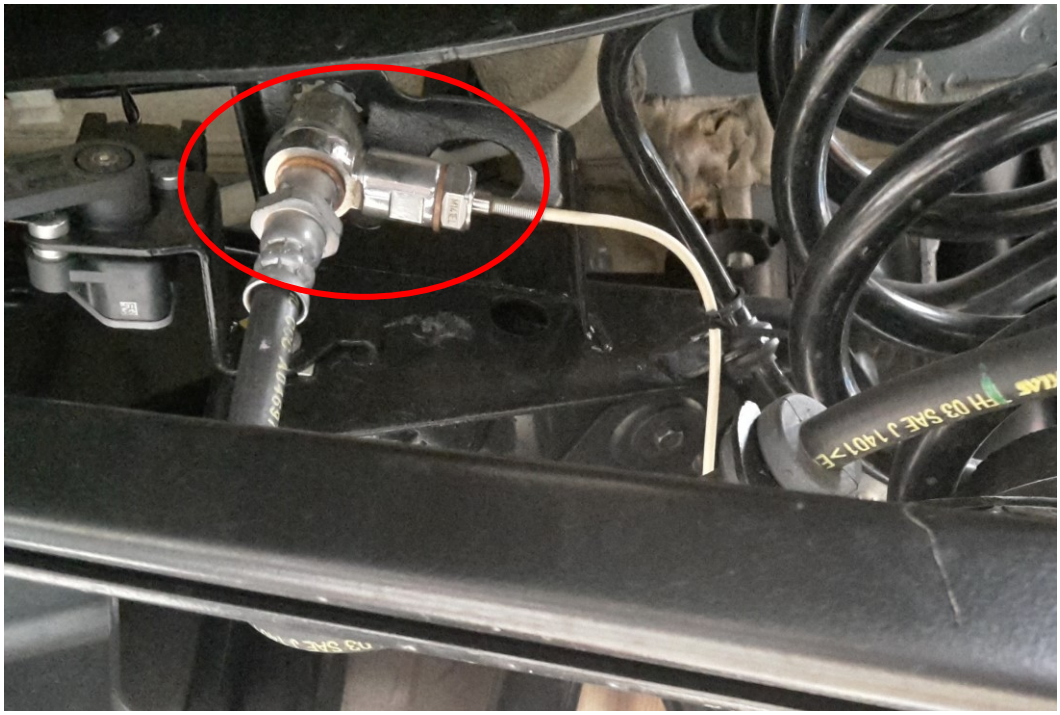

Figure 29. Brake line pressure (circled in red), mounted between the rigid brake pipe and the rubber hose of one of the wheels.

If a deeper analysis of the ABS system is needed, it is necessary to install a pressure sensor for each wheel.

It is worth to note that the ABS cycling during the brake pressure modulation generates high pressure spikes which introduce noise in the pressure measurement: installing the pressure sensors as close as possible to the wheels allows to take advantage of the damping effect of the pipes length and obtain more accurate measurements.

3.1.7 Brake Temperature

The brake temperature is measured using K-type thermocouples, which have a temperature range from – 200 °C to 1260 °C, with a maximum error of ±1,5 °C or 0,4%, whichever is larger.

The brake temperature must be measured on at least one front wheel and one rear wheel. If the vehicle is equipped with disk brakes, the thermocouple is installed in the inner brake pad, in the middle of the contact surface, at 4 mm of depth. The disc temperature is measured in the middle

of its thickness (in the middle of the thickness of the inner disk, if it is a vented disk), at a radial distance which is the average of the inner and outer radius of the contact are between pad and disk. The choice of the inner side is because is the one which reaches higher temperatures, therefore it is more suitable when assessing the cooling ability of the braking system. In the case of a drum brake, the temperature sensor is installed in the middle of the leading show, at a depth of 2,5 mm of the liner. Also in this case the leading shoe has been chosen because it is the most exploited when the vehicle is moving forward.

3.1.8 Wheel Speed

The wheel speed is measured using rotary encoders mounted externally on at least one front wheel and one rear wheel. The speed range should be enough to allow the vehicle to reach the maximum speed, or at least 250 km/h, although it depends on the wheel rolling radius, since the maximum rating of the sensor is an angular velocity. The sensor sends 30 pulses per complete rotation, providing an accuracy similar to the one provided by the ABS wheel speed sensor, but the direct connection between the external wheel speed sensors and the DAQ allows for a very low and known measurement latency, while the information provided by the ABS ECU via the CAN Bus network has a much lower and irregular sample rate, due to the shared and asynchronous nature of the CAN protocol.

3.1.9 Engine Speed and Coolant Temperature

The engine speed and coolant temperature are provided by the Engine Control Unit of the vehicle through the CAN Network. Although this communication protocol is asynchronous and does not provide a very high refresh rate for every variable, in this case the performance is enough, considering the speed at which these variables change and their lower priority in the brake performance measurement.

3.1.10 Data Acquisition System

It is a modular system able to collect, synchronize, store and filter data from all the sensors. It must have at least 8 analog input channels, 15 thermocouple input channels, 5 digital inputs and 1 CAN transceiver. It integrates the GPS receiver and each measured variable must be sample at a configurable rate, up to 2000 Hz for brake tests.

It incorporates a display and a keyboard to set-up the DAQ and configure the system for each brake test, showing the most important measured variables for each maneuver, to help the driver in the correct execution of the test and, at the same time, verify the validity of the data.

Figure 30. Data Acquisition System mounted instead of the front passenger seat.

3.2 Tested Vehicles

The vehicles experimentally tested in this thesis are listed in Table 1. Note that in the list there are both FCA and competitors vehicles.

Vehicle	Segment	Mass [kg]	Powertrain	
1	Crossover	1508	Diesel	77 kW
2	A	1103	Gasoline	63 kW
3	Sport	1742	Gasoline	317 kW
4	C	1431	Diesel	70 kW
5	SUV	1556	Diesel	88 kW
6	B	1238	Gasoline	51 kW
7	A	1031	Gasoline	63 kW
8	Crossover	1447	Gasoline	74 kW
9	Sport	1421	Gasoline	169 kW
10	A	-	Gasoline	51 kW
11	A	1346	Gasoline	63 kW
12	C	-	Diesel	88 kW
13	SUV	1575	Diesel	88 kW
14	Sport	1613	Gasoline	180 kW
15	SUV	1976	Gasoline/Electric	149 kW
16	D	2454	Diesel/Electric	208 kW
17	B	1024	Gasoline/Electric	70 kW
18	B	1448	Gasoline	- kW
19	C	1338	Gasoline	75 kW
20	A	-	Gasoline/Electric	66 kW
21	SUV	-	Diesel	230 kW
22	A	1236	Gasoline	63 kW
23	A	986	Gasoline	66 kW
24	Crossover	1863	Hybrid	165 kW
25	SUV	1657	Gasoline	136 kW
26	A	1172	Gasoline	51 kW
27	B	1290	Gasoline	88 kW
28	SUV	1765	Diesel	100 kW

Table 1. List of experimentally tested vehicles.

3.3 Braking system conditioning

When the braking system is new, or when the friction material (either the stator or the rotor) has been replaced, the braking system is not able to express its full potential, because of two reasons:

- The brake pads or liners, as well as brake rotors, have some surface irregularities that reduce the effective contact surface between the two, since only the most protruding portions of the two components will rub each other, while the hollowest portions of the surfaces will not be able to make any contact.
- The friction material needs to fully cure through the heating process of the brake operation before achieving a stable friction coefficient at the interface between stator and rotor.

Performing a certain amount of brake applications allows to wear out part of the pad/liner until its surface becomes complementary to the one of the rotor, gradually increasing the effective contact area until a full contact is achieved. In the meanwhile, the heat generated by the braking process, increases the temperature of the friction material, allowing its constituents to fully cure, until an almost stable chemical and mechanical condition is achieved.

It is important during this process to avoid excessive temperatures which could cause degradation to the organic components of the liner, as well as to increase its wear rate, which is exponentially dependent on the temperature.

The vehicles analyzed in this thesis have been conditioned performing 200 brake applications from 120 km/h to 80 km/h, with a deceleration of 0,4 g and a load of 50 kg plus the driver. Time between applications depends on the cooling ability of the braking system, but should be enough to ensure that the liners temperature is always below 200 °C.

3.4 Static tests

Once the vehicle has been conditioned, the first test relative to pedal feeling is performed with the vehicle stationary. It consists in pressing the brake pedal with a force that gradually increases up to 50 daN, while all the variables indicated at the beginning of this chapter (except for the ones relative to vehicle motion) are recorded at a sampling rate of 200 Hz.

The tests are performed in various conditions:

- Engine off, brake booster at atmospheric pressure. In this condition, the brake booster is not providing any assistance to the driver, therefore the output pressure at the Tandem Master Cylinder will be the lowest with respect to the force applied to the brake pedal. The performance measured in this condition represents the baseline to compare with when analyzing the assistance ratio provided by the brake booster when it is operative.

Moreover, it is possible to estimate the performance of the braking system in case of brake booster failure.

- Engine at idle, brake booster operative. Before starting the engine, the brake pedal is applied repeatedly until both chambers of the brake booster are at atmospheric pressure, then the engine is started and after a brief time in which the vacuum pressure in the booster stabilizes, the test is performed. The test is repeated with cold and warm engine, as well as with the air conditioning and all the electric devices in the vehicle turned on and off. These 4 combinations influence the engine idle angular velocity and the engine load: these variables influence the maximum level of vacuum achievable in the brake booster, particularly when the vacuum source is the intake manifold of a Spark Ignition engine.
- Engine warm and at idle after high speed operation, brake booster operative. When the engine is operated at high revolutions (4000-5000 rpm) the vacuum level in the brake booster reaches its maximum, both in case the vacuum source is the intake manifold or a crankshaft-driven pump. In the first case the combination of high engine speed and closed throttle valve when the engine is returned to idle generates a significantly higher vacuum in the intake manifold with respect to the engine running at constant speed at idle, while in the second case the achievable vacuum level is slightly dependent on the pump speed.

It is known that the brake booster performance depends on the vacuum pressure applied to it, and that each brake application introduces air to the device, therefore the amount of vacuum available immediately after a brake application is lower, until the optimal value is restored. This is usually not critical, but there might be real driving situations in which the brake application pattern can introduce more air to the booster than the one that can be extracted by the vacuum source, gradually decreasing the booster performance until the driver is forced to significantly increase the effort on the brake pedal to obtain the desired deceleration. An example of this worst-case scenario is a vehicle with a naturally aspirated engine and automatic gearbox, equipped with a conventional brake booster whose vacuum source is the intake manifold of the engine. If this vehicle is driven in a traffic jam, creeping at very low speed with the engine at idle thanks to the automatic gearbox, the stop-and-go driving style combines frequent brake applications with a relatively poor vacuum in the engine intake manifold, which can decrease the brake booster effectiveness. Similarly, a situation in which a vehicle is got out from a parking lot at high altitude above sea level (therefore, low ambient pressure) and with the engine cold, the intake manifold might not be able to provide in a short time an acceptable amount of vacuum in the brake booster, surprising the driver with a brake pedal harder to press than what it used to be.

Of course, these conditions are taken into account during the design process of the braking system, so that they are not a cause of concern for the final user, but specific tests are performed during the validation process of the vehicle, simulating the above mentioned scenarios and monitoring the vacuum pressure in the brake booster, to ensure that it stays within an acceptable range.

With the data gathered from static tests, two main analyses have been performed:

- TMC pressure as a function of Brake Pedal applied Force.
- Brake Pedal Stroke as a function of applied Force.

The behavior of the above-mentioned variables is described in the following paragraphs.

3.4.1 Tandem Master Cylinder Pressure as a function of Brake Pedal applied Force

As a first approximation, it is possible to consider the output pressure at the Tandem Master Cylinder as linearly proportional to the vehicle's deceleration. This is a valid assumption if the friction coefficient of the front and rear brakes is constant, if the grip at the tire-ground contact is enough to express the braking forces without locking the wheels and if the brake-force distribution between front and rear axles is constant. If all these conditions are satisfied, the interaction between pedal force and the TMC output pressure is very similar to the one between pedal force and the vehicle's deceleration.

The components that influence the TMC output pressure as a function of the applied force on the brake pedal are:

- Pedal lever ratio: the higher the ratio, the higher the pressure/force ratio
- TMC section area: the higher the area, the lower the pressure/force ratio
- Brake servo boost ratio: the higher the boost ratio, the higher the pressure/force ratio.

It is worth to note that the first two parameters (pedal lever ratio and TMC section area) have a direct influence also on the pedal stroke: any change in these two components that increases/decreases the pressure/force ratio will also increase/decrease the pedal stroke in direct proportion.

On the other side, the brake booster is able to increase the pressure/force ratio without affecting the pedal stroke.

An example of a typical TMC pressure curve as a function of the brake pedal force in a conventional braking system is shown in Figure 31, with and without the assistance of the brake booster.

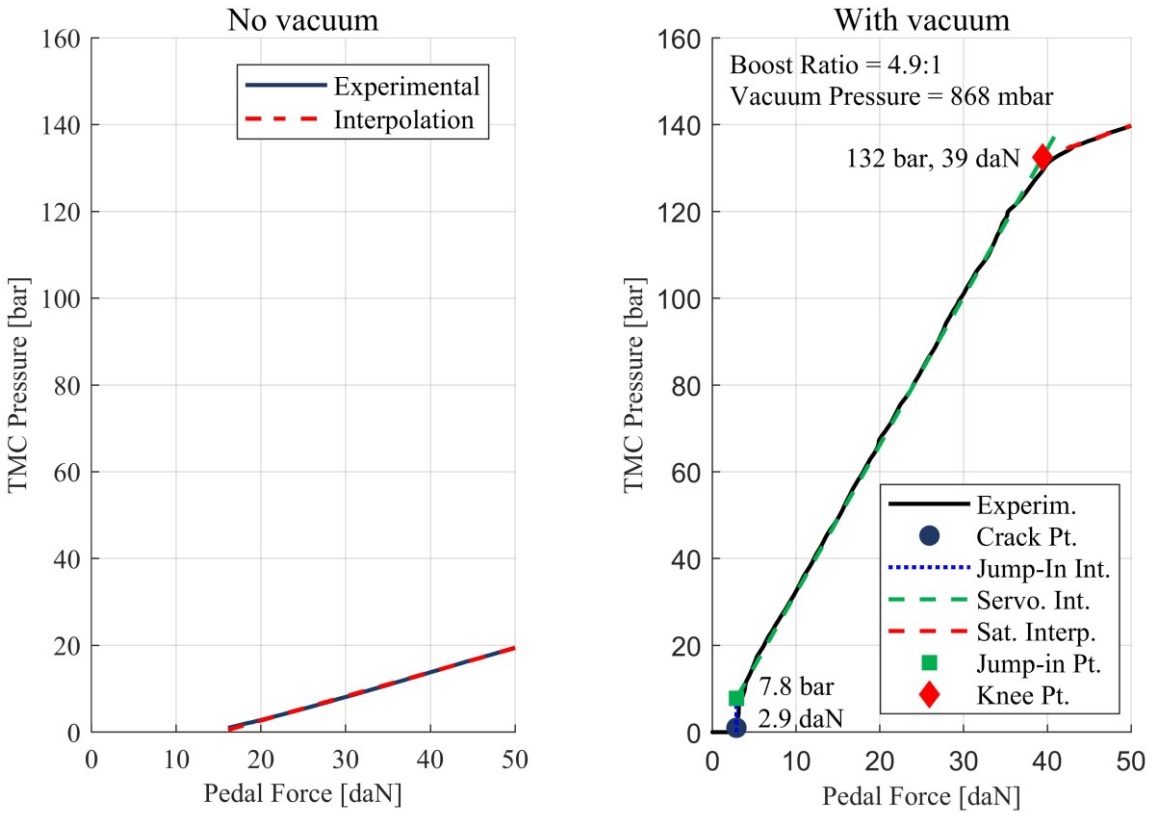

Figure 31. Tandem master cylinder pressure vs. applied force on the brake pedal without the contribution of the brake booster (left) and with the contribution of the brake booster (right).

From the test with the brake booster inoperative it is possible to make a linear interpolation of the Tandem Master Cylinder output pressure as a function of the Brake Pedal Force. This allows to obtain the minimum effort necessary to produce an output pressure from the Tandem Master Cylinder and the slope of the curve, which represents the ratio between the increment of TMC pressure as a function of the increment of applied force to the brake pedal.

When the brake booster is operative, the relation between pedal effort and TMC pressure is not anymore linear, but becomes representative of the relation between input and output force at the brake booster. The minimum force necessary to generate an output pressure at the TMC is much lower with respect to the case without servo assistance and the point at which it happens (2,9 daN, 0 bar) is defined as crack point. This is the effort necessary to close the communication valve between the front and the rear chamber of the brake booster. Any further effort allows to open the admission valve, which connects the rear chamber to the atmosphere, increasing its pressure and generating a force to the TMC which is translated into an output pressure. The pedal effort remains almost the same until a certain amount of TMC pressure is

reached (7,8 bar, in this case), when the servo plunger starts to contact the reaction pad. The operative point at which this happens (2,9 daN, 7,8 bar) is called jump-in point. From now, the TMC pressure becomes proportional to the pedal effort, showing a new operative region between points (2,9 daN, 7,8 bar) and (39 daN, 132 bar) which is defined as assistance region. In this condition the brake booster is assisting the driver amplifying the force he applies on the brake pedal, increasing the pressure in the rear chamber (and, therefore, the booster force) as long as the pedal effort increases. Comparing this part of the curve to the one of the figure on the left, it is immediate to note the difference in slope: the ratio between the two slopes is the amplification factor, or the boost ratio, provided by the brake booster. This region ends when the rear chambers reaches atmospheric pressure, achieving the maximum booster force allowed by the vacuum pressure available in the front chamber. From this point, any further increment in pedal effort is directly translated into TMC pressure, without any additional contribution from the brake booster, whose force remains constant. From the graph, it is possible to note this observing the change of slope, which becomes equal to the one of the left picture, where there is no booster contribution. The point at which the slope changes is named knee point, while the region beyond it is defined as saturation region.

As it has been shown in Chapter 2 during the description of the brake booster, this curve depends mainly on the difference between the atmospheric pressure and the pressure in the front chamber: the higher the difference, the higher the position of the knee point along the assistance line. Therefore, for a given braking system, the pedal effort necessary to achieve a certain level of TMC pressure depends mainly on the atmospheric pressure and on the vacuum pressure in the front chamber of the brake booster.

3.4.2 Brake Pedal Stroke as a function of applied Force

The movement of the brake pedal under the force applied to it, is the consequence of the internal clearance and of the compliance of the various components of the braking system.

Each component of the braking system absorbs part of the volume of the brake fluid, which can be quantified directly in volume units, or be transformed in pedal stroke length, dividing the volume by the section area of the TMC. The sum of the absorptions of all the components of the braking system determines the total absorption and, consequently, the pedal stroke.

Starting from the brake pedal, the bending moment generated by the force application produces an elastic deformation which is directly proportional to the applied force. Inside the brake booster, the stroke/force ratio is highly nonlinear, because it depends on the clearances of the communication and admission valves, on the stiffness of the internal springs, on the compliance of the reaction pad and on its distance from the plunger. The TMC has an initial dead stroke in which no pressure can be generated until the connection between the two chambers and the reservoir is closed, after which it has a small compliance proportional to the generated pressure.

The brake pipes and the ABS/ESP modulator also have a small fluid absorption proportional to the fluid pressure. The hose that connects the rigid pipes to the brake caliper (or to the drum brake) also contributes to the fluid absorption, usually in a non-linear manner, which also depends on the brake fluid temperature, due to the high content of rubber, whose stiffness is strongly affected by its temperature. The last three contributions to the fluid absorption are given by the bending compliance of the brake caliper, by the clearance between brake pad and brake rotor, and by the temperature-dependent compliance of the brake pad.

The result of all these contributions in terms of pedal stroke as a function of pedal effort is visible in Figure 32.

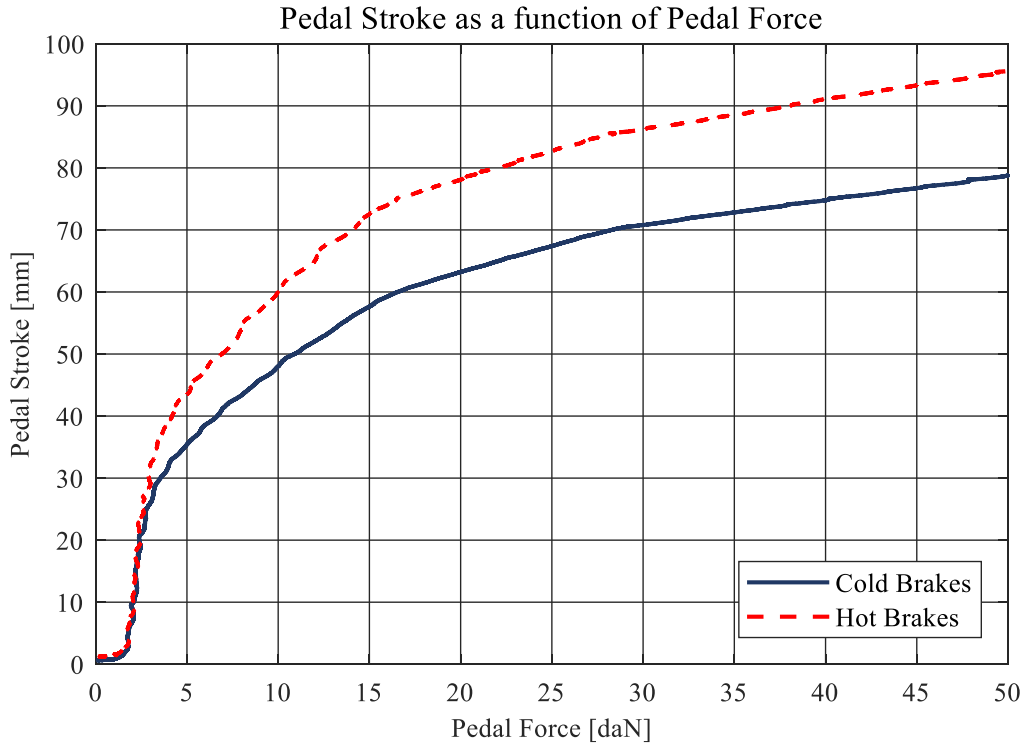

Figure 32. Brake pedal stroke vs. applied force with cold brakes and hot brakes.

The results of Figure 32 have been obtained a test performed with the brakes at ambient temperature and it has been repeated shortly after an AMUS brake test. As it will be described later, the AMUS brake test consists in 10 emergency braking maneuvers from 130 km/h up to a complete stop, repeated in the shortest time possible. The huge amount of heat generated during this test increases the brake rotors temperature up to 600-700 °C. Also, the brake pads suffer a high increase in their temperature, which determines a heat transfer to the brake fluid and, consequently, to the rubber hoses close to the wheels.

The temperature increase affects the compressibility of the brake pads, as well as the flexibility of the rubber hoses, which determine, in this case, an increase in the pedal stroke by 20-25 % with respect to the test with cold brakes.

From a pedal feeling point of view, the fact that the pedal stroke increases with the brakes temperature, together with an increased sensation of sponginess of the pedal, is perceived as a weakness of the braking system, being unable to withstand the demanded performance without showing the symptoms of thermal stress. On the other side, a brake pedal whose feeling is completely independent from the brake temperature might not warn the driver of an imminent boiling of the brake fluid, with a total loss of braking force. The final choice of the temperature influence on the pedal stroke depends on the vehicle manufacturer know-how and on the mission of the vehicle.

3.5 Dynamic Tests

The primary objective of the braking system is to reduce the vehicle speed and the static tests are not able to show the ability of the vehicle in fulfilling this task. Within the vehicle dynamics requirements of every vehicle it is reasonable, if not mandatory, to include the possibility to finely modulate the vehicle deceleration through the action on the brake pedal, and the ability to exploit the maximum tire-ground grip coefficient to minimize the stopping distance in emergency situations. The following described tests will show how these features are assessed and the main parameters of influence.

3.5.1 Progressive Braking

The progressive braking test consists in braking a vehicle from the speed of 120 km/h, increasing the vehicle deceleration as linearly as possible until the maximum value – typically limited by the tire-ground grip coefficient – is achieved in 6 seconds, while the vehicle speed is still above 30 km/h. At least 0,85 g of deceleration must be reached before locking the wheels. The maneuver can be performed either by a human driver or by a robot that acts on the brake pedal: in any case, the closed-loop control of the brake pedal force to obtain a linear deceleration increase over time is quite challenging, requiring some training for the human driver and a fine PID tuning for the robot. The final choice depends on the know-how and on the tools available at the testing facility, keeping in mind that the learning curve of a skilled driver is faster, while the high accuracy and repeatability of the robot requires longer installation and tuning times. The vehicles analyzed in this thesis have all been tested by experienced human drivers.

The test is performed at various temperature levels, from the lowest to the highest, considering the temperature of the front discs at the beginning of the maneuver as the reference value. Before passing from a temperature level to the next one, at least three correct repetitions must have been done. Once the test at the highest temperature has been completed, the brakes are cooled down and a further test at low temperature level is performed, to check if there has been any permanent change in the friction material after the thermal cycle: this further level is named with the temperature value, followed by the word “recovery”.

In the recent past, the temperature levels were: 50 °C, 100 °C, 150 °C, 200 °C, 250 °C and 100 °C *recovery*. Nowadays the stress requirements have increased, therefore the temperature levels are: 50 °C, 100 °C, 200 °C, 300 °C, 400 °C and 100 °C *recovery*. The majority of vehicles analyzed in this thesis have been tested with the new methodology, with a few vehicles tested only with lower temperatures. For what concerns the temperature level at 50 °C, it is particularly time-consuming to cool down the brakes in order to perform the three repetitions, because of the high ambient temperatures and/or because of the residual braking torque which generates heat even if the brakes are not applied: for this reason, the number of repetitions has often been only one or two.

In Figure 33, a single measurement of a tested vehicle is shown.

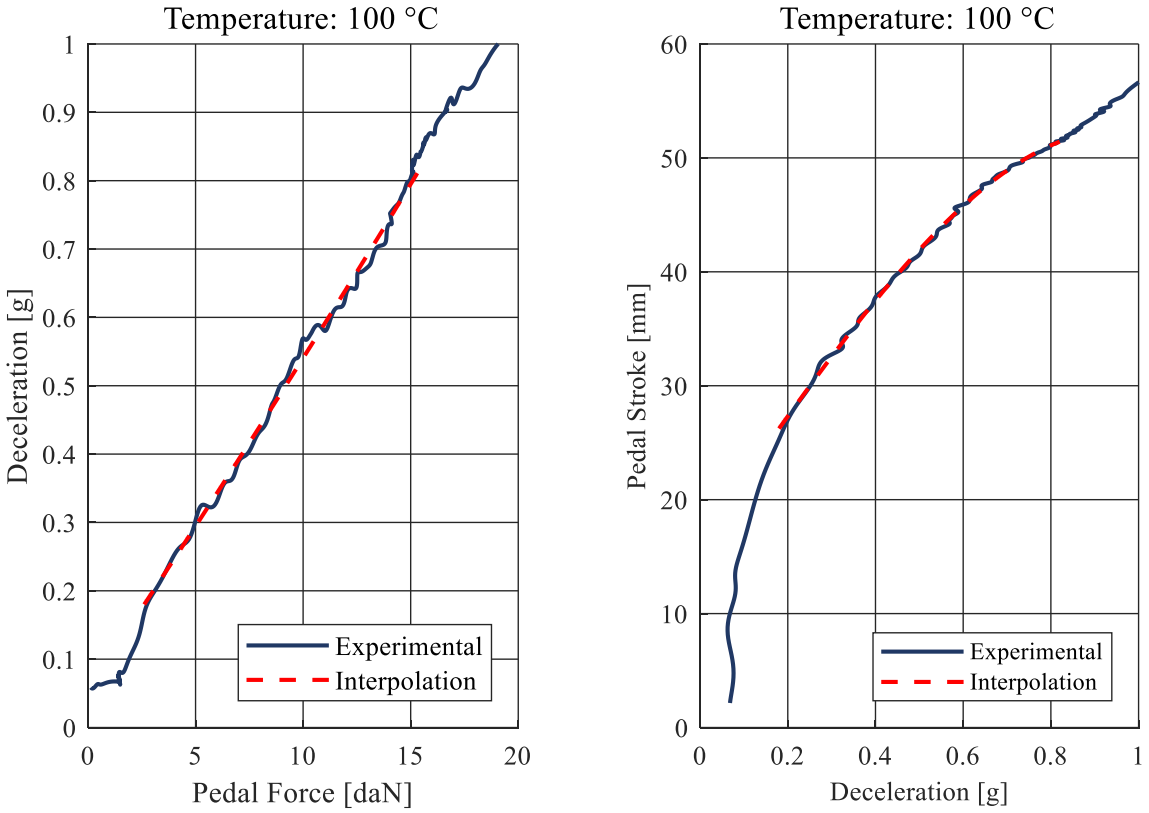

Figure 33. Measurement of the vehicle deceleration vs. brake pedal force (left). Measurement of the brake pedal stroke as a function of the vehicle deceleration (right).

Figure 33 on the left shows the deceleration of the vehicle as a function of the pedal force, while, on the right, shows the pedal stroke as a function of the deceleration. The range of interest is the one in which the deceleration is between 0,2 and 0,8 g. The choice of the range of deceleration depends on the fact that, being the initial speed of the test 120 km/h, the dissipative forces of the vehicle (in particular, the aerodynamic force) generate a significant deceleration even if the vehicle is not braked: this is visible from the plots shown, observing that they don't intersect the origin of the axes. A finer analysis of the pedal feeling for low decelerations is

obtainable by a similar test, in which the initial speed is 50 km/h and the maximum deceleration achieved is 0,4 g: such test was not available at the time of this work, therefore it has been neglected. For what concerns the higher end of the deceleration, the probability of locking one or more wheels at decelerations above 0,8 g increases significantly, therefore this limit allows to have more repeatable results.

Both plots have been interpolated with a least-square polynomial fit: a second order polynomial has been used for the deceleration-force curve, while a third order polynomial has been used for the stroke-deceleration curve. For all the tested vehicles this interpolation methodology has been valid between 0,2 and 0,8 g of deceleration, with coefficients of determination R^2 above 0,95. In some circumstances the interpolation was not able to fit well the curve and it has been chosen to discard the maneuvers in which this happened, because a deeper analysis of the maneuvers in which this phenomenon occurred has shown that the application of the brake pedal was incorrect, leading to sudden changes in the vehicle deceleration and showing results excessively different from the average of the vehicle.

Besides the shape of the curve, the values of pedal force and stroke necessary to develop decelerations of 0,2 – 0,4 – 0,5 – 0,6 – 0,8 g have been recorded, with the purpose of a quick comparison between different vehicles.

Considering that for each temperature level at least three repetitions should be done, when the number of repetitions is three or less than three, the results are averaged, both in terms of polynomial fit coefficients and in terms of absolute force/stroke values at the predetermined deceleration levels. If the number of repetitions is higher than three, the combination of three repetitions which are better fitted by a common polynomial are selected for computing the result.

Figure 34 shows the result obtained from the combination of three repetitions at the same temperature level.

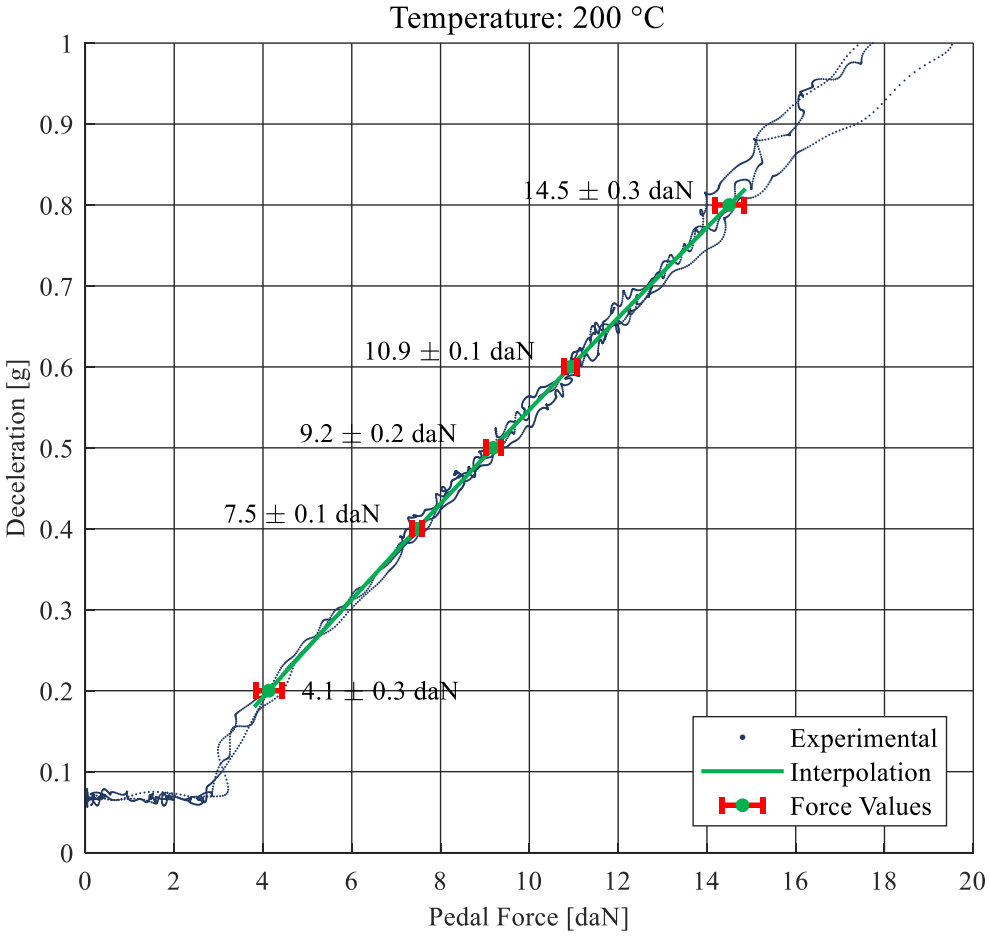

Figure 34. Interpolation of the vehicle deceleration vs. brake pedal force from 3 repetitions of a progressive braking maneuver.

From Figure 34 it is possible to see the superimposition of the three acquisitions, together with the green line which represent the polynomial fit, obtained from the average of the coefficients of the fit of the single curves.

The values of force at the decelerations of 0,2 – 0,4 – 0,5 – 0,6 – 0,8 g are also represented, together with their standard deviation.

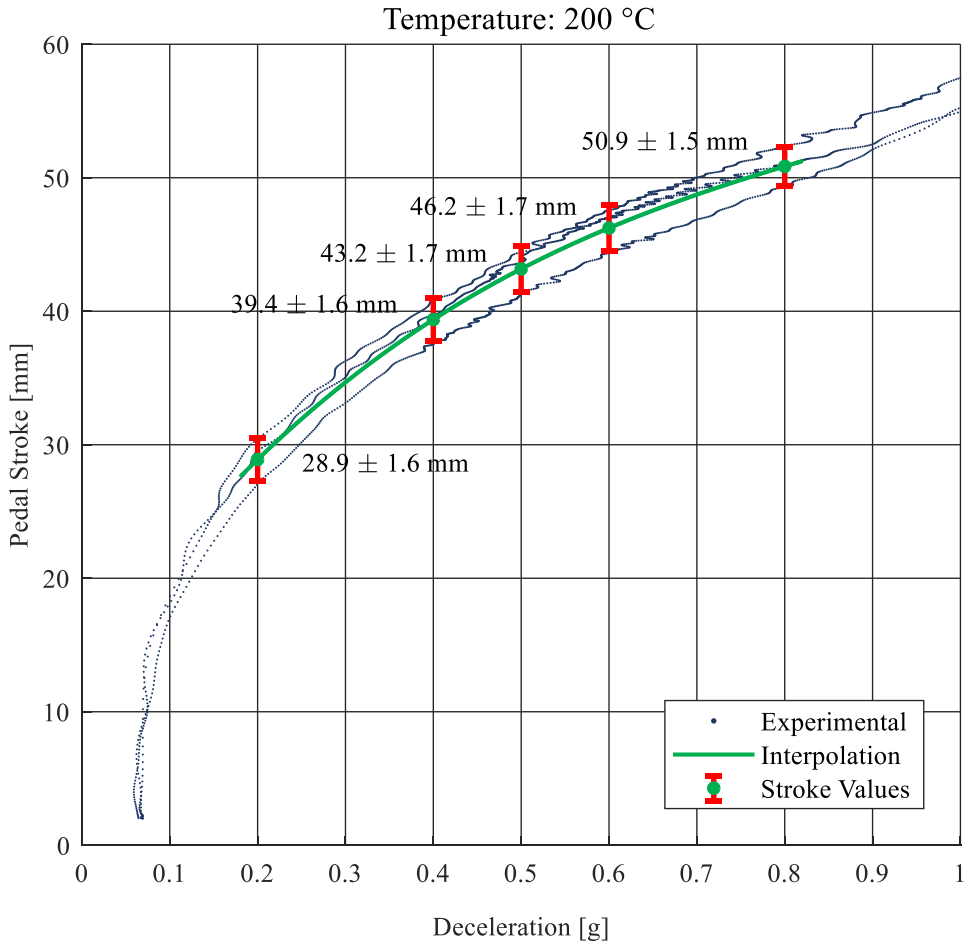

Figure 35. Interpolation of the brake pedal stroke as vs. vehicle deceleration from 3 repetitions of a progressive braking maneuver.

In the analysis of the pedal stroke as a function of the vehicle deceleration, the methodology of representation of the results is the same.

Since the test is performed at different temperatures, it is useful to compare how the same vehicle changes as the temperature increases.

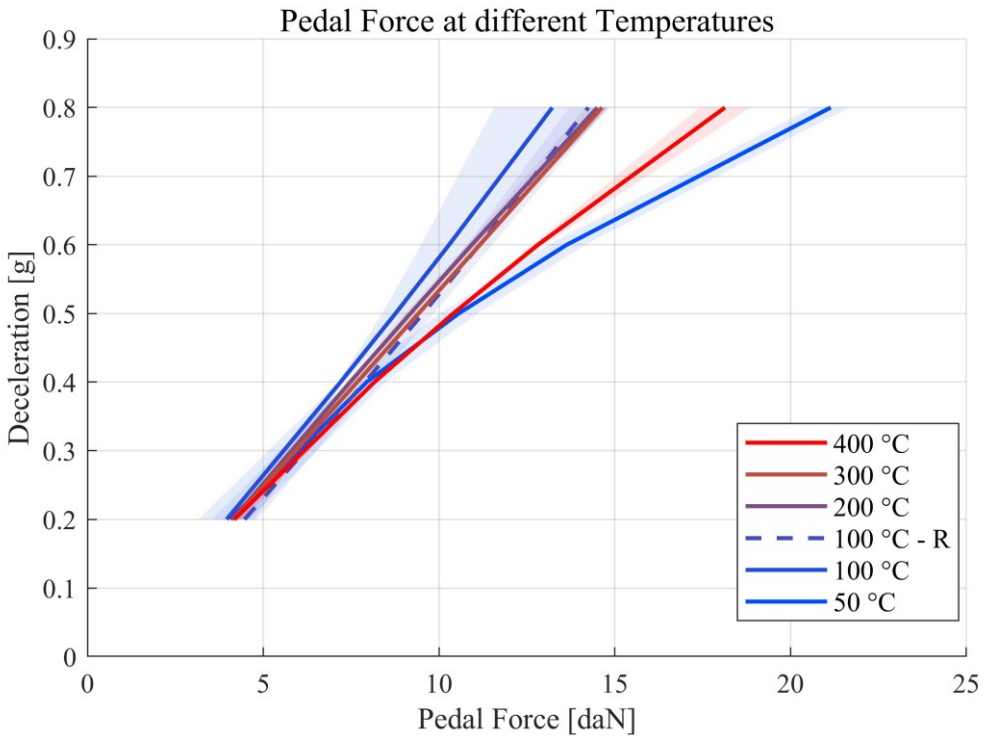

Figure 36. Interpolated results of the vehicle deceleration vs. brake pedal force at different brake temperature levels.

Looking at the deceleration as a function of the pedal force in Figure 36, the first outcome is that, for this vehicle, the results between 100 °C and 300 °C are very similar, with a significant increase of the pedal force at the highest decelerations from an initial temperature of 400 °C. It is important to remember that the reference temperature is measured at the beginning of the maneuver and that the deceleration is linearly increased as the vehicle slows down, therefore the higher deceleration levels are usually expressed by a braking system whose temperature is 100-150 °C higher with respect to the beginning of the maneuver. If the vehicle is not a sports car, it is typical to see a degradation in the friction coefficient between brake stators and rotors when the temperature is above 350-400 °C.

Another important result is noting that there is minimum difference between the initial performance at 100 °C and the performance at 100 °C after having completed the test cycle, this means that, even after having experienced some fading, the braking system has not suffered a permanent damage.

For what concerns the test at 50 °C, it is very common to have results not coherent with the rest of the values at different temperatures: when the friction material is very cold, its performance may be impaired.

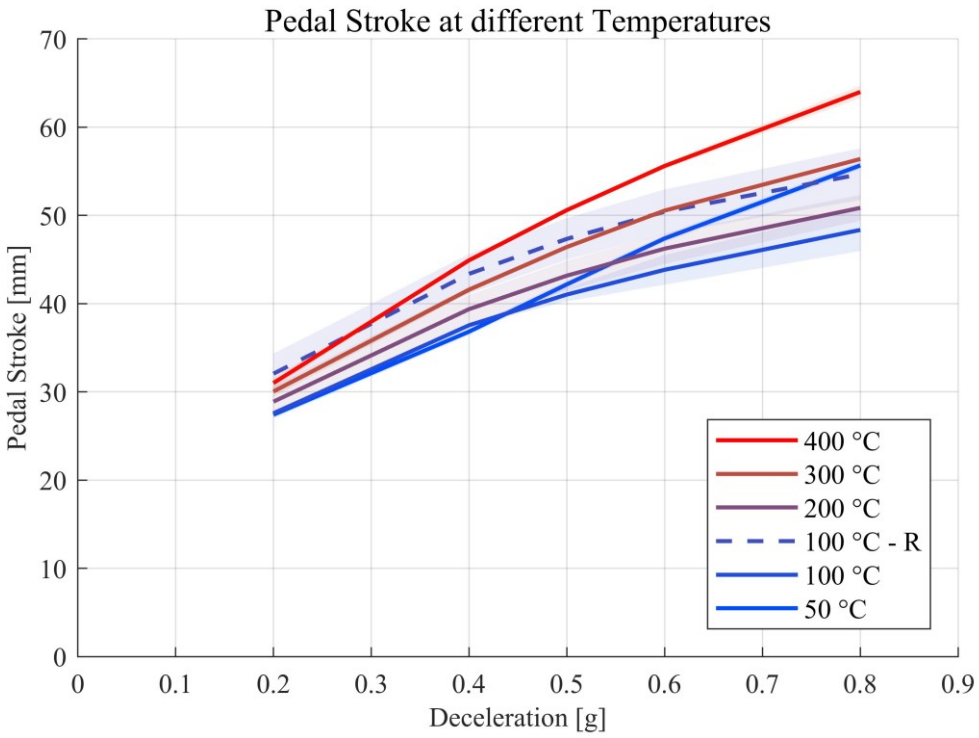

Figure 37. Interpolated results of the brake pedal stroke vs. vehicle deceleration at different brake temperature levels.

In Figure 37, the stroke as a function of the vehicle deceleration is analyzed at the different temperatures. In the range from 100 °C to 400 °C the pedal stroke gradually increases in the whole range of decelerations, with a higher dispersion as the deceleration increases. This is a common behavior, since the brake pads become more compressible as the temperature increases, as well as the rubber hoses connecting the rigid brake lines to the brake calipers tend to expand more under the effect of the brake fluid pressure, when its temperature is increased. Once again, the behavior at 50 °C is inconsistent with the rest of the results.

For what concerns the behavior at 100 °C after the complete cycle – named "100 °C - R" – it shows a longer pedal stroke with respect to the initial test performed at the same temperature. This does not necessarily indicate a permanent modification of the pedal feeling: since the test is repeated as soon as the front discs temperature drops from 400+ °C to 100 °C, the brake pads and the brake fluid, whose thermal inertia is higher than the one of the discs, might still be at a higher temperature with respect to the one at the beginning of the test.

3.5.2 Emergency braking

Keeping in mind that the possibility to modulate the vehicle deceleration is a legal requirement, it is reasonable to assume that the differences between one vehicle and another are not of a safety concern, but they can influence, sometimes significantly, the comfort, the perceived quality and the driving pleasure of a vehicle. On the other side, the maximum deceleration

achievable belongs to the safety field of a vehicle and it is immediate to conclude that the higher the deceleration, the safer is the vehicle.

Since the introduction as a standard equipment for all the new passenger vehicles of the Anti-lock Braking System combined with the Electronic Brake-force Distribution, the design process of the braking system has focused in providing enough brake force to completely exploit the grip of the four tires in any loading condition, creating the ideal conditions for the ABS/EBD to minimize the stopping distances while maintaining the vehicle stability and steerability. For this reason, the maximum deceleration and the stopping distances are mainly influenced by the friction coefficient at the tire-ground contact and by the tuning of the ABS.

While the methodology of the stopping distance assessment is widely known, consisting in stabilizing the vehicle at a certain speed and then suddenly applying as much force as possible to the brake pedal until the vehicle stops, the criterion used to measure the mean deceleration and the stopping distance is more heterogeneous, since various standards and regulations suggest different methods.

The objective of this thesis, for what concerns the stopping distances, is to find a correlation between an objective measurement and a subjective evaluation, therefore, the reference chosen for the measurement of the stopping distances are two widespread automotive magazines, which assign a numeric evaluation to the braking system considering, among other factors, the stopping distances. The two magazines used as a reference are the Italian *Quattroruote* and the German *Auto Motor und Sport*.

Stopping distances have also been measured for all the vehicles analyzed in this thesis, but the results obtained, were too different with respect to the values obtained by the magazines, because the tires used were different, the asphalt grip and temperature were different and probably even the rate of application of the maximum force to the brake pedal was different, since the drivers and their training are not the same.

Apart from the stopping distances on dry asphalt, other emergency braking maneuvers include the emergency braking on a split surface in which the left and right side of the vehicle are running on different surfaces: in one case there is wet asphalt on one side and a surface which reproduces the friction coefficient of ice on the other side; in another test there is dry asphalt on a side and dry setts on the other side. The aim of these “μ-split” tests (being μ the symbol typically used to define the friction coefficient) is to assess the ability of the ABS to achieve short stopping distances while maintaining the vehicle stability even if a yawing torque is generated from the difference in longitudinal force among the two sides of the vehicle. The surface irregularity of the setts paving, moreover, causes the wheels on this surface to bounce repeatedly, alternating moments in which the tire in not in contact with the ground, to other

ones in which it has a high grip on the ground: this friction oscillation can interfere with the cyclic brake-force modulation of the ABS, impairing the braking effectiveness.

A further test performed by both magazines is the repetition of 10 emergency braking maneuvers on dry asphalt in the shortest possible time, to see if the braking system shows symptoms of fading under a prolonged stress. The test conditions vary whether the maximum vehicle speed is higher than 180 km/h or not: if it is higher, the initial speed is 130 km/h and the vehicle is loaded with 2 passengers + 20 kg; if it is lower, the initial speed is 100 km/h and the vehicle is fully loaded.

For all these tests, the braking distance measurement considerations are the same, therefore a description of the methodology needed to fulfill this task, will be provided in the following paragraphs.

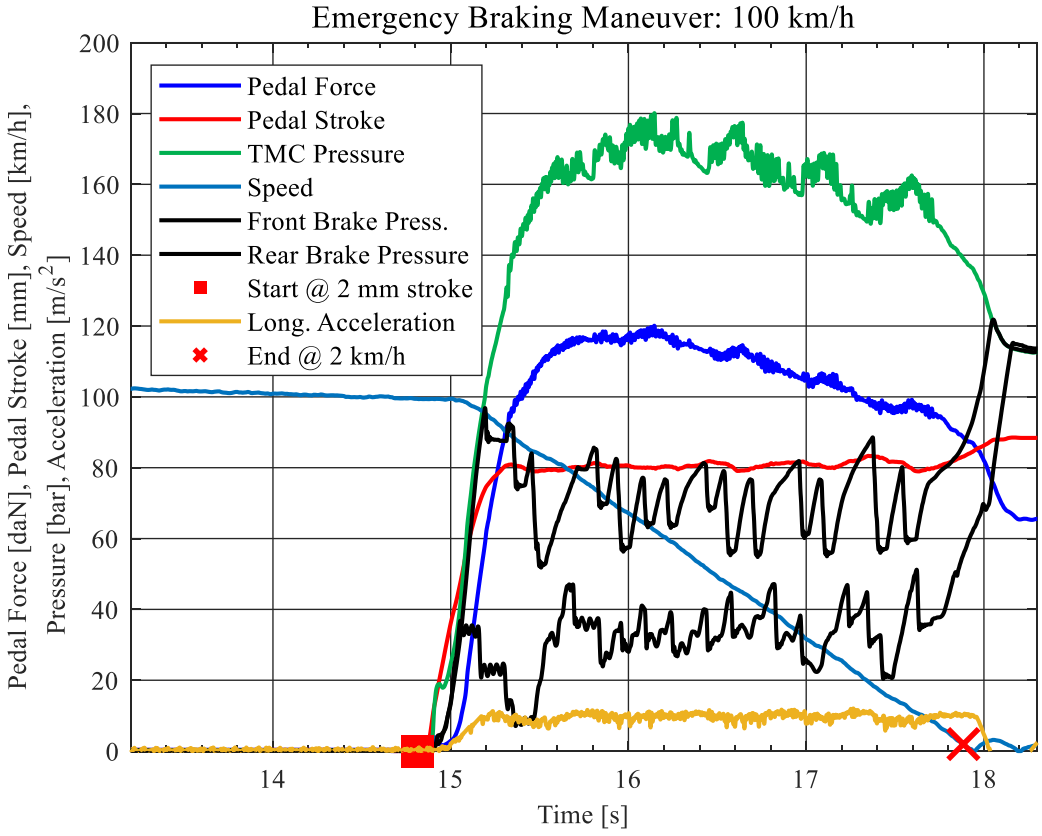

Figure 38. Time evolution of the brake pedal force and stroke, tandem master cylinder pressure, front and rear brakes pressure, longitudinal acceleration and vehicle speed during an emergency braking maneuver.

In Figure 38 are represented the main variables involved in an emergency braking maneuver and their evolution over time.

In this specific test, the initial speed was 100 km/h, it is possible to note that the driver has applied more than 100 daN of force on the brake pedal, far more than the necessary to trigger the ABS, whose activity is visible by the oscillating pressures measured at the front and rear

calipers, much lower than the one measured at the TMC output. It is also visible that the deceleration of the vehicle needs some time to build up, before reaching a quasi-constant value until the vehicle stops: this is one of the reasons why there are different methods in the measurement of the stopping distance and why they provide very different results.

The marker “End @ 2 km/h” indicates when the measurement of the stopping distance ends. The choice of interrupting the measurement at a very low speed, such as 2 km/h, instead of when the vehicle comes to a halt, does not introduce a significant error in the distance measurement, but it is very useful when the speed and distance are measured by a GPS device, because the roof-mounted antenna is not able to discriminate between the whole vehicle translation and the body rotation from the pitched state assumed during the braking and its normal state when it becomes stationary. This effect is well visible in Figure 38, where the measured speed comes to a very low when the vehicle stops and then increases again due to the body pitch motion, until it finally becomes zero. To provide an idea of the magnitude of these errors, the interruption of the distance measurement at 2 km/h, assuming a deceleration of 10 m/s^2, shortens the braking distance by 1,5 cm, much less than the measurement accuracy; including the pitch-back of the body in the measurement increases the braking distance of more than 10 cm. Moreover, the first error can be easily compensated during the correction of the braking distance as a function of the nominal initial speed instead of the actual initial speed, while the second error is much harder to manage.

When it comes to choose the starting point of the distance measurement, the variety of options and the variability of the final results become very high, therefore it is almost impossible to compare stopping distances measured with different methods. Two different methods, among the most commonly used, will be described.

If the objective is to measure the braking distance in the most complete way, including the initial transitory phase in which the deceleration is built up, the starting trigger should be as early as it is possible to determine the action of the driver on the brake pedal. In this case, the displacement by 2 mm of the brake pedal, distance which is equivalent to the stroke of the electric switch that activates the stop lights of the vehicle, is used to determine the start of the braking action. Similarly, a load cell on the brake pedal can be used to provide a trigger when the driver’s foot touches the brake pedal. The choice of the trigger, as well as the sampling rate of the signal that determines the start of the braking maneuver is critical, because even the smallest time delay influences the measured distance: a timing error as small as 50 ms at a speed of 100 km/h generates an error of 1,4 m in the final result.

To better understand the issues in the determination of the starting point, it is possible to look in detail the time evolution of the input signals at the beginning of the braking maneuver.

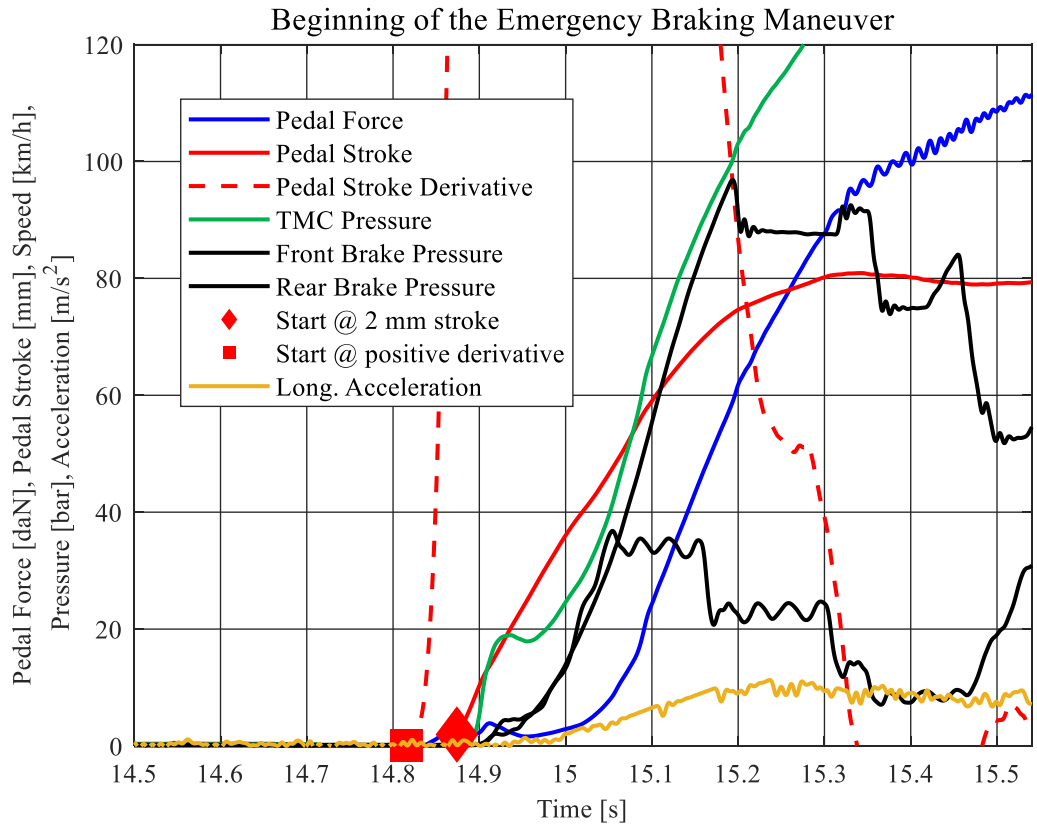

Figure 39. Close-up of the initial moment of an emergency braking maneuver, illustrating the time evolution of the brake pedal force and stroke, tandem master cylinder pressure, front and rear brakes pressure, longitudinal acceleration and the time derivative of the brake pedal stroke.

Figure 39 shows a detail of Figure 38 with, in addition, the time derivative of the pedal stroke: the moment in which it becomes positive is the moment in which the brake pedal starts to move under the effect of the applied force. The delay between this very first moment, and the moment in which the pedal moves by 2 mm is, in this case, approximately 50 ms, with the measurement error consequences previously mentioned. It is evident that placing the trigger at 1, 2 or 3 mm of stroke makes a significant difference. Similar conclusions are possible if the measured variable is the applied force on the pedal.

As a further error source, particularly in the case of magazines assessments, whose evaluation can influence the sales of a vehicle, if the magazine's tester uses a vehicle's signal to detect the start of the braking maneuver, such as the voltage potential at the stop lights or a message in the CAN Bus network, an unfair manufacturer could implement a test-beating software in the vehicle that recognizes a braking test and delays the propagation of the measured signals by an amount of time small enough to not be detected by the tester, but sufficient to start the distance measurement 1-2 m after the actual starting point.

A workaround which provides more reliable and repeatable results is to measure the Mean Fully Developed Deceleration MFDD, which is required by some regulations and it is performed by

other car magazines. It consists in measuring the deceleration when it has already stabilized, typically starting at the 80% of the initial speed and ending at the 10% of the initial speed. From the MFDD and the initial vehicle speed it is possible to compute the braking distance. In this case, such distance will result to be lower with respect to the one measured from the very beginning, because it does not consider the initial transitory in which the deceleration has to ramp-up and the ABS needs to seek the optimal performance.

Whichever is the method used, the time evolution of the traveled distance $S(t)$ can be computed as the time integral of the vehicle speed $V(t)$:

$$S(t) = \int V(t)dt \tag{3.1}$$

This is typically internally computed by the GPS receiver or by the Data Acquisition System as an array of travelled distance values as a function of time. Being an indefinite integral, the actual value of the travelled distance can be offset by a constant, therefore this information is useful if it is used to compute the travelled distance between two time instants.

If the method of the Mean Fully Developed Deceleration MFDD is used, it is possible to compute it using [3]

$$\text{MFDD} = \frac{V_\text{b}^2 - V_\text{e}^2}{2\,(S_\text{e} - S_\text{b})} \tag{3.2}$$

where:

V_0 = initial vehicle speed,
V_b = Vehicle speed at 0,8 V_0,
V_e = Vehicle speed at 0,1 V_0,
S_b = travelled distance between V_0 and V_b,
S_e = travelled distance between V_0 and V_e.

Knowing the MFDD, the braking distance D_MFDD is computed as

$$\text{D}_\text{MFDD} = \frac{V_\text{nom}^2}{2\ \text{MFDD}} \tag{3.3}$$

where V_nom is the nominal initial speed of the braking maneuver. To ensure accurate results, the actual initial speed V_0 should be equal to $V_\text{nom} \pm 2\ \%$.

If it is preferred to take into account of the initial transient of the braking maneuver, if the time t_1 at which the maneuver starts and the time t_2 at which the maneuver ends are recorder, the braking distance between the two triggers is D_trig

$$D_{trig} = S(t_2) - S(t_1) \tag{3.4}$$

If a distance vector is not available, but it is only possible to use the time history of the vehicle speed, the same result is obtained using

$$D_{trig} = \int_{t_1}^{t_2} V(t)dt \tag{3.5}$$

Being V_1 the initial speed of the vehicle speed at the time t_1 and V_2 the final speed of the vehicle speed at the t_2, it is possible that V_1 does not coincide with the nominal initial speed V_{nom}, as well as that the final speed V_2 is slightly higher than zero. A compensation of these errors is possible, combining Equations 3.2 and 3.3 to obtain the corrected braking distance $D_{trig,c}$

$$D_{trig,c} = D_{trig} \frac{V_{nom}^2}{V_1^2 - V_2^2} \tag{3.6}$$

4. Subjective Evaluation and correlation with Objective Measurements

To understand how the interactions between pedal force, stroke and vehicle deceleration influence the brake pedal feeling, it is necessary to collect data about the subjective evaluation of the pedal feeling from experts and normal drivers, to find possible correlations between the objective measurements on the braking system and the driver's perception.

The collection of data about the subjective feeling of the brake pedal has been done using the evaluations on the braking system of two of the most widespread automotive European magazines: the Italian *Quattroruote* and the German *Auto Motor und Sport*. The evaluations and the rating of these magazines have a role in the customer perception of the appeal of a new vehicle, influencing the sales of the reviews models. For this reason, automotive manufactures follow closely the test methods of the most widespread magazines and their evaluation criteria, including in the design process of their vehicles the fulfillment of the same tests the magazines will perform when the vehicle will be on the market, to ensure good ratings.

As the evaluation of the vehicles provided by the automotive magazines is done by experts, it is necessary to consider also the perception of common drivers, the actual users of the vehicles, because they are the customers of the vehicle manufacturer and their satisfaction is fundamental for building customer loyalty and increase sales. To this purpose, a customer interview performed between March 2016 and July 2017 involving the owners of new vehicles within six months from their purchase, has been used to gather additional information on the pedal feeling.

The obtained data will be compared with previous studies, to verify the consistency of results.

4.1 Auto Motor und Sport

Auto Motor und Sport, frequently referred to as AMS or AMUS, is a German magazine, first issued as *Das Auto* in 1946 and now published every two weeks. The number of copies sold in Germany and abroad, thanks to the various international versions made available even outside Europe, combined with the thorough and scientific testing methodology used in their reviews, makes AMUS a reference source of information of car enthusiast and people willing to be prepared before buying a new vehicle.

Every new issue of the magazine, in addition to providing news, motorsport updates and investigations related to the automotive field, contains detailed reports on a small number of vehicles recently launched in the market, with the aim of testing their features and comparing their performance against similar vehicles.

To do so, the comments of the journalist in the test article are supported by the results of measurements of the vehicle dynamics performance and of its fuel economy, and by a numerical evaluation of the various aspects of the vehicle, providing an individual score to each characteristic and an overall rating determined by the sum of the individual scores: such report is useful to easily compare different vehicles.

A total of 650 points can be assigned to each vehicle: 500 of them related to the vehicle itself and its driving characteristics, 50 to its environmental impact and 100 points for the costs of ownership.

The 500 points assignable to the vehicle are divided into five sub-categories, each one worth 100 points:

- Chassis: evaluates the roominess, dimensions and versatility of the vehicle, as well as the equipment and the quality of manufacturing;
- Safety: evaluates how many safety devices are present in the vehicle, the performance of the headlights, the braking performance and the driving safety;
- Comfort: evaluates the ability of the suspensions to filter the road asperities, the comfort of the seats, the infotainment and other devices that enhance the ride comfort, the climate control system and the acoustic comfort of the vehicle;
- Drivability: evaluates the engine and gearbox performance, the acceleration of the vehicle, its maximum speed and fuel efficiency
- Handling: evaluates the road holding capability of the vehicle, as well as its maneuverability and off-road performance.

Within the Safety category, which includes the braking performance evaluation, a particular item of the list is dedicated to the rating of the brake pedal feeling (*pedalgefühl* in German), assigning up to five points in this regard.

ERGEBNISSE

Fahrzeugtyp (Maximalpunktzahl)		BMW 740i	Mercedes S 450 4Matic
Karosserie			
Raumangebot	(20)	11	12
Außenabmessungen	(10)	3	3
Kofferraum	(15)	7	7
Zuladung	(10)	6	8
Variabilität/Funktionalität	(10)	7	7
Instrumente/Anzeige	(5)	5	4
Bedienung	(10)	9	8
Rundumsicht	(10)	7	7
Qualitätsanmutung	(10)	10	10
Summe	**(100)**	**65**	**66**
Sicherheit			
Sicherheitsausstatt./-assistenz	(40)	32	31
Licht	(10)	10	9
Bremsweg kalt (100 km/h)	(10)	3	3
Bremsweg kalt (130 km/h)	(5)	3	2
Bremsweg warm (130 km/h)	(10)	7	4
Bremsweg (190 km/h)	(5)	4	3
Pedalgefühl	(5)	5	5
Fahrsicherheit	(15)	14	14
Summe	**(100)**	**78**	**71**
Komfort			
Federungskomfort	(25)	22	24
Sitze vorn	(15)	14	15
Sitze hinten	(10)	10	10
Multimedia	(20)	20	19
Komfort-Assistenzsysteme	(10)	10	10
Klimatisierung	(10)	10	10
Innengeräusch-Messwerte	(5)	4	5
Geräuscheindruck	(5)	4	5
Summe	**(100)**	**94**	**98**
Antrieb			
Laufkultur	(10)	9	10
Durchzugskraft	(10)	8	9
Leistungsentfaltung	(5)	4	5
Schaltung/Getriebeabstufung	(10)	9	9
Beschl./Höchstgeschwindigkeit	(15)	11	11
Zwischenbeschleunigung	(5)	4	4
Testverbrauch	(20)	5	5
Lademöglichkeiten	(10)	–	–
Reichweite Elektro	(10)	–	–
Reichweite	(5)	4	3
Summe	**(100)**	**54**	**56**
Fahrverhalten			
Fahrdynamik	(20)	10	10
Handling/Fahrspaß	(25)	22	20
Lenkung	(20)	19	19
Wendekreis	(10)	0	1
Traktion/Wintertauglichkeit	(15)	11	15
Geradeausl./Windempf.	(10)	10	10
Summe	**(100)**	**72**	**75**
Umwelt			
Well-to-Wheel-CO_2-Emission	(30)	8	8
Emissionen nach NEFZ	(15)	9	8
Stand- und Fahrgeräusch	(5)	5	5
Summe	**(50)**	**22**	**21**
Eigenschaftswertung	**(550)**	**385**	**387**
Kosten			
Grundpreis*	(25)	24	25
Ausstattung*	(10)	10	7
Aufpreisgestaltung	(5)	4	4
Wiederverkaufschancen	(10)	8	8
Festkosten für 5 Jahre*	(10)	10	10
Wart./Reparatur 100 000 km*	(15)	15	13
Kraftstoffkosten 100 000 km*	(15)	15	15
Garantie	(10)	7	5
Summe	**(100)**	**93**	**87**
Gesamtwertung	**(650)**	**478**	**474**

Figure 40. Auto Motor und Sport score table (Source: Auto Motor und Sport magazine, published on September, 28, 2017).

Although the methodology used by *Auto Motor und Sport* to assess the pedal feeling is not known, there are 12 vehicles among the ones experimentally analyzed in this thesis work that have also been evaluated by the German magazine between 2014 and 2017: they are built by different manufacturers, 4 of them are city-cars, 6 vehicles belong to the small-medium B-C segments, there is 1 SUV and 1 sports vehicle. All the vehicles have received a pedal feeling rating of 4-5 points, therefore it is not expected a big difference between them.

An analysis of the results given by the static tests has not given a clear evidence of difference in the characteristics of the brake booster or in the relationship between pedal force and stroke with the vehicle at standstill: the vehicles are different with respect to each other, but the evaluation difference was not consistent with such differences.

As the attention is brought to the results of dynamic tests, in particular to the progressive braking maneuver, it is possible to see a difference between the vehicles that received five points and the ones which received only four.

Looking in Figure 41 at force-deceleration curves obtained during the progressive braking maneuver performed at 100 °C of all the vehicles together, it is possible to see that, for low deceleration values, the vehicles with the maximum rating are enclosed in a narrow band, while the other vehicles show higher or lower deceleration values per a given pedal force.

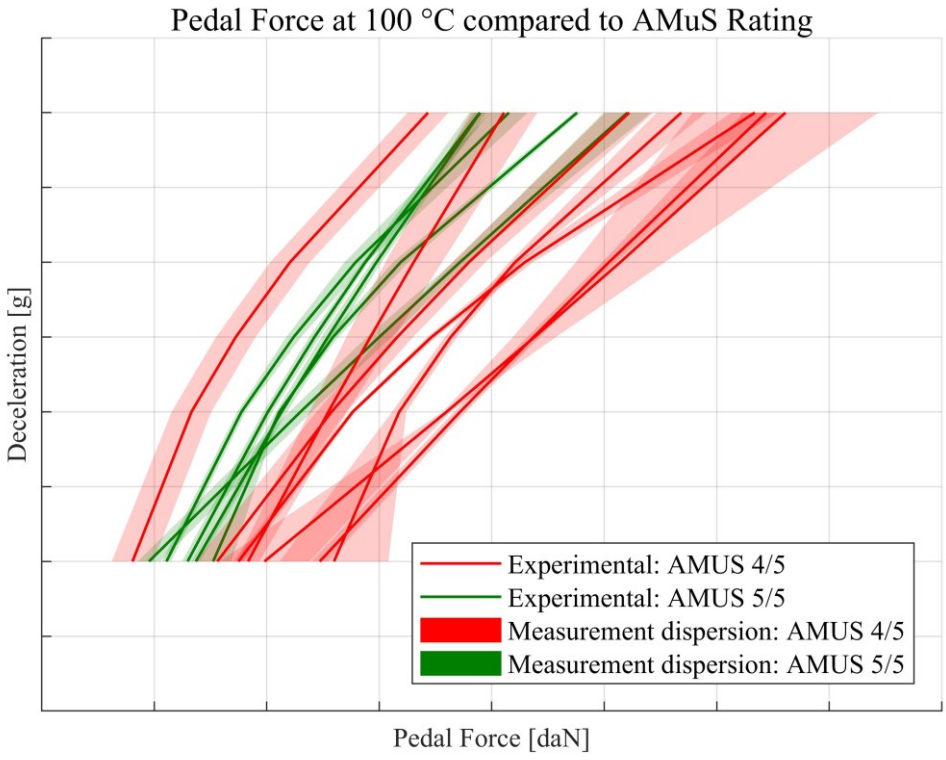

Figure 41. Experimental curves of vehicle deceleration vs. brake pedal force of the vehicles also evaluated by Auto Motor und Sport.

Even if the difference is quite visible, it is useful to understand if it depends on the effective value of force to obtain a certain deceleration, or if it depends on the average slope of the curve.

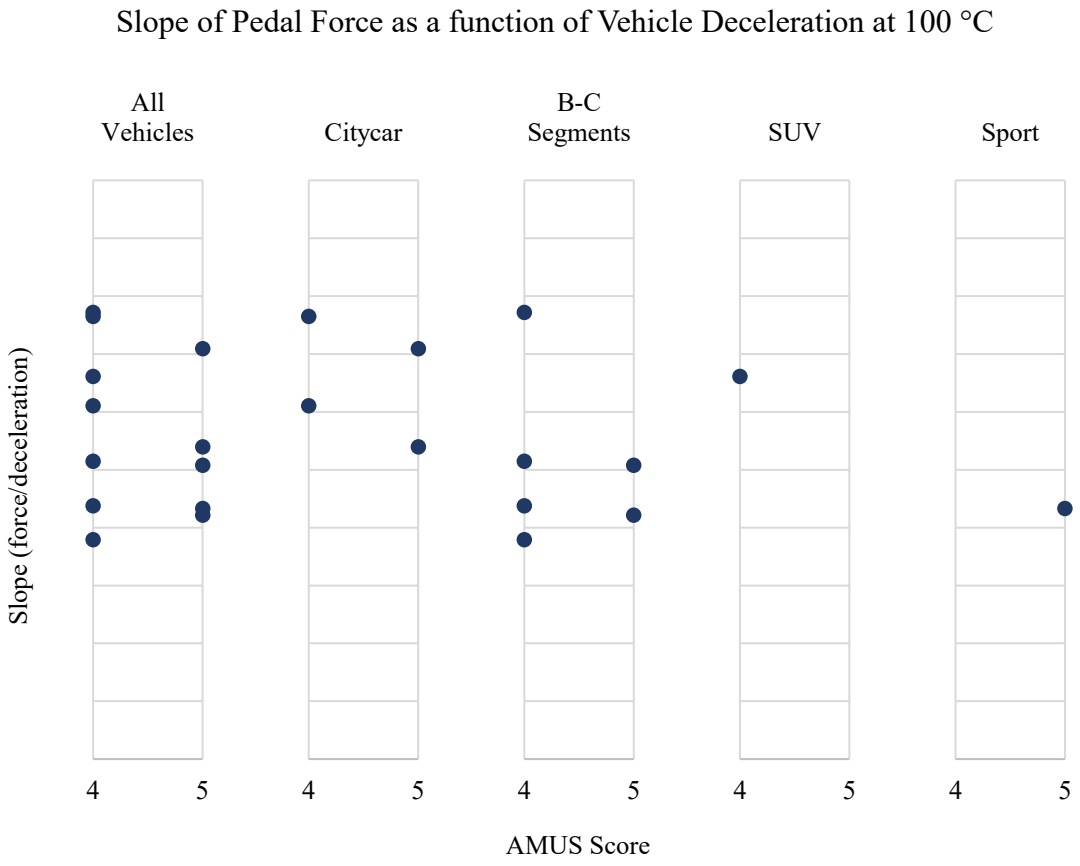

Figure 42. Comparison of the mean slope (between 0,2 g and 0,8 g) of the pedal force vs. vehicle deceleration, against different Auto Motor und Sport pedal feeling ratings and different vehicle segments.

The slope of the pedal force as a function of the vehicle deceleration does not seem to influence the pedal feeling rating, meaning that there is no correlation with the increment is pedal force to obtain a certain increment of vehicle deceleration. Also, separating the results considering the different segments of the vehicles does not provide additional information.

If the analysis is brought to the values of pedal force to obtain determined levels of deceleration, a correlation becomes visible in Figure 43:

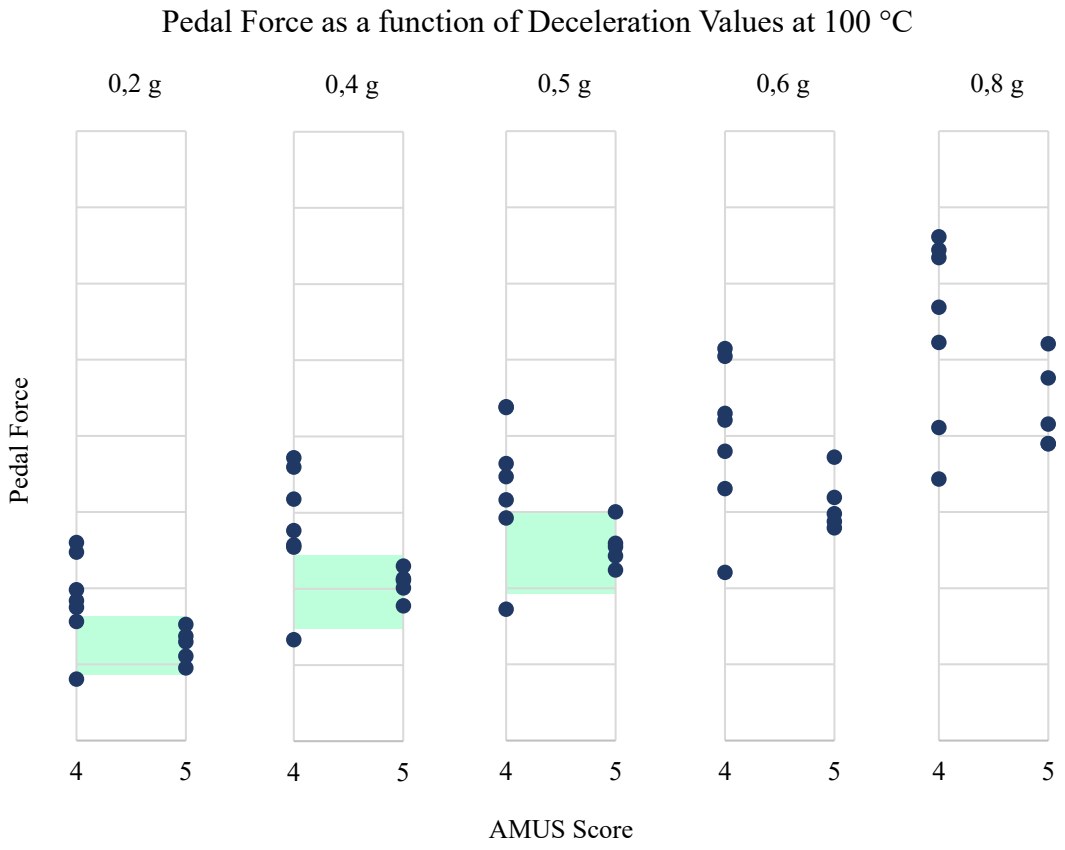

Figure 43. Comparison of the values of pedal force required to achieve various levels of vehicle deceleration and the associated pedal feeling ratings from Auto Motor und Sport.

The analysis with cold brakes shows that for low deceleration values, up to 0,5 g (approximately equivalent to 5 m/s^2) the pedal force values of the vehicles with the maximum rating are within an identifiable range (highlighted in green), while the vehicles with a lower rating show pedal force values outside such range. At higher deceleration values the two groups of vehicles show overlapped results, not allowing to come to further conclusions.

It is reasonable, however, that the discriminant is mainly visible at low deceleration values, since the vast majority of brake applications develop decelerations below 0,3 – 0,4 g.

Moreover, except for one vehicle, the vehicles with a lower rating require a higher effort on the brake pedal, with respect to the top rating vehicles, to obtain decelerations in the range 0,2 – 0,5 g, allowing to formulate two alternative hypotheses:

- The only vehicle below the green area scored a low rating because of other reasons, allowing to conclude that the lower the effort, the better the pedal feeling;
- If the brake pedal returns too low resistance, the feeling is actually not appreciated.

Extending the analysis to other vehicles might help to understand which hypothesis is the correct one.

Now it is possible to perform the same analysis at the pedal stroke. At first, the curves of the pedal stroke as a function of the vehicle deceleration for all the vehicles is represented in Figure 44:

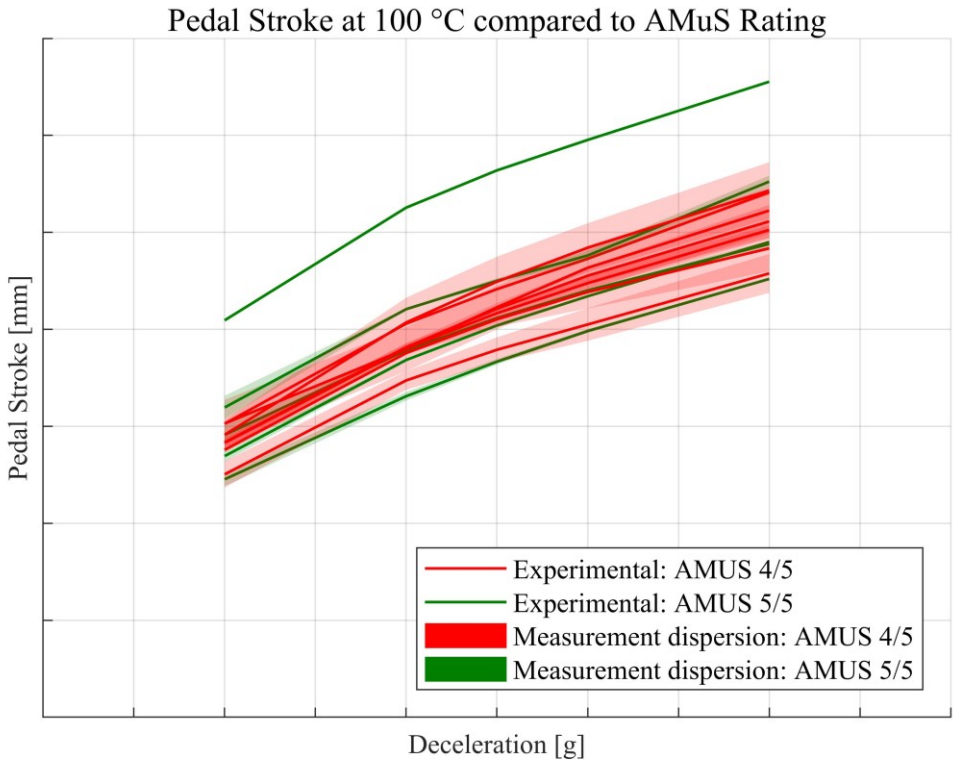

Figure 44. Experimental curves of brake pedal stroke vs. vehicle deceleration for the vehicles also evaluated by Auto Motor und Sport.

Differently to the pedal force case, the pedal stroke curve of the vehicles with the maximum rating is spread over the curves of the vehicles with a lower rating, not allowing to conclude anything at first sight.

As for the pedal force, it is possible to look in detail to the pedal stroke average slope as a function of the deceleration, separating the results per AMUS rating and vehicle segments.

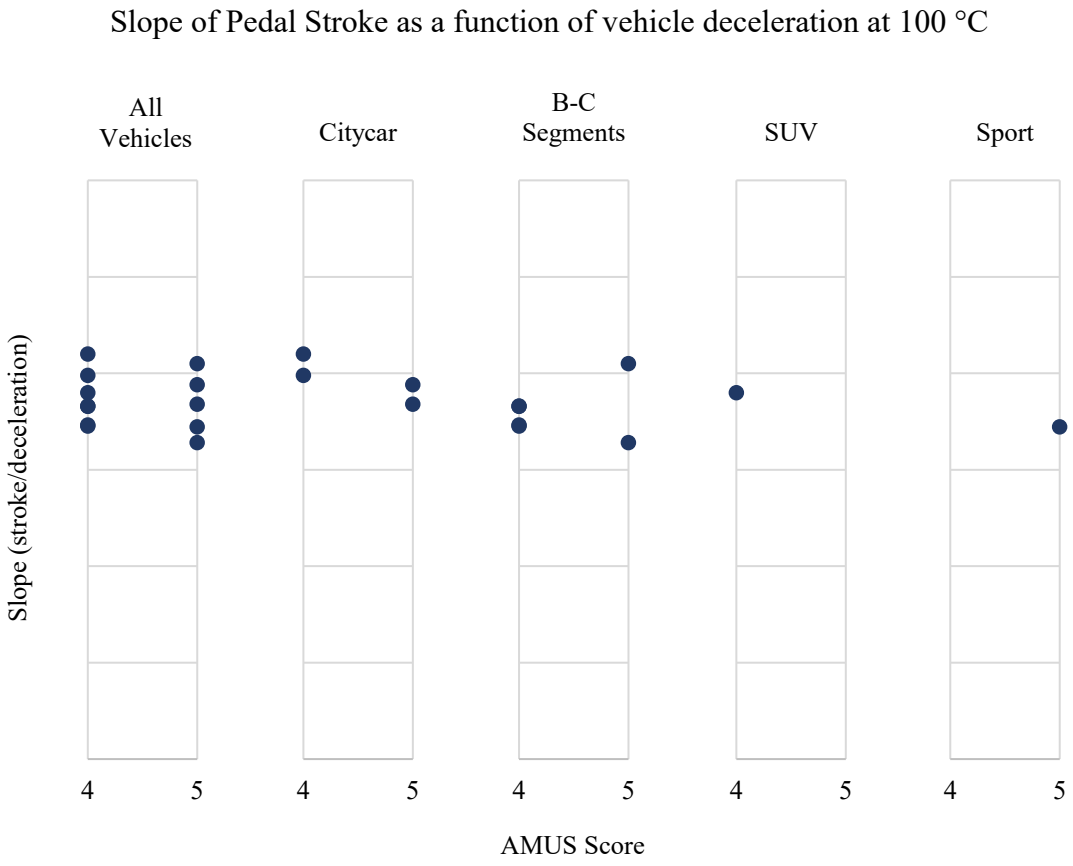

Figure 45. Comparison of the mean slope (between 0,2 and 0,8 g) of the pedal stroke vs. vehicle deceleration, against different pedal feeling rating from Auto Motor und Sport and different vehicle segments.

The increment of pedal stroke to obtain a certain increment of vehicle deceleration does not show differences between vehicle segments and between different ratings.

Also, the result is similar looking in Figure 46 at the absolute pedal stroke values at the various deceleration levels:

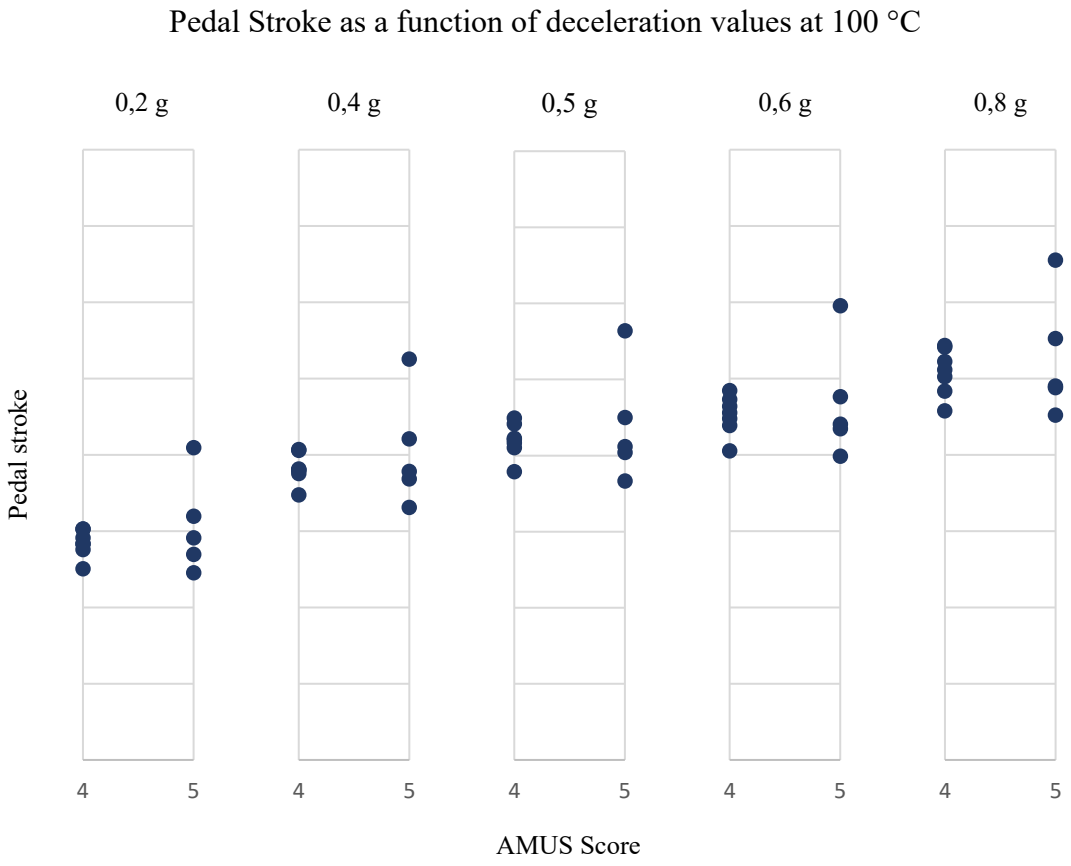

Figure 46. Comparison of the values of brake pedal stroke required to achieve various levels of vehicle deceleration and the associated pedal feeling ratings from Auto Motor und Sport.

It is visible the pedal stroke increases as the deceleration increases, but there is no difference among vehicles with different scores. It is possible, therefore, to conclude that the pedal stroke does not influence the magazine rating.

The search of possible correlations has also been conducted looking at the relative difference in the pedal feeling with cold brakes (at 100 °C) and hot brakes (at 300 °C), and in the relative difference in the cold pedal feeling before and after the heating cycle of the whole progressive braking test. Since the magazine also tests the vehicles performing repeated emergency braking maneuvers, the aim of these comparisons is to assess if the magazine tester is influenced by possible differences in the braking performance of the vehicle before, during and after an intense operation of the braking system.

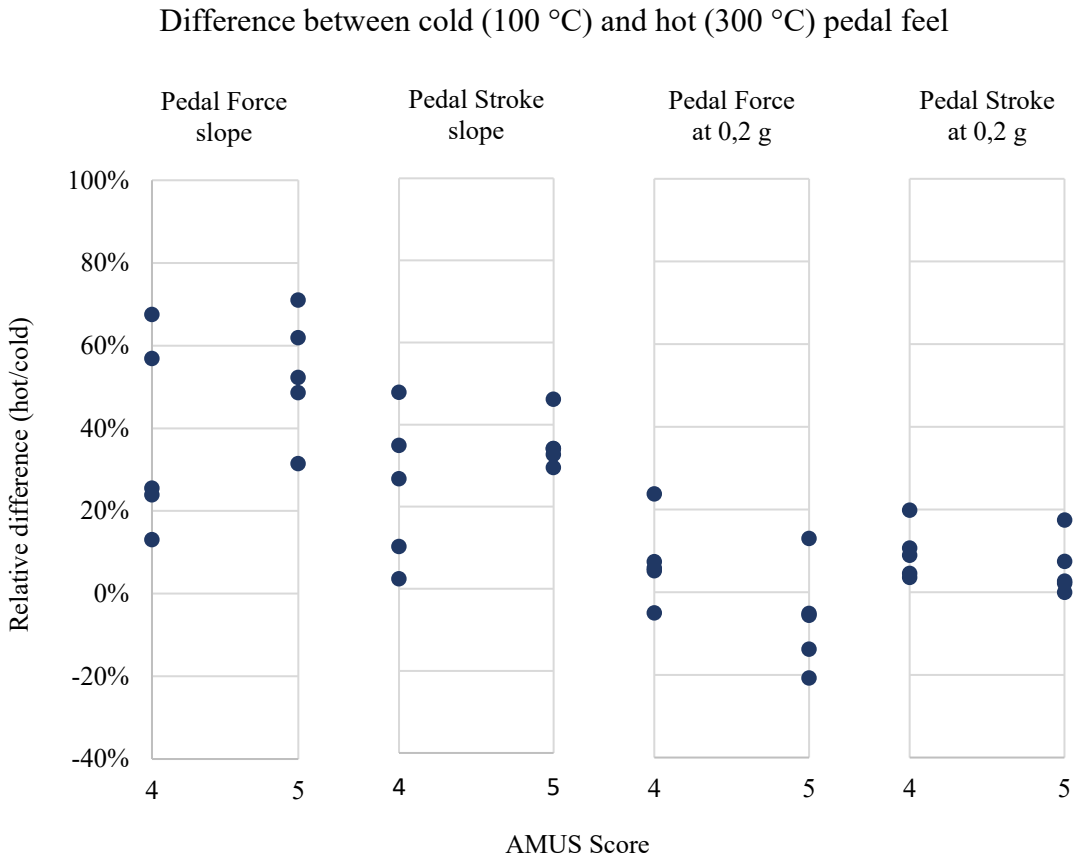

Figure 47. Comparison of the relative difference between cold and hot brakes pedal feeling and its rating from Auto Motor und Sport.

Looking at Figure 47, the average slope of pedal force and pedal stroke as a function of the deceleration (along the whole curve, between 0,2 and 0,8 g) does not influence the rating of the vehicles. Also, the difference in pedal force and pedal stroke to obtain a low deceleration (which seems to be more significant for the pedal feeling rating) between cold and hot brakes does not indicate an influence of this parameter on the evaluation of the pedal feeling.

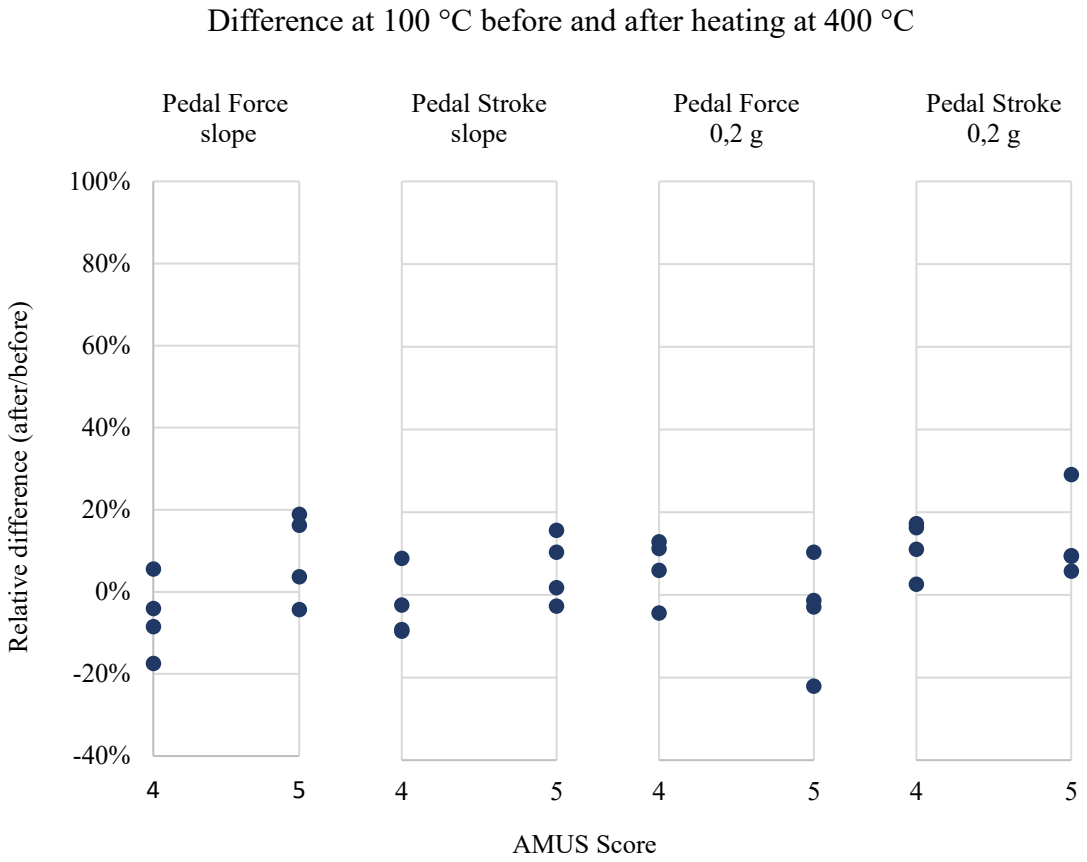

Figure 48. Comparison of the relative difference in pedal feeling of cold brakes (100 °C) before and after the execution of the full progressive braking test cycle, which heats up the braking system up to above 400 °C.

The same conclusion can be drawn with the differences in pedal feeling with cold brakes, before and after heating the brakes up to 400 °C. Even if the differences shown in Figure 48 are quite small for all the vehicles, neither the slope, neither the absolute values at low deceleration, for both the pedal force and stroke, show an influence on the magazine evaluation.

It is possible to conclude, therefore, that the magazine rating indicates that vehicles that require a low effort to provide low-medium decelerations are the most appreciated from a pedal feeling point of view. It might be possible that an excessively low resistance of the brake pedal negatively affects the pedal feeling, but further investigations are necessary to confirm this hypothesis.

4.2 Quattroruote

The Italian magazine *Quattroruote* has been published monthly since 1956 and, similarly to *Auto Motor und Sport*, it quickly became a reference it its country because of the foundation of a testing facility that allowed to deeply analyze each vehicle and provide to the audience a large quantity of data and measurements to support the description and evaluation of the journalists in the test articles. Since 1995, *Quattroruote* owns a test track with dedicated areas to assess

the vehicle performance, handling, comfort, fuel consumption and active safety with a repeatable methodology.

As *Auto Motor und Sport*, *Quattroruote* includes an evaluation table for each tested vehicle, assigning a maximum of 5 points (with honors) – named stars – to various attributes.

Each evaluation carries a brief comment that justifies the score assigned or emphasizes a characteristic of the vehicle.

The scores are assigned to the seating position, the instrumentation and commands, the infotainment, the climate control, the visibility, the trims, the equipment, the safety features, the driving assistance devices, the roominess, the luggage compartment, the comfort, the engine, the acceleration with and without gear changes, the gearbox, the steering, the brakes, the handling, the fuel economy and the warranty.

For what concerns the evaluation of the braking performance, there is not an explicit evaluation of the brake pedal feeling, although it is occasionally mentioned in the score description if it is particularly appreciated or unsatisfactory. What the description mentions more often, if not always, is the stopping distance of the vehicle in various situations, as well as its resistance to fading.

LA PAGELLA

POSTO GUIDA ★★★★★	Posizione di guida ideale per il tipo di vettura, con volante verticale ampiamente regolabile e seduta piuttosto bassa, a soli 34 cm dall'asfalto.
COMANDI E STRUMENTI ★★★★☆	I moduli opzionali dell'infotainment montati sull'esemplare in prova hanno portato in dote i comandi sul volante. Controlli clima migliorabili.
AUDIO E NAVIGATORE ★★★★☆	Il sistema di serie ha le funzioni di base, compresa la connettività Bluetooth per il telefono. Il resto, dal mirroring al navigatore, va ordinato a parte.
CLIMATIZZAZIONE ★★★★☆	L'abitacolo piccolo si raffredda (e si riscalda) molto in fretta. L'impianto è a due zone separate e, a richiesta, si possono avere i sedili climatizzati.
VISIBILITÀ ★★★☆	Lievemente migliore di quella della Boxster, soprattutto di lato e dietro. Indispensabili, comunque, sensori di parcheggio e retrocamera.
FINITURA ★★★★★	La sensazione di ben fatto pervade un po' tutta la vettura ed è all'altezza delle aspettative. Il margine di miglioramento è veramente esiguo.
ACCESSORI ★★★	Sulla variante S alcuni equipaggiamenti, soprattutto quelli orientati al miglioramento delle prestazioni dinamiche, potrebbero essere di serie.
DOTAZIONI DI SICUREZZA ★★★☆	È di serie il sistema multicollisione, che prova a ridurre le conseguenze di un impatto, frenando anche dopo l'apertura dell'airbag.
ASSISTENZA ALLA GUIDA ★★★☆	Non molto per la verità (e tutto a richiesta): regolatore di velocità attivo, in grado di frenare "delicatamente", e assistente dell'angolo buio.
ABITABILITÀ ★★★	L'abitacolo offre ospitalità per una coppia di adulti anche di statura superiore alla media. Pure lo spazio tra i sedili è più che sufficiente.
BAGAGLIAIO ★★★☆	La Cayman si pregia di due vani per i bagagli, uno anteriore a pozzetto e uno posteriore, il cui accesso è agevolato dal portellone.
CONFORT ★★☆	Nota dolente, non tanto per l'assorbimento delle sospensioni (che, anzi, sono molto efficienti), quanto per il rumore di rotolamento e i fruscii.
MOTORE ★★★★★	Un signor quattro cilindri, forse tra i migliori in circolazione, per potenza, coppia, allungo e guidabilità. Non fa rimpiangere il vecchio "flat-six".
ACCELERAZIONE ★★★★★	Quattro secondi netti per passare da 0 a 100 orari (con il launch control) sono una prestazione superlativa. Meglio anche del dato dichiarato.
RIPRESA ★★★★★	Tempi di tutto rispetto, che mettono in rilievo l'elasticità del boxer turbo. La spinta è già consistente e corposa a partire da 2.400 giri.
CAMBIO ★★★★★	Il "Doppelkupplung" ha tante doti, dal funzionamento puntuale e rapido alla corretta rapportatura. Ottimo in pista quanto su strada.
STERZO ★★★★★	La sua dote è senz'altro la capacità di "parlare" al guidatore, trasmettendo informazioni ed emozioni. Non è neanche così rapido da generare apprensione.
FRENI ★★★★★	Al di là di un feeling inaspettatamente imperfetto in pista, le prestazioni dell'impianto lasciano poco spazio alle interpretazioni. Potente e infaticabile.
SU STRADA ★★★★★	Il risultato finale è semplicemente strepitoso, tanto che proprio nella guida la 718 Cayman trova la sua ragion d'essere. Pilota e macchina sono un tutt'uno.
CONSUMO ★★★☆	Non è un'utilitaria, ma nemmeno un'avida succhiabenzina: usandola nei limiti ci si può persino sorprendere. Tirando, invece, la musica cambia.
GARANZIA ★★	L'aspetto "normale" di tutta la macchina: la garanzia è di due anni, tre sulla verniciatura e 12 sulla corrosione passante.

Legenda (vale per tutte le tabelle della prova): ★ Insufficiente ★★ Sufficiente ★★★ Discreto ★★★★ Buono ★★★★★ Ottimo ☆ Vale ½ stella ★★★★★★ Con lode

Figure 49. Quattroruote score table (source: Quattroruote magazine n. 745).

The results that the magazine provides on the braking tests, include:

- Stopping distance on dry asphalt from 100 km/h, driver and instrumentation only;
- Stopping distance on dry asphalt from a higher speed V_2, driver and instrumentation only;
- Stopping distance from 100 km/h on a split surface: dry asphalt and dry setts;
- Stopping distance from 100 km/h on a split surface: wet asphalt and artificial ice;
- Optional: stopping distances of 10 repeated emergency braking maneuvers from 100 km/h on dry asphalt, in full load conditions. If the vehicle is a sports car, the initial speed is raised to 130 km/h, always in full load conditions.

The initial speed V_2 used in the high-speed braking test is chosen between 130 – 160 – 180 – 200 km/h and depends on the maximum speed of the vehicle.

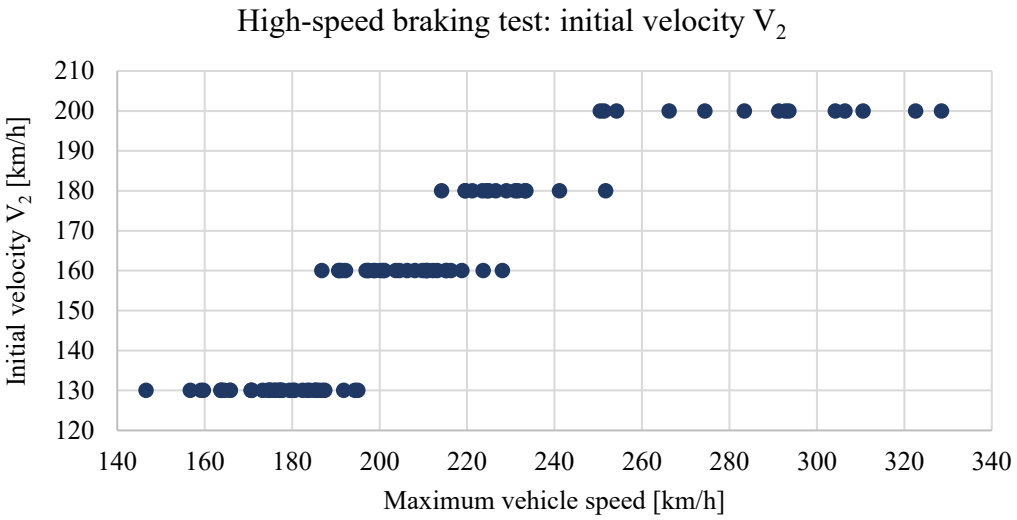

Figure 50. Initial vehicle speed V_2 of the high-speed braking test performed by Quattroruote vs. maximum vehicle speed.

If the maximum speed is lower than 180 km/h, V_2 is 130 km/h; if the maximum speed is higher than 250 km/h, V_2 is 200 km/h. The V_2 values of 160 km/h and 180 km/h are used of intermediate values of maximum speed, but it is not possible to determine a precise range, since in several occasions more vehicles are tested together in a "comparison test" and V_2 is unique for all the vehicles of the test, even if their maximum speeds are significantly different.

Since it is not available a numerical evaluation of the pedal feeling, and even a qualitative description of it is not systematically present, it has been decided to analyze how are correlated the stopping distances to the final score on the braking system, using the results of 96 vehicles, reviewed by *Quattroruote* between October 2016 and October 2017.

The vehicles have been divided in two groups, depending on the presence in the published data of the fading test with 10 repeated braking maneuvers: 41 vehicles did not perform the test, while the remaining 55 vehicles did.

The minimum score for the braking performance among the vehicles was 2,5 stars, while the best vehicle achieved 5 stars with honors, that has been translated in the numerical value of 5,5.

Starting from the group of vehicles that did not perform the fading test, for each vehicle have been collected the mean decelerations developed in the braking maneuvers previously mentioned (with the exception of the fading test), using directly the result provided by the magazine, if published, or calculating it from the published stopping distance and the initial speed:

$$\mathrm{a_{avg}} = \frac{\mathrm{V}^2}{2\mathrm{d}} \tag{4.1}$$

where $\mathrm{a_{avg}}$ is the mean deceleration, V the initial speed and d the stopping distance.

A comparison between the computed mean deceleration and the one published by the magazine, where both the stopping distance and the mean deceleration were available, has shown that the proposed formula returns the same results of the magazine.

The values of deceleration obtained in the four braking maneuvers have then been normalized, assigning to the best deceleration of each type of maneuver i a partial score $\mathrm{ps}_{i,\max}$ which depends on the maximum total score ts achieved by the group of vehicles and on the maximum possible score $\mathrm{ts}_{\max}$ (equal to 5,5 in this case):

$$\mathrm{ps}_{i,\max} = \frac{\max(\mathrm{ts})}{\mathrm{ts}_{\max}} \tag{4.2}$$

Similarly, the lowest value of deceleration in each maneuver will be assigned a partial score $\mathrm{ps}_{i,\min}$ which depends on the lowest score achieved by the group of vehicles:

$$\mathrm{ps}_{i,\min} = \frac{\min(\mathrm{ts})}{\mathrm{ts}_{\max}} \tag{4.3}$$

Now, it is possible to assign a score to the intermediate values of deceleration a_i, with a linear interpolation between the minimum and maximum values:

$$\mathrm{ps}_i = \frac{\mathrm{a}_{i,\max} - \mathrm{a}_i}{\mathrm{a}_{i,\max} - \mathrm{a}_{i,\min}} \mathrm{ps}_{i,\max} + \frac{\mathrm{a}_i - \mathrm{a}_{i,\min}}{\mathrm{a}_{i,\max} - \mathrm{a}_{i,\min}} \mathrm{ps}_{i,\min} \tag{4.4}$$

At this point, each value of deceleration has an individual score between 0 and 1, where 1 corresponds to a 5 stars with honors performance, while 0 corresponds to a 0 stars performance.

For each braking maneuver it is possible to see how the partial scores computed are related to the total scores assigned by the magazine.

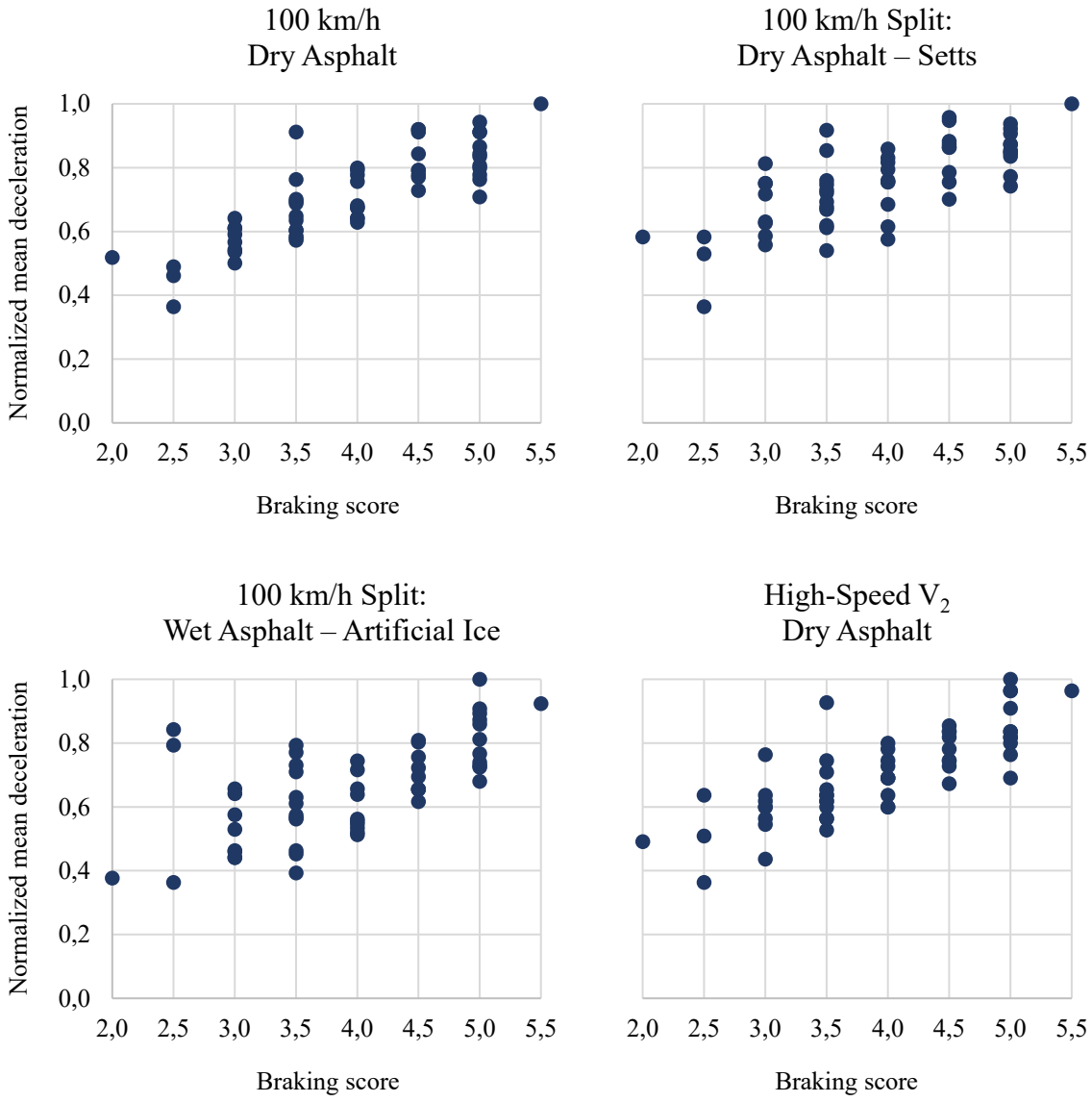

Figure 51. Normalized mean deceleration values in the four main braking maneuvers performed by Quattroruote as a function of overall braking score.

It is visible from Figure 51 how the deceleration increases with the total score, although there are some exceptions: some vehicle may have received a high partial score in a certain maneuver, but have performed poorly in the other ones, obtaining a low overall score.

Assuming that the total score is based on a weighted sum of the partial scores above mentioned plus a constant term, a multiple linear regression has been used to compute the weights, obtaining a constant term of −0,31, and the following weight coefficients:

Braking maneuver	Absolute weight	Relative weight
100 km/h Dry Asphalt	3,21	52,3 %
100 km/h Split: Dry Asphalt – Setts	0,32	5,3 %
100 km/h Split: Wet Asphalt – Artificial Ice	1,87	30,5 %
High-Speed V_2 – Dry Asphalt	0,73	11,9 %

Therefore, summing each partial score multiplied by its absolute weight, plus the constant term, should return the total score assigned by the magazine. It is possible to compare in Figure 52 the actually assigned total scores and the estimated ones.

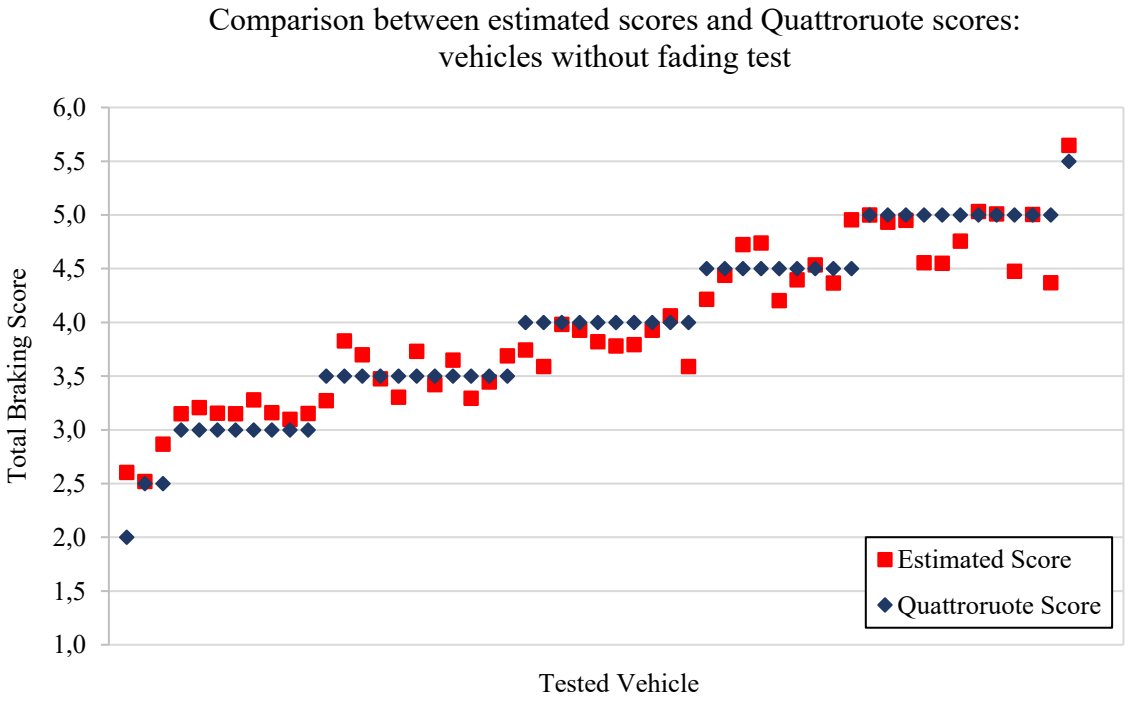

Figure 52. Comparison between the estimated and actual scores assigned by Quattroruote for the group of vehicles which did not undergo the fading test of the magazine.

The estimated values have not been rounded on purpose and the vehicles have been sorted from the lowest to the highest actual score for sake of clarity. Rounding them with a half point resolution, as the magazine rating, did not affect significantly the coefficient of determination. It is visible a slight overestimation of the score for the low performing vehicles, while the top performing vehicles are slightly underrated.

It must be noted that the multilinear regression is valid under the assumption of using continuous variables, while the score of the magazine is discrete. Moreover, some brake tests provide correlated results, such as the decelerations on dry asphalt from 100 km/h and from high speed: since these two results are often correlated, the weight estimation from the multilinear regression can give much more importance to a maneuver with respect to the other one, even if the actual weights used by the magazine were more equally distributed.

The same methodology has been applied to the group of vehicles which also undergo the fading test. The parameter used to assign a score for the fading performance was the ratio between the mean decelerations of the last braking maneuver and the first one. If the brake applications are numbered from 1 to 10, the fading performance parameter fp is:

$$\mathrm{fp} = \frac{a_{avg,10}}{a_{avg,1}} \tag{4.5}$$

and it will be equal to 1 if the first and last decelerations are identical, lower than 1 if the deceleration has decreased during the fade test, higher than 1 if the deceleration has increased at the end of the fade test. Also, this parameter has been normalized using the same procedure of the other four partial scores.

The five partial scores can now be compared against the overall magazine score.

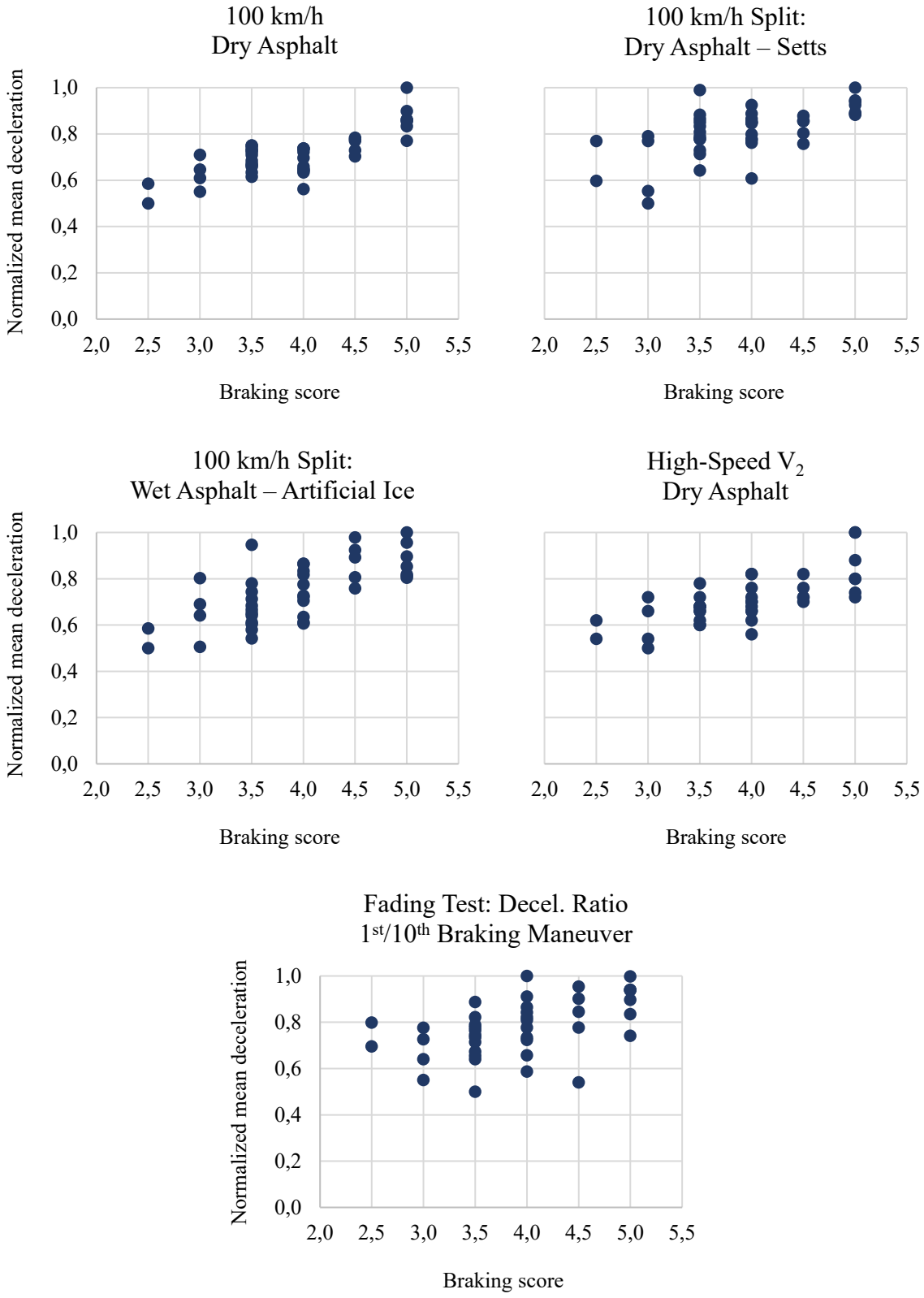

Figure 53. Normalized mean deceleration values vs. Quattroruote braking score in the five main braking maneuvers performed by the magazine.

As in the group of vehicles without the fade test, all the partial scores represented by the normalized mean deceleration values increase as the overall evaluation increases.

The multiple linear regression of the overall braking score as a function of the five partial scores returned a constant term of −0,96 and the following weight coefficients:

Braking maneuver	Absolute weight	Relative weight
100 km/h Dry Asphalt	2,63	40,0 %
100 km/h Split: Dry Asphalt – Setts	0,97	14,8 %
100 km/h Split: Wet Asphalt – Artificial Ice	2,02	30,7 %
High-Speed V_2 – Dry Asphalt	0,07	1,1 %
Fade Test: Decel. Ratio 1st/10th Braking Maneuver	0,88	13,3 %

The comparison of the estimated total braking score provided by the weighted sum of its partial scores and the total braking score provided by Quattroruote is visible in the following plot.

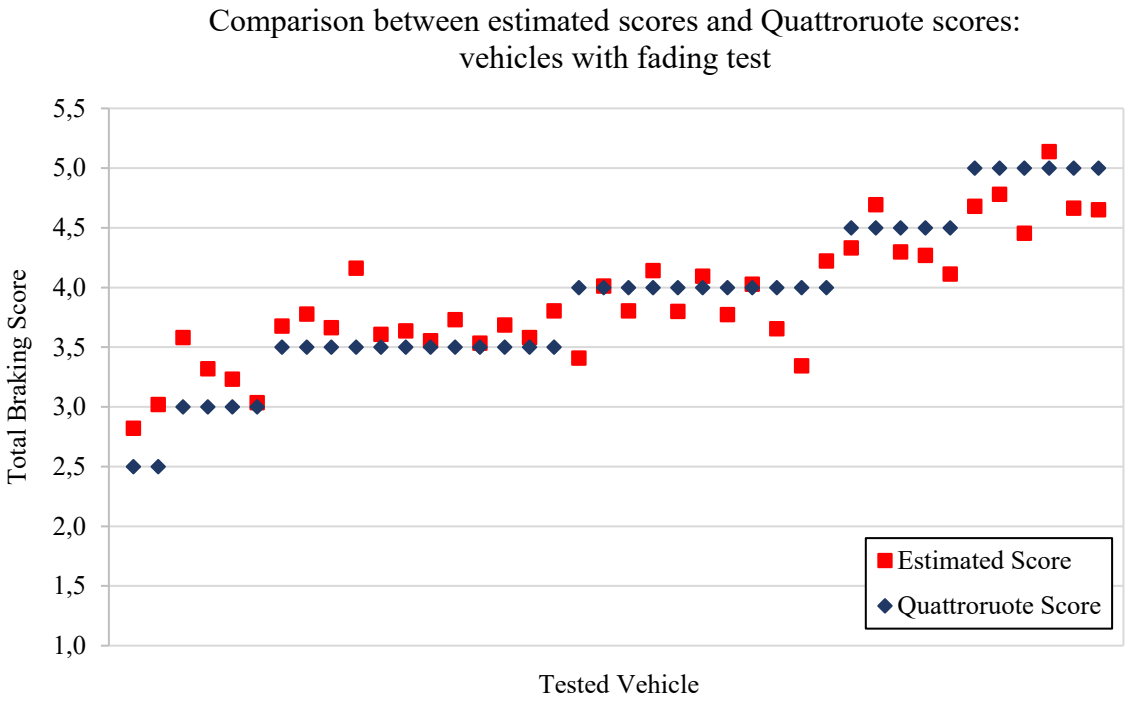

Figure 54. Comparison between the estimated and actual scores assigned by Quattroruote for the group of vehicles which performed the fading test of the magazine.

Even with this group, there is a slight overestimation of the score obtained by low performing vehicles, while the best performers received an underestimated evaluation. The almost negligible weight assigned to the high-speed braking test compared to the braking test on dry

asphalt from 100 km/h confirms the behavior of the linear regression when more variables are correlated to each other, as it was described for the previous group of vehicles.

In conclusion, it is possible to state that the rating used by Quattroruote is mainly based on the deceleration achieved by the vehicles in the various braking tests, with a strong influence from the cold performance on dry asphalt and on the slip surface composed by wet asphalt and artificial ice: these two tests seem to contribute to more than 70 % of the total score. The errors in the estimation, however, indicate that there are more variables than the ones used in the linear regression and, for the fading test, the parameter used could be incorrect. It is also possible, looking at the evaluation of vehicles which performed very well in all the tests except for one, that a penalty algorithm is used by the magazine to limit the maximum score achievable by such vehicles. It is reasonable to assume that the dynamic behavior of the vehicle during the braking maneuver, such as the amount of steering corrections necessary to maintain the straight line during the split surface braking tests, also contributes to the final evaluation of the vehicle.

All these undocumented variables, together with the low resolution of the final score (only 10 levels from minimum to maximum, with respect to the 100 ones of AMuS), make very difficult to infer the contribution of the pedal feeling from the evaluation of *Quattroruote*, although it is possible that it has been taken into account in the evaluation.

4.3 Customer Satisfaction Survey

The last method used to compare objective parameters of the pedal feeling with its subjective evaluation is based on the results of a customer satisfaction interview performed between March 2016 and May 2017, in which people who had recently bought a new vehicle were asked about their satisfaction with the braking system of the vehicle: the interviewer collected the vehicle model and all its technical specification, together with possible complaints from the interviewed person. The result of the survey is, for each sampled vehicle model, the percentage of users complaining about their braking system with respect to the total number of interviews, separating the results depending on the type of complaint: noise, vibration, parking brake issues, deviations from the straight line during braking, insufficient braking force, etc.

The results of interest are the ones related to the pedal feeling, in particular:

- Complaints about the low responsiveness of the braking system
- Complaints about the propensity of the vehicle to lock the wheels during braking.

The first complaint category is interpretable as a low deceleration of the vehicle with respect to how much the driver actuated the brake pedal or, vice-versa, as an excessive perceived effort on the brake pedal to obtain the desired deceleration.

The second complaint category, although its description might be misleading, since all the vehicles mentioned in the survey were equipped with anti-lock braking systems, is interpretable as a tendency of the vehicle to decelerate more than what the driver expected, basing on his action on the brake pedal.

The correctness of these interpretations is verified by analyzing in detail the complaint as the interviewed person describes it, such as: “If I hit the brakes, it takes too much time to slow down the vehicle”, or: “The brakes are too sharp, sometimes I feel that if I did not fasten the seat belt, I would hit the steering wheel when I brake”, which are assigned to the first and second category respectively.

Approximately 8500 interviews have been used, related to 19 vehicles models. Some vehicles are listed more times, because they have different powertrains (which could change the vacuum source of the brake booster or the curb weight of the vehicle in a significant way) and/or are equipped with different brakes.

Each of these vehicles, with their percentages of complaints, has been associated to the progressive braking curves provided by the vehicle manufacturer, which also include a tolerance range of $\pm 3\,\sigma$, to take into account the tolerance chain due to the manufacturing variability of all the components of the braking system. If the average performance of each component coincides with the nominal performance designed by the manufacturer and the performance distribution is gaussian, the range of $\pm 3\,\sigma$ allows to represent the 99,7 % of the produced vehicles.

Some of the vehicles analyzed did not receive any complaint, others have received complaints about the low responsiveness of the braking system and only one vehicle model has been complained to have a too sensitive brake pedal.

Superimposing the progressive braking curves from the least complained to the most complained ones allows to create a map of possible regions to be avoided in the pedal feeling design:

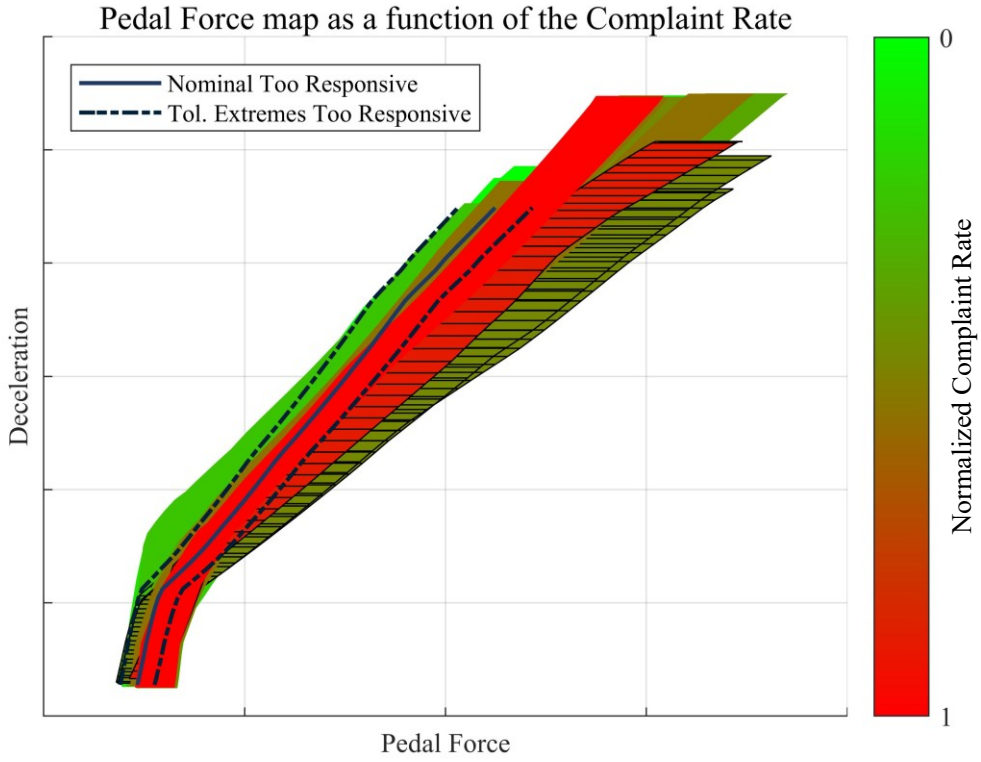

Figure 55. Map of the vehicle deceleration vs. brake pedal force colored as a function of the complaint rate for lack of responsiveness of the braking system, including the tolerance range of manufacturing variability.

The green curves belong to the vehicles with no or low complaints on the lack of responsiveness of the brake pedal, while the red curves are the most complained. The blue curve represents the curve of the only vehicle complained to be excessively prompt. The curves marked with black lines belong to light commercial vehicles, they have been highlighted as sometimes the design criteria for these vehicles are different with respect to passenger vehicles.

Being the curves overlapped from the least complained to the most complained, some of the best curves are hidden behind the worst ones. Processing the same plot of Figure 55 with only the nominal curves, without the width given by the tolerances chain, allows to see all the curves, although the map could be more difficult to understand. The result is shown in Figure 56, highlighting the commercial vehicles with dashed lines.

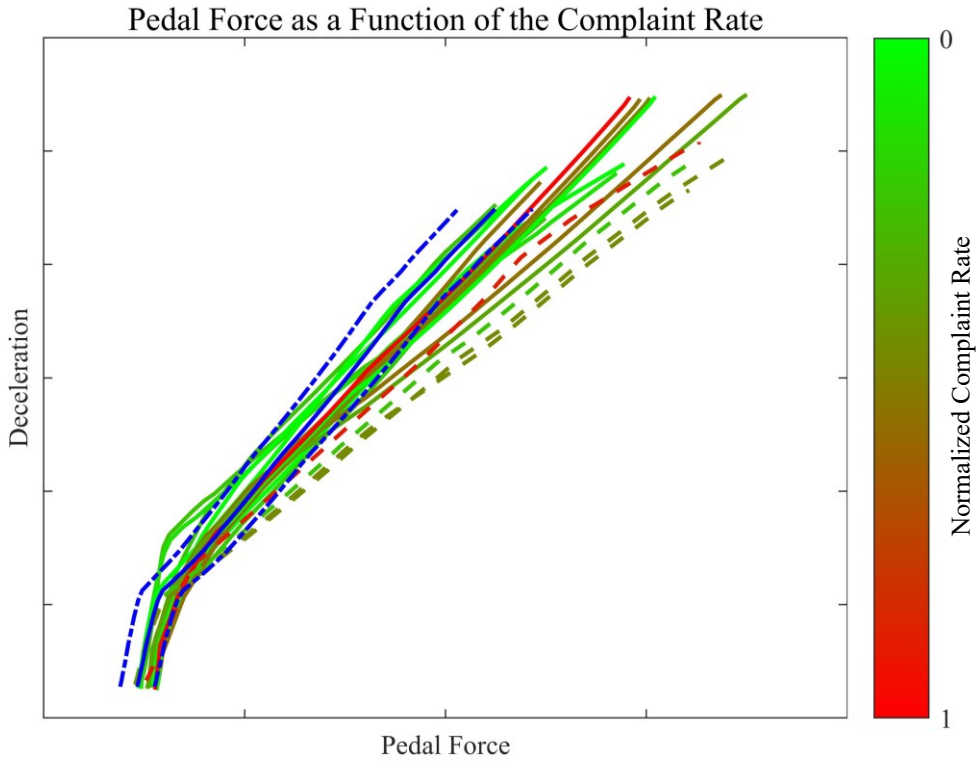

Figure 56. Vehicle deceleration vs. brake pedal force nominal curves colored as a function of the complaint rate for lack of responsiveness of the braking system.

Note that the blue curve in Figure 56, which belongs to the vehicle with an excessively prompt braking response, has been shown with its tolerance extremes: the supplier of one of the components of the braking system has had an offset production, whose average was not centered on the design values. Although they have supplied only components within the tolerance range, the distribution was not anymore gaussian: the consequence is that the actual curve of the vehicles used by the interviewed customer was more close, if not beyond, the upper/left tolerance extreme, probably causing the excessively prompt response even if the nominal curve is in between the ones of the other vehicles. Even if it were in its tolerance range, however, the “blue” vehicle is one of the vehicles which require the least effort on the brake pedal for each deceleration value.

Looking at all the vehicles, if the attention is focused on the lower end of the curves, the one related to the lower deceleration values, which is the range most used by common drivers, it is visible that the most complained curves tend to require a higher effort on the brake pedal, given a certain desired deceleration level.

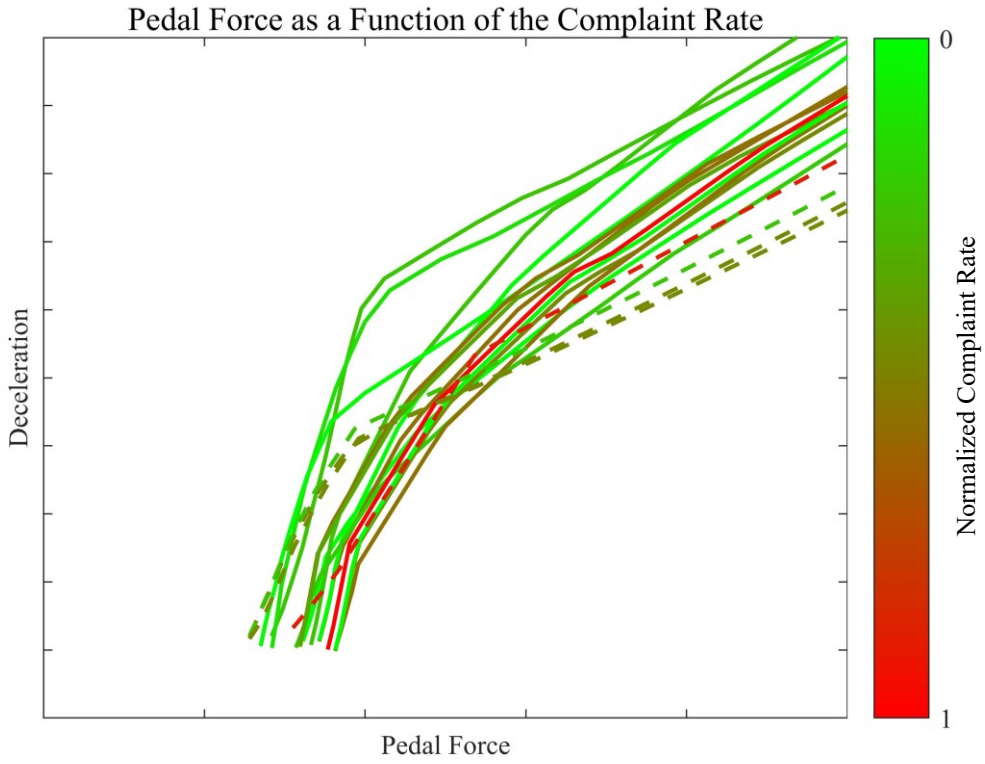

Figure 57. Close-up for low deceleration values of the curves of vehicle deceleration vs. brake pedal force colored as a function of the complaint rate for lack of responsiveness of the braking system.

In the detailed view of Figure 57 it is more visible that the most complained vehicles require higher efforts with respect to the least complained vehicles. It is also possible to compare, as in Figure 58, the pedal effort necessary to develop the values of deceleration of 0,2 – 0,4 – 0,5 g against their complaint rate and look for analogies with the results obtained by the vehicles that achieved the maximum pedal feeling score in the tests of *Auto Motor und Sport.*

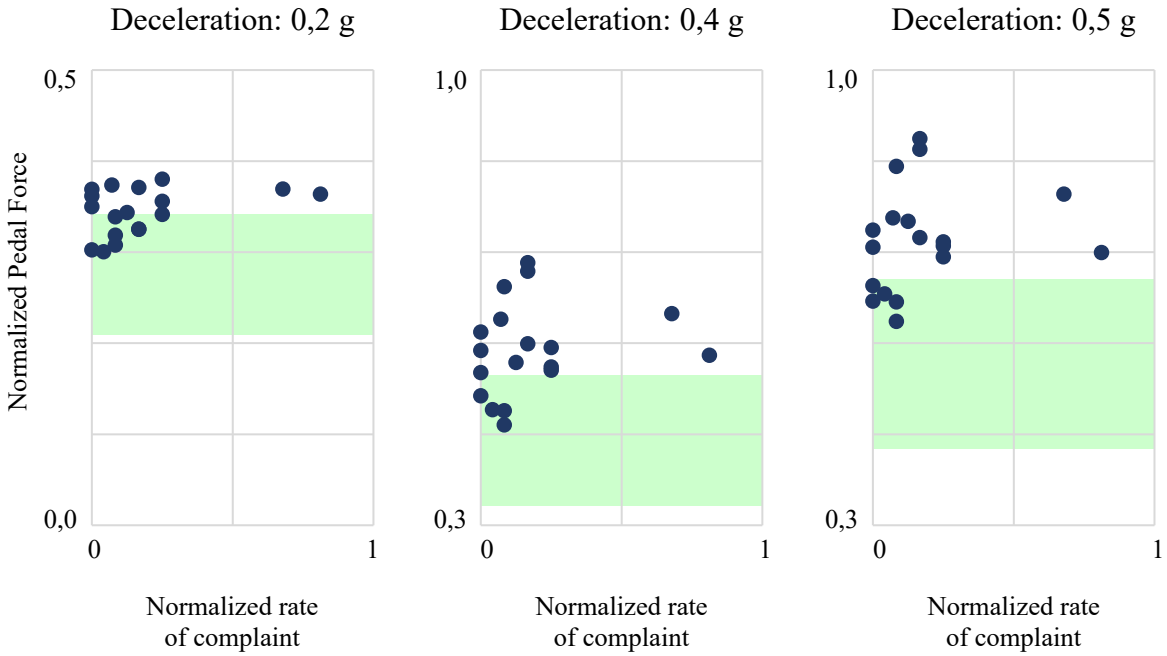

Figure 58. Normalized pedal vs. complaint rate for lack of responsiveness of the braking system for 3 values of vehicle deceleration.

The highlighted areas in green are the ones that correspond to the pedal effort necessary to achieve the maximum pedal feeling score in the German magazine, while the dots represent the efforts required by the vehicles sampled in the customer satisfaction interview as a function of the rate of complaint for low brake responsiveness.

There is not a clear evidence that a lower pedal effort is better, but it is possible to state that the most complained vehicles fall outside of the ranges of efforts which were most appreciated by AMuS. It is also possible to note that there are vehicles without any complaint both within and outside the top rating area, although there are not vehicles very complained in it.

It must be considered that, when the rating (or the complaint) is given by different people, their evaluation criteria are heterogeneous and, for normal drivers, it is probably based on what they were used to: since all the interviewed people have recently purchased the vehicles under investigation, they might still be in the learning process necessary to properly use the vehicle commands. A further point to consider is that, depending on the vehicle segment, the customers might be used to that kind of vehicle or not, i.e.: a consumer who is now driving a B-C segment vehicle has probably used similar vehicles prior to the purchase of the last one, while the new owner of a small SUV, which is a new segment in the market, could have used larger SUVs in the past, or medium sedans, leading to a different pedal feeling perception depending on the previously used vehicle. Similarly, changing brand within a segment could have the same consequences. For this reason, keeping in mind that lower efforts are generally more

appreciated, the benchmark for the pedal feeling of a new hypothetic vehicle should be not only the best competitor of its segment, but also the most driven vehicles of the targeted customers.

The same analysis can be performed on the pedal stroke, although, similarly to the results obtained from *Auto Motor und* Sport, there is less evidence with respect to the pedal force.

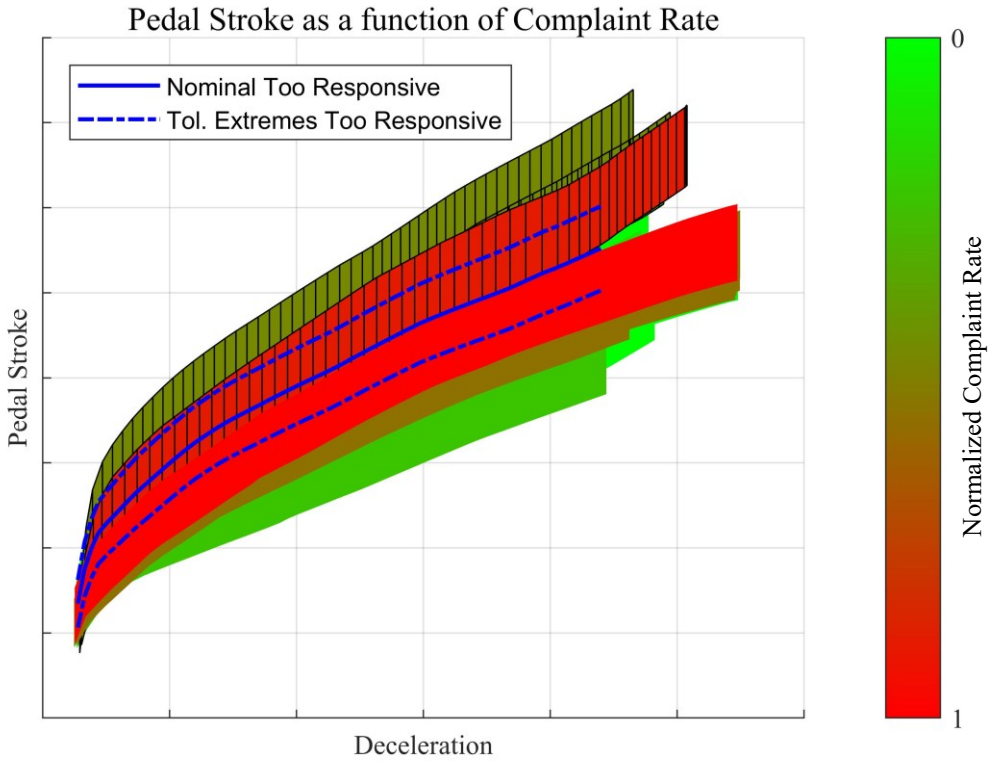

Figure 59. Map of the brake pedal stroke vs. vehicle deceleration colored as a function of the complaint rate for lack of responsiveness of the braking system, including the tolerance range of manufacturing variability.

In the case of the pedal stroke, the curves containing the tolerance ranges overlap more with respect to the ones of the pedal effort, making less easy to understand the map in Figure 59. It is still possible to see that light commercial vehicles (dashed in black) tend to have longer strokes, while the vehicles with the lowest strokes are less complained.

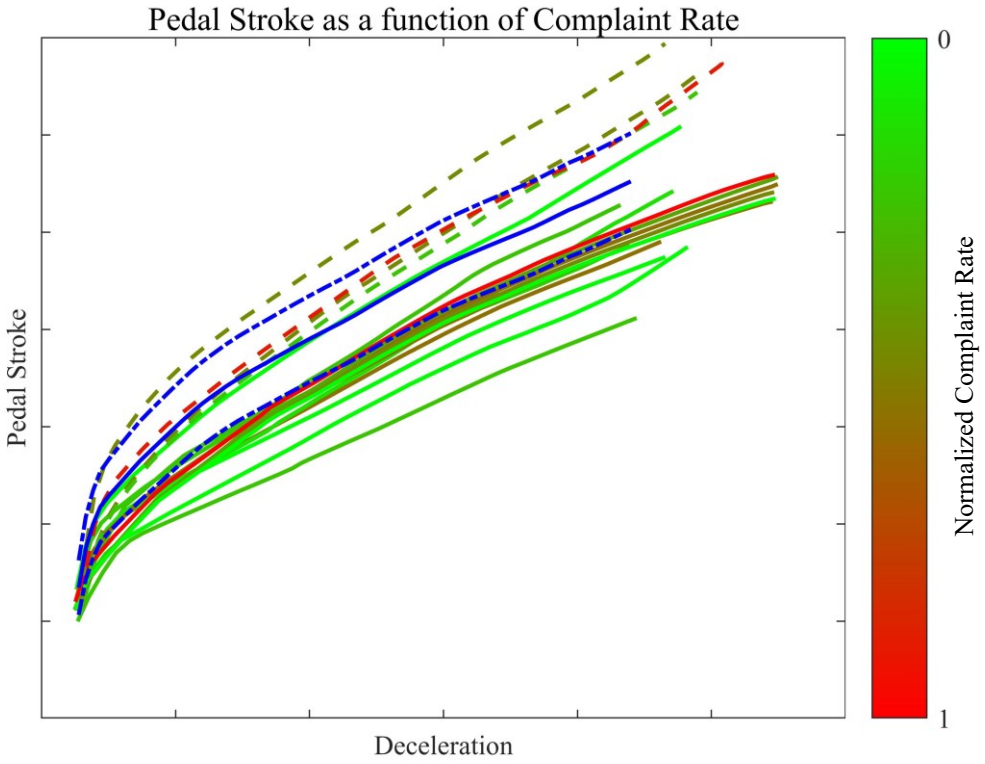

Figure 60. Brake pedal stroke vs. vehicle deceleration curves colored as a function of the complaint rate for lack of responsiveness of the braking system.

When all the curves are visible, as in Figure 60, it is possible to note that there are many vehicles with an average stroke that are not or little complained. This is even better visible comparing the required strokes at the various deceleration values. It is still evident the longer stroke of commercial vehicles (dashed lines), while the excessively prompt vehicle (shown in blue) has a relatively long stroke.

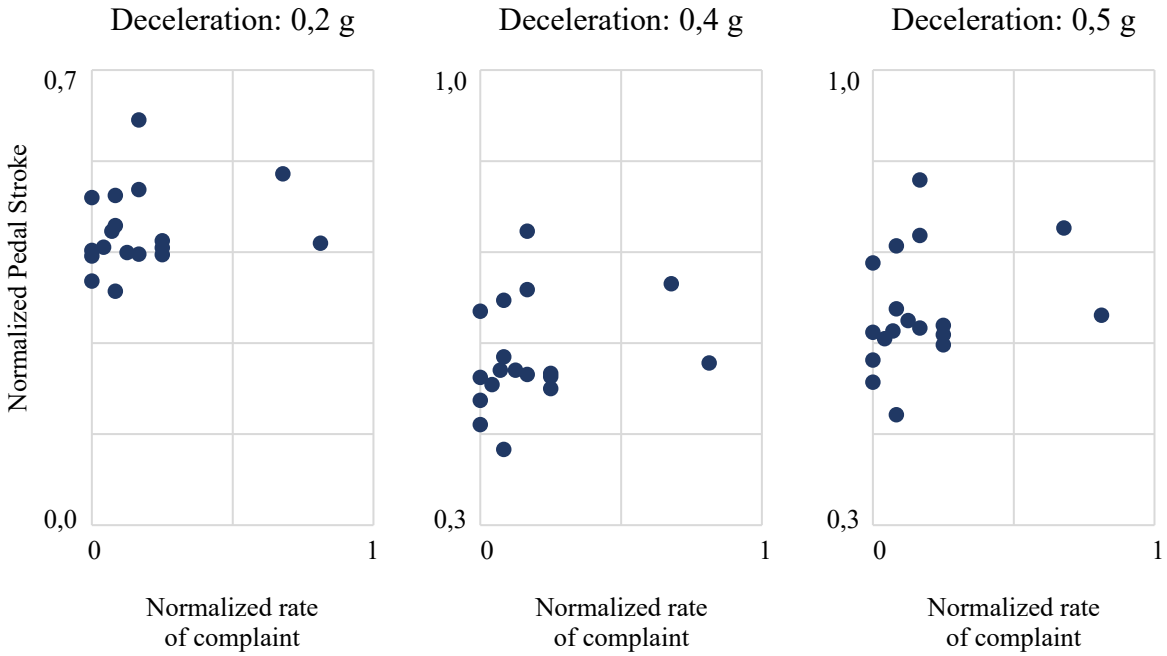

Figure 61. Normalized pedal stroke vs. complaint rate for lack of responsiveness of the braking system for three levels of vehicle deceleration.

As it can be seen in Figure 61, the pedal stroke is almost independent on the complaint rate, making difficult to state which is a possible range of most accepted strokes.

Even considering the sum of the normalized pedal force and stroke, there was no clear evidence of correlation with the complaint rate for lack of responsiveness of the braking system.

It is possible to conclude, then, that the customer satisfaction interview showed results which are compatible with the optimal pedal force values obtained with the analysis of the *Auto Motor und Sport* rating, although the evidence is less clear, being present many vehicles outside the optimal force ranges that still are little or no complained. Once again, this is possibly caused by the different evaluation criteria of each single interviewed driver.

4.4 Comparison with previous studies

The results obtained with the analysis of the *Auto Motor und Sport* ratings and the customer satisfaction interview are now compared with two previous studies, to check if there are consistencies in the pedal feeling evaluation. Both tests have been performed by FCA: the first one in Brazil in 2009, the second one more recently in Italy. The Brazilian test defined a map on the deceleration as a function of the pedal force plot for the progressive braking maneuver, indicating three regions associated to the subjective evaluation of the pedal feeling, normalized to the SAE ratings 6 – 7 – 8. The higher the SAE rating, the higher the appreciation of the pedal feeling. The Italian study has defined an ideal progressive braking deceleration as a function of pedal force curve, which is the result of a pedal feeling test which involved 15 people, some experts in braking system, some not.

In Figure 62, the results obtained in this thesis will be overlapped to the results of these studies.

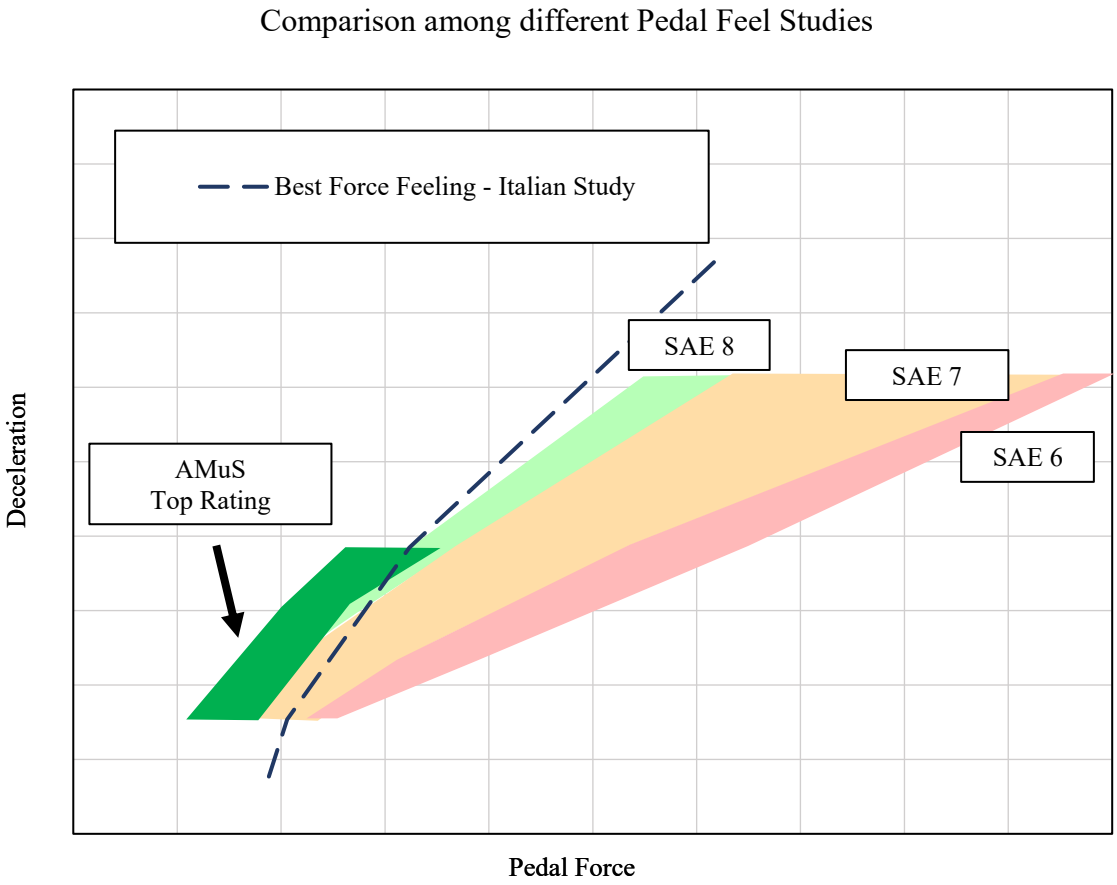

Figure 62. Comparison of the pedal feeling results obtained in this thesis (dark green area) against the results obtained in previous studies.

The three SAE areas represent the results of the Brazilian Study, while the dashed green line the shows the results of the Italian Study. The result of this work, represented by the "AMuS Top Rating" area, seems to be consistent with the ones of the previous studies, indicating a trend of reduction of applied forces on the brake pedal. This result is also compatible with a general tendency in the automotive field to reduce all the command efforts, including the steering wheel and clutch pedal effort.

5. Identification of the main parameters of a Braking System

During the development of a new vehicle, it is possible that the performance of the prototype is different with respect to the expectations given by the design model. Similar issues can arise during the analysis of conformity of production of an assembled vehicle, therefore, it is useful to define a simplified model to estimate the actual performance of each component of the braking system, to understand which element is out of tolerance.

A thorough approach would require disassembling the components of the braking system and to bench test each one of them separately, but such activity is very time consuming and the tools needed to perform these specific tests are often available only at the supplier of each component.

The model proposed aims to gather the main parameters of the braking system of a vehicle using the static tests and progressive braking maneuvers already implemented during the pedal feeling analysis. A further constraint to be considered is the preference of not using systems for the direct measurement of the braking torque or the wheel forces: such systems are not used during the normal testing of the pedal feeling and their adoption would require additional time to prepare the vehicle before the testing activity.

In this simplified model of a braking system, it will be considered a brake pedal with constant lever ratio, a brake booster whose performance curve will be approximated by four segments, a hydraulic pump with identical pressure for both circuits, a fixed rear pressure limiter, front brakes and rear brakes with fixed friction coefficient.

In the following paragraphs, a method of identification of each parameter of the braking system will be proposed: some parameters depend on the knowledge of other components of the braking system or of the vehicle, therefore, the order used in the analysis of each component does not follow the arrangement of a braking system layout from one end to the other end, but is functional to obtain all the necessary data for the successive steps.

5.1 Tandem Master Cylinder

The tandem master cylinder is mainly characterized by the internal section area of the cylinder and the maximum stroke of its pistons. The maximum stroke is designed to exceed the maximum stroke permitted by the brake pedal travel from its rest position up to the contact against the vehicle firewall, therefore, it does not influence the performance of the braking system. The section area, instead, directly influences the relationship between the input force and the output pressure. As the tandem master cylinder houses two pistons who can move relatively to the cylinder surface while maintaining a tight seal for the brake fluid, its

manufacturing tolerances are quite tight, allowing to assume that the nominal diameter of the tandem master cylinder is a suitable source for computing its section area.

If the design diameter value is not available, it is often reported on the cylinder body in millimeters or as a fraction of an inch. Performing the necessary unit conversions, the section area is easily computable from the diameter d_{tmc}

$$A_{tmc} = \frac{\pi d_{tmc}^2}{4} \tag{5.1}$$

5.2 Brake Pedal Ratio

The brake pedal is the first device that amplifies the driver effort, transmitting a higher force to the brake booster thanks to the different arm lengths at the input and output points of force exchange. The geometry of the pedal and the position of its hinge, behind the dashboard, makes difficult to reliably measure the distance from the fulcrum of the points of application and transmission of the force. A more convenient approach is to measure the applied force to the brake pedal, the output pressure at the tandem master cylinder and to compute the input force at the tandem master cylinder. If the brake booster is made inoperative by depleting the vacuum stored in its front chamber, the input force at the tandem master cylinder becomes equal to the output force of the brake pedal.

The tandem master cylinder input force F_{tmc} can be computed from its output pressure p_{tmc} and its section area A_{tmc}

$$F_{tmc} = p_{tmc} A_{tmc} \tag{5.2}$$

If the brake booster is inoperative, the output force of the brake pedal $F_{bp,o}$ is equal to the input force at the tandem master cylinder, allowing to compute the brake pedal ratio R_{bp} using the measured applied force $F_{pb,i}$

$$R_{bp} = \frac{\Delta F_{bp,o}}{\Delta F_{bp;i}} = \frac{\Delta F_{tmc}}{\Delta F_{bp,i}} \tag{5.3}$$

The incremental form of the equation is necessary because it is required a certain amount of force at the tandem master cylinder before it starts to generate an output pressure: such force is not known, but it can be assumed as constant. Analyzing the increment of output pressure as a function of the increment of pedal force allows to exclude the influence of the initial resistance of the brake pump.

It is worth to note that, as the pedal rotates during its travel, the angle between the pedal and the booster rod slightly varies, introducing a minimum variation of the pedal ratio as a function of the pedal stroke. Computing a mean value for the pedal ratio is usually sufficient for the purpose of this work.

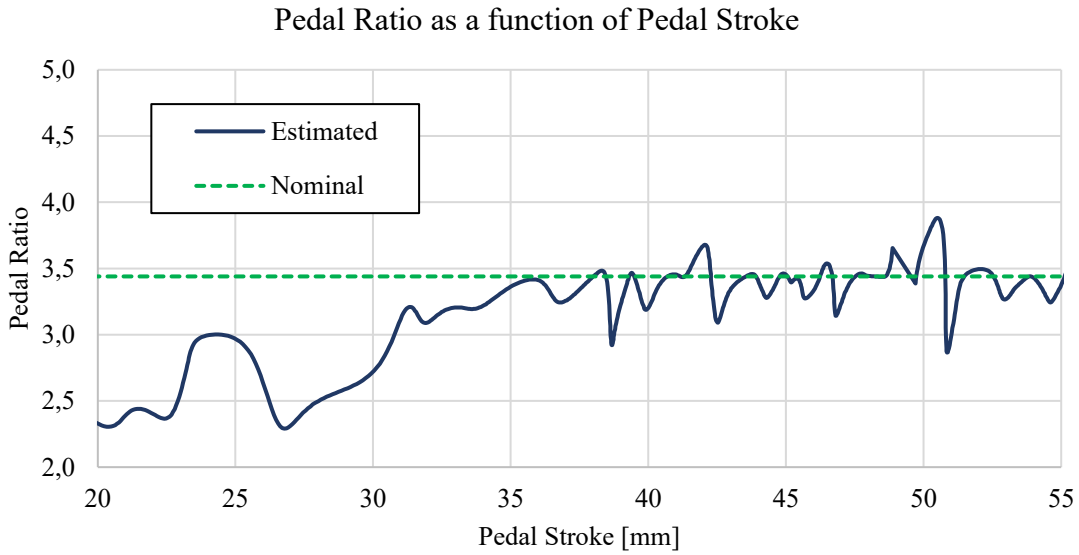

Figure 63. Estimated pedal ratio as a function of pedal stroke, compared to the nominal value of pedal ratio.

In Figure 63 it is shown an experimental test on a vehicle whose nominal pedal ratio was known and it is visible that, once the estimated pedal ratio stabilizes, its value is very close to the nominal one. It is important to remember, however, that the effective pedal ratio depends on the point of application of the force, as it has been explained in the description of the brake pedal in Chapter 2. In other tests, the estimated pedal ratio was systematically different from the nominal one, with little difference among various repetitions of the same test.

Although the pedal ratio is not used to estimate other parameters of the braking system, it is advisable to average the results obtained from different people acting on the brake pedal, to reduce the influence of the contact point between shoe and pedal.

5.3 Brake Booster

The brake booster is a fundamental component in the definition of the pedal feeling, as its non-linear characteristic of output force as a function of input force strongly influences the shape of the function between the vehicle deceleration and the applied pedal force.

It is possible to evaluate its contribution analyzing the difference in the tandem master cylinder pressure as a function of the brake pedal force, when the brake booster is fully operative (maximum vacuum pressure in the front chamber) and when it is not (no vacuum pressure in the front chamber).

Since the brake booster is often supplied with the tandem master cylinder, in a single assembly, it is common to refer to the performance of the brake booster as an output pressure as a function of the input force. If it is necessary to isolate the behavior of the brake booster, it is sufficient to obtain the brake booster output force, which is equal to the input force at the tandem master cylinder, from the output TMC pressure, using equation (5.2).

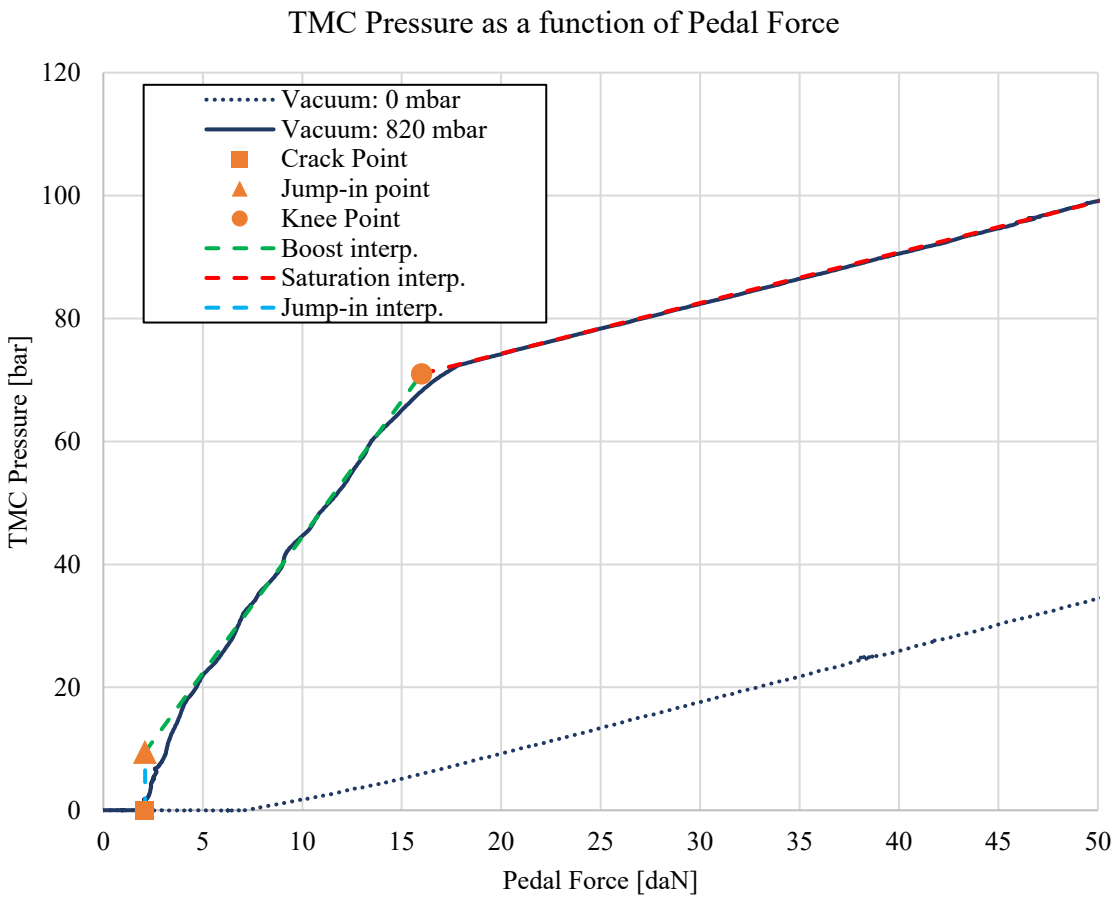

Figure 64. Tandem Master Cylinder pressure as a function of brake pedal force, with and without vacuum pressure in the front chamber of the brake booster.

In a brake booster, the main design parameters are the crack force, the Jump-in pressure, the knee force/pressure and the boost ratio.

During the static test, in which the brake pedal is gradually depressed until an actuation force of 50 daN is reached, it is possible to see in the curve with the brake booster operative two main linear regions: the boost linear region, where the brake booster is contributing proportionally to the input force, and the saturation region, in which the brake booster has reached its maximum contribution. The intersection between these two regions is the knee point, in which the change of slope occurs and, from that point, any further increment of the TMC pressure will be given only by the increment of pedal effort.

The minimum pedal force needed to overcome the internal springs of the brake booster is defined as crack force, and can be extrapolated as the maximum force that does not produce and output TMC pressure.

During the Jump-in phase, in theory, the brake booster increases the TMC output pressure without any increase in the input force, until the Jump-in pressure value is reached, which corresponds to the working point in which the plunger starts to touch the reaction pad in the brake booster. The Jump-in pressure value can be extrapolated by intersecting the interpolation line of the boost linear region with a vertical line starting from the crack point.

Some brake boosters have an internal components design that tends to smooth the transition from the jump-in phase to the boost phase, therefore the jump-in point becomes a virtual point that does not belong to an actual working point of the brake booster. In these cases, it is possible to define a loop-in point, which corresponds to the TMC pressure actually generated by the brake booster at a certain pedal force level, in a working area in which the jump-in phase has been completed: for the brake booster in Figure 64, the loop-in pressure could be measured when the pedal force is 5-6 daN. In any case, the shape of the brake booster function can be approximated by using three contiguous segments.

The boost ratio can be estimated from the linear interpolation of the boost region when the brake booster is operative, and the pressure-force curve when the brake booster is not operative. Being

$$p_{\mathrm{tmc}} = \mathrm{c}_{11} + \mathrm{c}_{12} F_{\mathrm{bp,i}} \tag{5.4}$$

$$p_{\mathrm{tmc}} = \mathrm{c}_{21} + \mathrm{c}_{22} F_{\mathrm{bp,i}} \tag{5.5}$$

the interpolation equations of the boost region and of the no-boost curves respectively, the coefficients c_{12} and c_{22} determine the slope of the two lines, therefore, the boost ratio R_{bb} can be computed as the ratio

$$R_{bb} = \frac{c_{12}}{c_{22}} \tag{5.6}$$

If the parameters of the brake booster are needed as a function of the input force at the booster rod, it is possible to convert the pedal force to the input force using the pedal ratio computed at the equation (5.3). If the pedal ratio has been computed using the same tester that performed the static test for the brake booster analysis (it is possible to use the same no-vacuum test for both), the possible error on the application point of the brake pedal force is eliminated during the conversion.

Similarly, if the analysis must be performed as a function of the output force, instead of the TMC pressure, it is possible to pass use equation (5.2), being the input pressure at the tandem master cylinder equal to the output pressure of the brake booster.

5.4 Wheel Brakes

In this paragraph, the main parameters that determine the performance of a disc brake will be analyzed. The method used to retrieve them can be adapted to the case of a drum brake, although the vehicle used in this demonstration had four disc brakes with floating calipers.

Recalling the description of the disc brake from Chapter 2, the braking moment τ depends on the outer and inner radiuses of the contact area between pads and disc, on the friction coefficient between them, on the brake circuit pressure and on the area of the caliper piston:

$$\tau = 2\mu\left(p\frac{\pi d^2}{4} - F_r\right)\left(\frac{2}{3}\frac{r_{ext}^3 - r_{int}^3}{r_{ext}^2 - r_{int}^2}\right) \tag{5.7}$$

The geometry of the disc and the pads is easily measurable on the disc itself, allowing to obtain the external and internal radiuses of the contact surface between pads and disc. The diameter of the piston is also directly measurable by disassembling the brake caliper, a typical operation needed during the replacement of the brake linings.

The brake circuit pressure at the caliper can be measured using a pressure sensor on the brake line, while the resisting force F_r that opposes to the movement of the caliper to allow the contact between pads and disc can be approximated by reducing the brake pressure of a fixed amount p_{res}, between 1 and 2 bar. Therefore, the net useful pressure p_{net} can be computed as:

$$p_{net} = \begin{cases} 0, & p \le p_{res} \\ p - p_{res}, & p > p_{res} \end{cases} \tag{5.8}$$

Now it is possible to rearrange the equation (5.7) making explicit the friction coefficient and including p_{net} in the formula:

$$\mu = \frac{\tau}{2\left(p_{net}\frac{\pi d^2}{4}\right)\left(\frac{2}{3}\frac{r_{ext}^3 - r_{int}^3}{r_{ext}^2 - r_{int}^2}\right)} \tag{5.9}$$

At this point, to determine the friction coefficient it is necessary to know the braking torque. Because the front and rear brakes are different, the front and rear axles contribute in different proportions to the total braking force of the vehicle, making difficult to estimate the correct braking moment for each axle.

To better understand how it is possible to estimate the braking forces, it is useful to recall from Chapter 2 the weight distribution equations and how a tire exerts its longitudinal forces on the ground.

Combining equations (2.21), (2.22) and (2.23), the vertical force at each axle as a function of the vehicle deceleration can be expressed as:

$$F_{\mathrm{z,f}} = \mathrm{m}\left(\frac{\mathrm{gb} + a\mathrm{h}}{\mathrm{w}}\right) \tag{5.10}$$

$$F_{\mathrm{z,r}} = \mathrm{m}\left(\frac{\mathrm{ga} - a\mathrm{h}}{\mathrm{w}}\right) \tag{5.11}$$

where a and b are the distances between the center of gravity and the front and rear axles respectively, h the center of gravity height from the ground, w is the wheelbase, g the gravity acceleration, m the vehicle mass and a the longitudinal deceleration of the vehicle.

The vertical force is directly related to the longitudinal force exerted by the tires, through the tires longitudinal friction coefficient μ_{x}:

$$F_{\mathrm{x,f}} = F_{\mathrm{z,f}}\,\mu_{\mathrm{x,f}} \tag{5.12}$$

$$F_{\mathrm{x,r}} = F_{\mathrm{z,r}}\,\mu_{\mathrm{x,r}} \tag{5.13}$$

The longitudinal friction coefficient of the tires is not fixed, but depends on both the vertical force and on the wheel slip ratio σ defined as in equation (2.19). Note that the tire model used in this example does not belong to the tested vehicle, as it was equipped with 15-inch rims, while the model is based on a tire of a different manufacturer that fits on a 16-inch rim: at the moment of the test, it was not available a vehicle with the same tires used in the model.

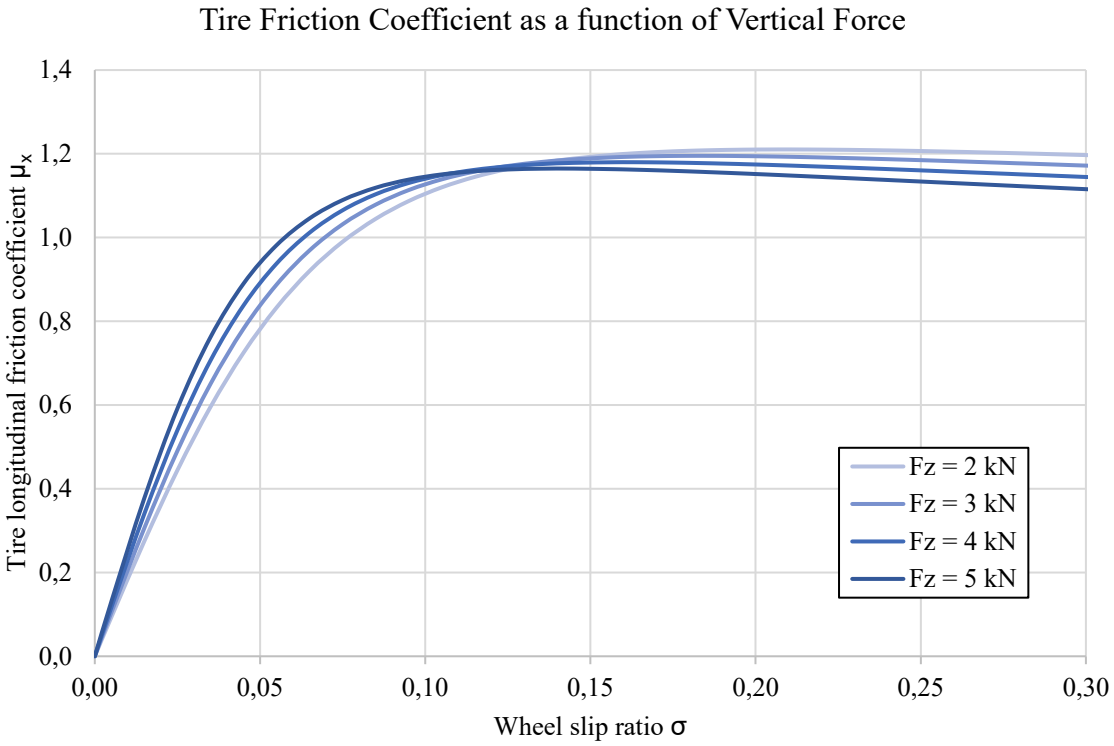

Figure 65. Tire longitudinal friction coefficient as a function of slip ratio and vertical force. The vertical force is referred to a single tire.

A previous study internally developed in the company estimated the braking forces during an emergency braking maneuver with the ABS engaged: as the Anti-lock Braking System modulated the brake pressure to keep the slip ratio in the range that corresponds to the peak tire friction coefficient, once the deceleration and the weight transfer has stabilized, it was possible to average the brake pressure at the front and rear axle, assume front and rear tires peak friction coefficients, and obtain the average force at the front and at the rear wheels to compute the friction coefficient at the brake pads. The drawback of this method is that it relied on the assumption of the tire peak friction coefficient and on the ability of the ABS to maintain during the whole braking maneuver the optimal slip ratio at both front and rear wheels to achieve the maximum braking force. Moreover, the friction coefficient of the brake pads is slightly dependent on the applied pressure, therefore, the estimated friction coefficient could be affected by the relatively high pressure generated during emergency braking maneuvers.

Estimating the slip ratios at the front and rear wheels during a progressive braking maneuver would allow to estimate the friction coefficient of the brake pads in more stable conditions and at lower brake pressures, reducing the wear of the tires in case more repetitions of the test are needed.

To estimate the wheel slip ratios, the first attempt has been to compare the angular wheel velocities provided by the ABS or by additional wheel speed sensors, with the vehicle velocity

obtained from the GPS or from an optical speed sensor. The problem with this method is that the wheel slip ratios during a progressive braking maneuver are smaller of an order of magnitude with respect to an emergency braking maneuver: 1 – 3 % with respect to the 10 – 30 % operative range of the ABS. Measuring such small differences poses a problem of synchronization of the vehicle speed signal with the wheel speed signals, as it can be visible in Figure 66.

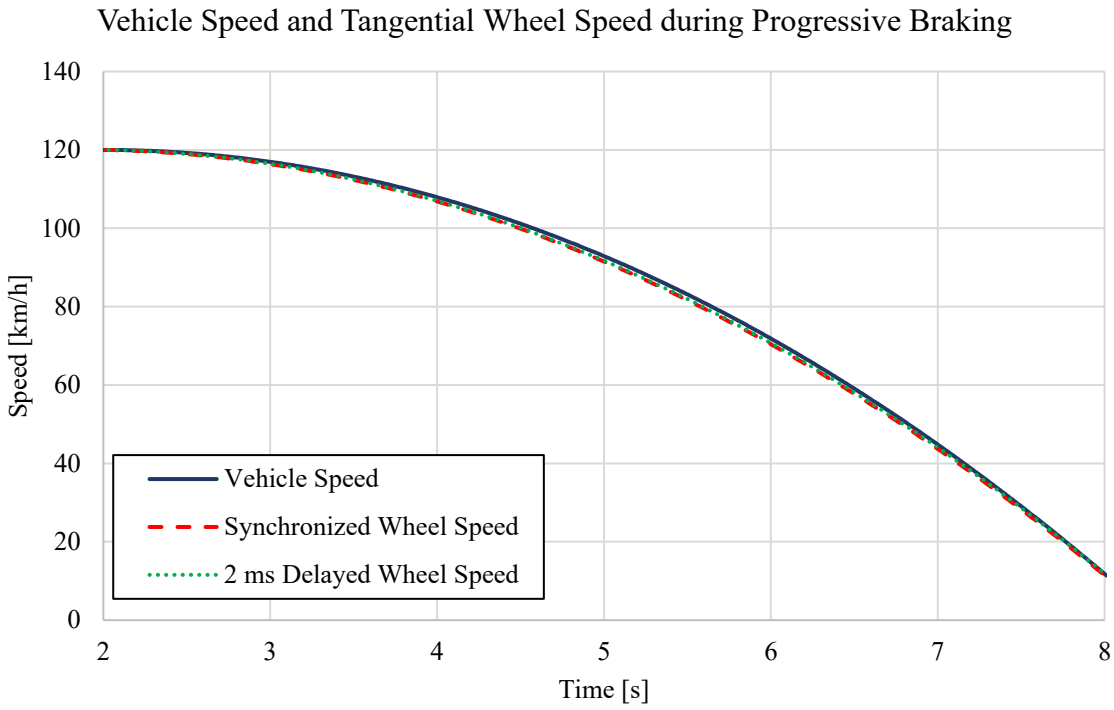

Figure 66. Simulation of the time history of the vehicle speed and of the actual and delayed tangential speeds of one wheel during the progressive braking maneuver.

In this simulation of progressive braking, the deceleration of the vehicle is linearly increased from 0 to 1 g in 6 seconds and the wheel speed of one tire has been considered, assuming a constant longitudinal stiffness, neglecting the load transfer of the vehicle. Ideally, the wheel speed is measured and recorded by the data acquisition system in the same moment of the vehicle speed provided by the GPS: in reality, the two signals are asynchronous and the time needed for the measurement, processing and storage of the data is different, as it depends on the sensor used, on the communication protocol between the sensor and the data acquisition system, on the DAQ itself and on the sampling rate used. These delays are generally very small and the manufacturer of each sensor provides some information about its delay or a form of compensation, in order to perform satisfactorily in most applications. During the tests performed in this work, it became evident that some delay between the wheels speed measurement and the wheel speed occurred, as the calculated wheel slip ratios had no physical meaning. To understand how such delay influences the slip ratio measurement, a detail of

Figure 67 is proposed in Figure 68, showing both the actual wheel speed and the delayed wheel speed signal, compared to the vehicle speed.

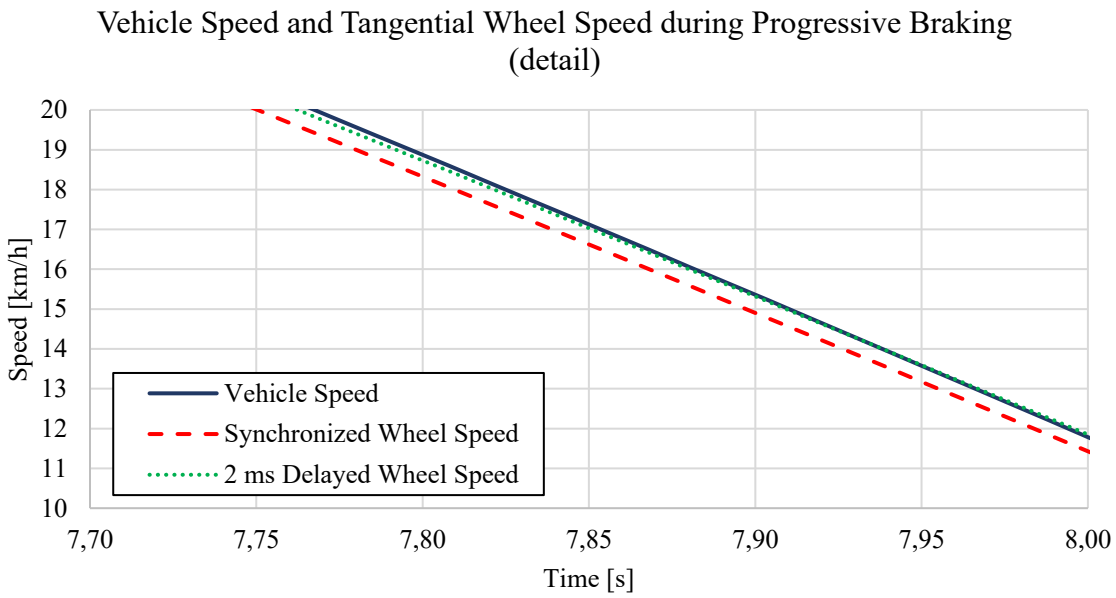

Figure 67. Detailed view of the vehicle speed, the actual wheel speed and the delayed wheel speed signal as a function of time, during a progressive braking maneuver.

As the vehicle speed is decreased and the deceleration increases, at a certain point, which depends on the amount of delay and on the sample rate of the DAQ system, the delay in the wheel speed signal makes it to report a higher speed that may become even higher than the measured wheel speed. As a consequence, the wheel slip ratio is not anymore somehow proportional to the vehicle deceleration (and to the braking forces), but goes back to zero or even becomes negative.

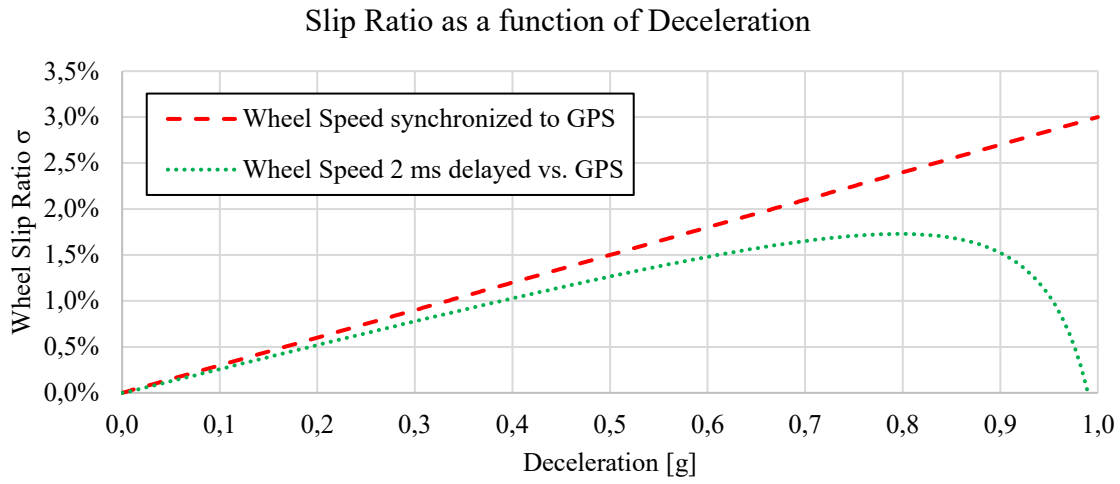

Figure 68. Wheel Slip ratio as a function of vehicle deceleration, estimated from the actual wheel speed and the delayed wheel speed signal.

Although the simulation in Figure 68 made evident the error of the wheel slip ratio, during the experimental activity it was very difficult to identify all the sources of delay, although it always resulted the wheel speed to be in delay with respect to the GPS speed.

Using the wheel speed provided by the ABS, the information is read from the packets flowing in the High-Speed CAN bus of the vehicle, allowing an approximate 100 Hz reading of each wheel speed. Apart from the internal delay of the ABS in measuring and computing the wheel speed, the CAN protocol is asynchronous and several ECUs might attempt to transmit their data packets at the same time: to avoid data collisions, an arbitration method is used to let the transmission of the highest priority packet, while the other ECUs will attempt a new transmission as soon as possible, following the priority order of each packet. For this reason, the delay of each wheel speed packet from the measurement of the wheel speed to the data transmission is not fixed, because it depends on priority of other messages flowing in the same medium, making the ABS an unreliable source of wheel speed information for this specific application.

If an external wheel speed sensor is used, this is directly connected to the DAQ system. However, the wheel speed sensor working principle is to provide a certain number of electrical pulses per wheel rotation (30, in this case), and the DAQ is able to compute the average wheel speed between two pulses only after the second pulse has been sampled, recording this information until a further pulse is generated by the wheel speed sensor.

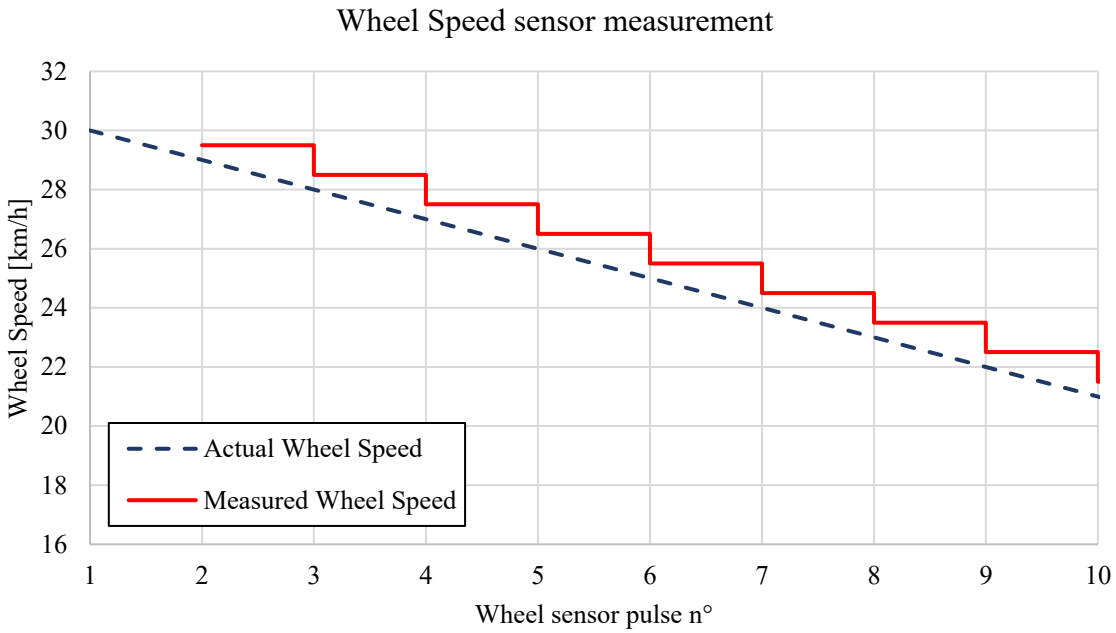

Figure 69. Comparison between the actual wheel speed, and the wheel speed signal provided by the periodic pulses of a wheel speed sensor.

The delay in the wheel speed measurement depends on the wheel speed, as it corresponds to the time interval between two pulses of the wheel speed sensor: as the speed decreases, therefore, the delay increases.

Moreover, an additional, speed-independent and undocumented delay of 8 ms has been found on the DAQ system between the wheel speeds measurement and the GPS velocity: as several different models of DAQ systems are used in the company, it was impractical to take into account of the delays of each possible combination of sensors and DAQ system, therefore it has been discarded the idea of directly comparing the wheels speeds against the vehicle speed.

A different approach, that resulted to be effective, required the use of the tire model and only the wheel speeds of the front and rear axles from the ABS system. As the wheel speeds come from the same source, the delay is less critical, and the variability of the delay due to the CAN arbitration can be considered as randomly varying sample by sample, without systematic influences on the wheels speed signals.

The longitudinal force that slows down a vehicle F_{x} is generated by two main components: the total braking force $F_{\mathrm{brk,tot}}$ coming from the two axles and the resisting force F_{res} generated by the aerodynamic forces, the tires rolling resistance, the internal frictions in the transmission, etc.:

$$F_{\mathrm{x}} = F_{\mathrm{brk,tot}} + F_{\mathrm{res}} \tag{5.14}$$

The total force can be obtained knowing the vehicle mass and the vehicle longitudinal acceleration a_x by means of an accelerometer:

$$F_{\mathrm{x}} = m a_{\mathrm{x}} \tag{5.15}$$

while the resisting force can be estimated from the vehicle speed V and the coast-down coefficients F_0 and F_2 of the vehicle:

$$F_{\mathrm{res}} = F_0 + F_2 V^2 \tag{5.16}$$

To estimate the braking forces at the front and rear axles, $F_{\mathrm{x,f}}$ and $F_{\mathrm{x,r}}$ respectively, it is necessary to know the vehicle speed and the vertical load on each axle, in order to obtain the friction coefficient at the tire – ground contact. The axles vertical load is known from Equations (5.10) and (5.11), while the vehicle speed can be estimated using the tire model, the wheels velocities and the total braking force obtained from equations (5.14), (5.15) and (5.16).

Considering a certain time instant in the braking maneuver, if a certain vehicle speed V_{est}, is assumed, and it is chosen so that it is higher than both front and rear wheels speeds, it is possible to obtain the wheels slip ratios of front and rear axles by using V_{est} as a reference vehicle speed:

$$\sigma_{\mathrm{f,est}} = 1 - \frac{v_{\mathrm{f,avg}}}{V_{\mathrm{est}}} \tag{5.17}$$

$$\sigma_{\mathrm{r,est}} = 1 - \frac{v_{\mathrm{r,avg}}}{V_{\mathrm{est}}} \tag{5.18}$$

where $v_{\mathrm{f,avg}}$ and $v_{\mathrm{r,avg}}$ are, respectively, the front and rear average tangential wheel speeds.

Knowing the vertical force at the front and rear axles, it is possible to use the tire model to compute the front and rear friction coefficients and, eventually, the front and rear braking forces $F_{\mathrm{brk,f}}$ and $F_{\mathrm{brk,r}}$:

$$F_{\mathrm{brk,f}} = F_{\mathrm{z,f}}\, \mu_{\mathrm{x,f}} \left(\frac{F_{\mathrm{z,f}}}{2}, \sigma_{\mathrm{f,est}} \right) \tag{5.19}$$

$$F_{\mathrm{brk,r}} = F_{\mathrm{z,r}}\, \mu_{\mathrm{x,r}} \left(\frac{F_{\mathrm{z,r}}}{2}, \sigma_{\mathrm{r,est}} \right) \tag{5.20}$$

The vertical force used in the tire model must be halved, as it must be referred to one tire and not to the whole axle. If the assumed vehicle speed V_{est} is correct, the sum of the braking forces at the front and rear axles should be equal to the total braking force obtained from equation (5.14). If it is not, it is possible to iterate the process varying V_{est} until the error on the total braking force is minimized.

Once the process has been repeated for the whole braking maneuver, it will be available a time history of the vehicle speed V, which is not anymore an assumption, but it has been derived from the tire model, the wheels speed and the vertical load on front and rear axles.

In the following figures, a progressive braking maneuver and the results obtained are shown.

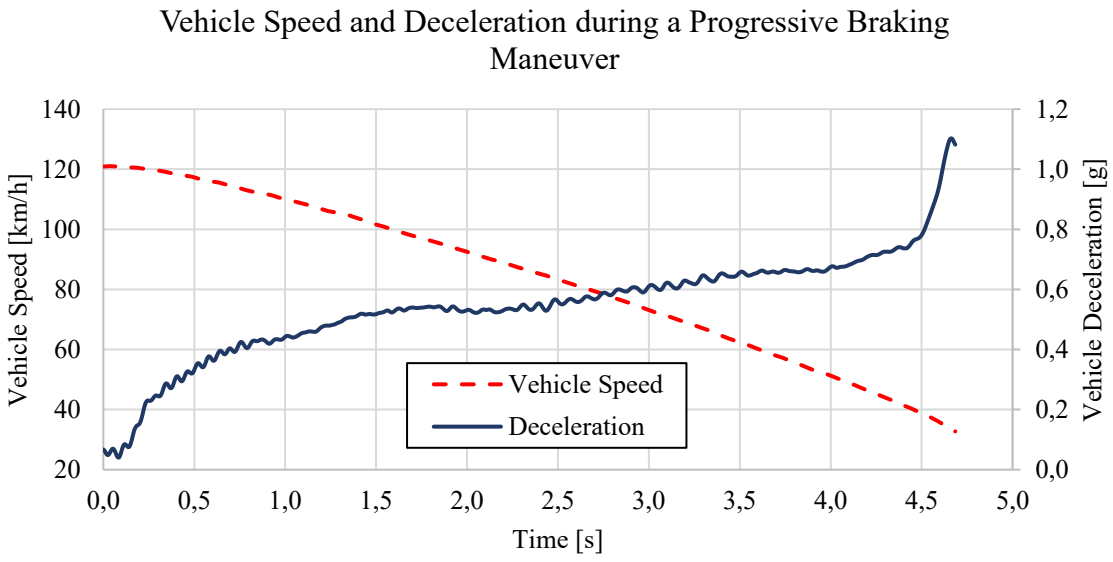

Figure 70. Time evolution of the vehicle speed and its deceleration during a progressive braking maneuver.

As it is visible in Figure 70, among all the repetitions performed with this vehicle, there was not a linear increase of the vehicle deceleration as a function of time; also, the duration of the maneuver has been shorter than the 5-6 seconds recommended. Although this is not an ideal condition, the intermediate range of decelerations, which will be used for the estimation of the brake pads friction coefficient, is sufficiently linear.

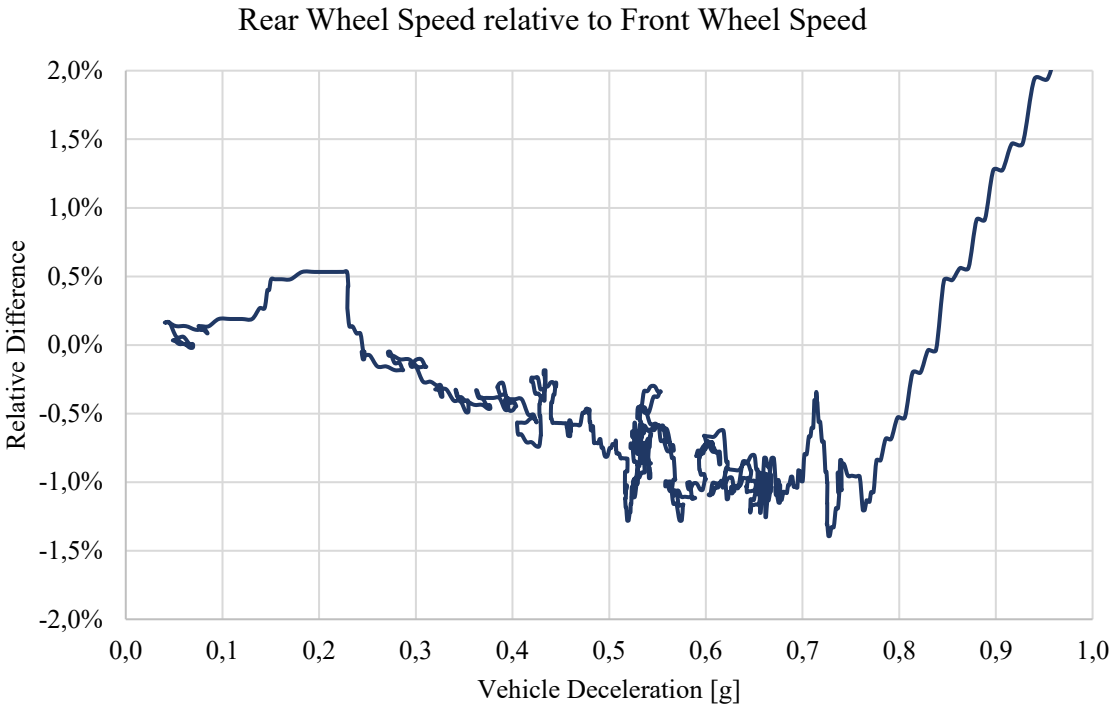

Figure 71. Relative difference between rear and front wheel velocities as a function of vehicle deceleration.

In Figure 71 it is shown the relative wheel speed difference between front and rear axles, obtained from the wheel velocities given by the ABS. The resolution of the measurement is enough to obtain a variable result as a function of the vehicle deceleration, showing the influence of the weight transfer on the front and rear tires exploitation.

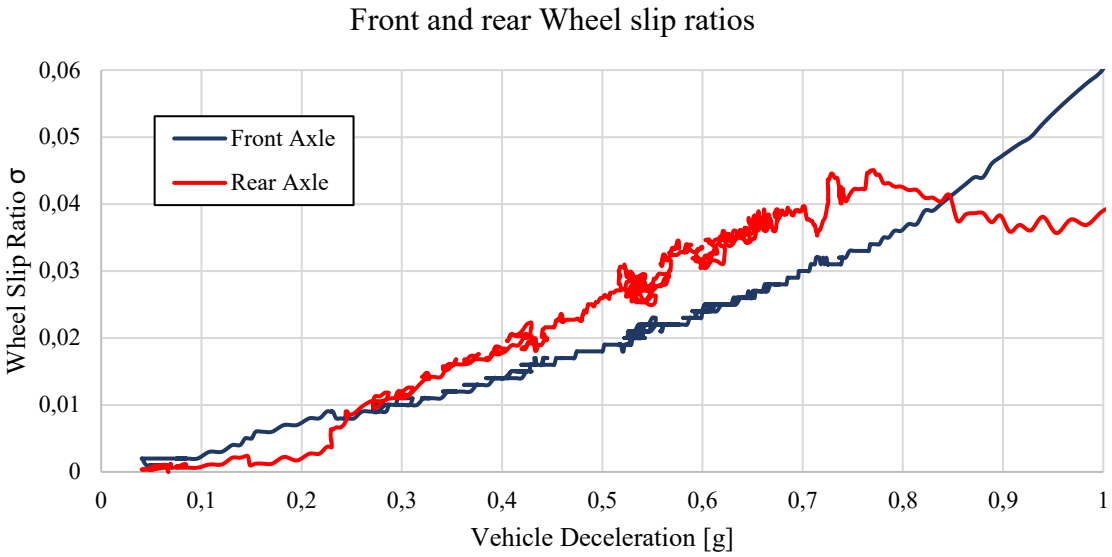

Figure 72. Front and rear wheel slip ratios (average between left and right wheels) estimated from the tire model and the wheels speed from the ABS.

In Figure 72 it is visible that the rear tires have a higher slip ratio with respect to the front ones at low decelerations, while at the higher decelerations the phenomenon is reversed, as the EBD intervenes to limit the rear pressure. Note that, although normally the EBD intervenes activating the isolation valves at the rear wheels to maintain the rear pressure constant from a certain value of deceleration, in this case, there have been EBD interventions since the lowest values of deceleration, repeatedly reducing and restoring the rear pressure until a constant value has been maintained at the highest levels of deceleration. This visible from the front and rear pressure evolution vs. vehicle deceleration and vs. time in Figures Figure 73 and Figure 74 respectively.

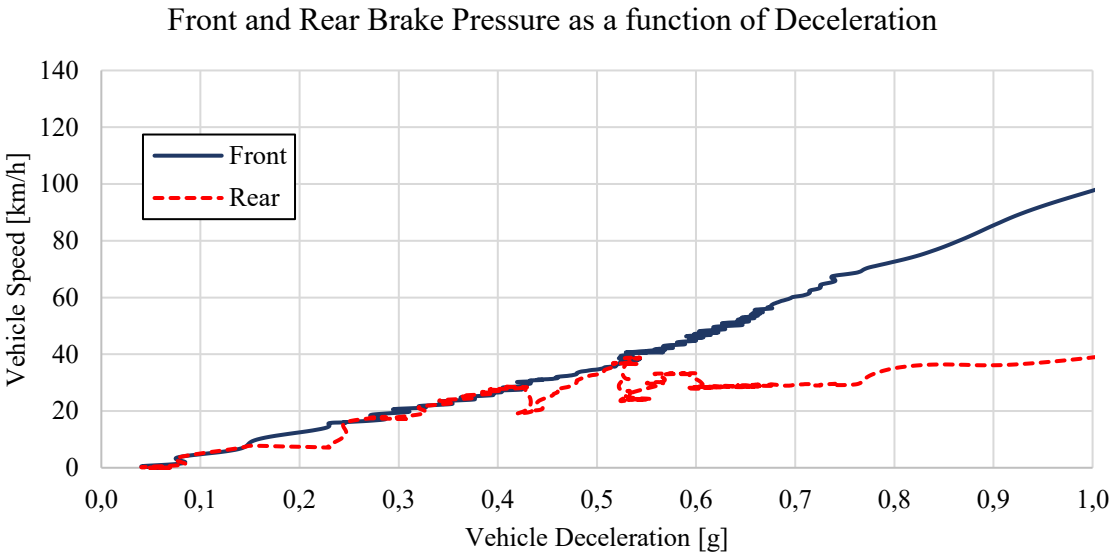

Figure 73. Front and rear brake pressure as a function of vehicle deceleration, during a progressive braking maneuver.

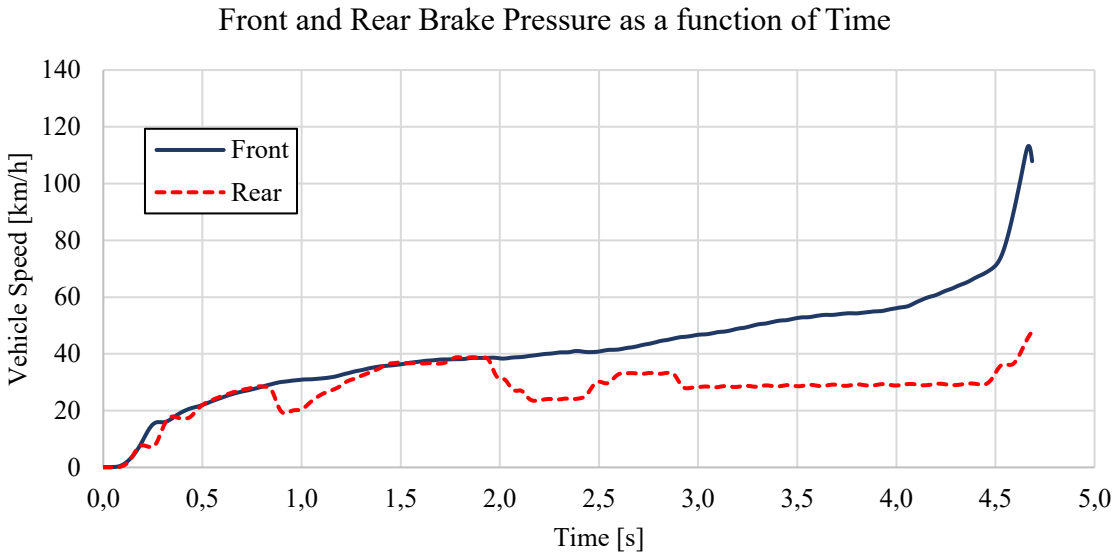

Figure 74. Front and rear brake pressure as a function of time, during a progressive braking maneuver.

These pressure oscillations across the whole deceleration range might affect the estimation of the rear pads friction coefficient. This effect has also occurred in other braking maneuvers with the same vehicle, therefore, it should be considered as a characteristic of the EBD strategy.

Knowing the vehicle deceleration and the position of the vehicle center of gravity, it is now possible to compute the weight transfer and, therefore, the vertical load acting on the front and rear axles.

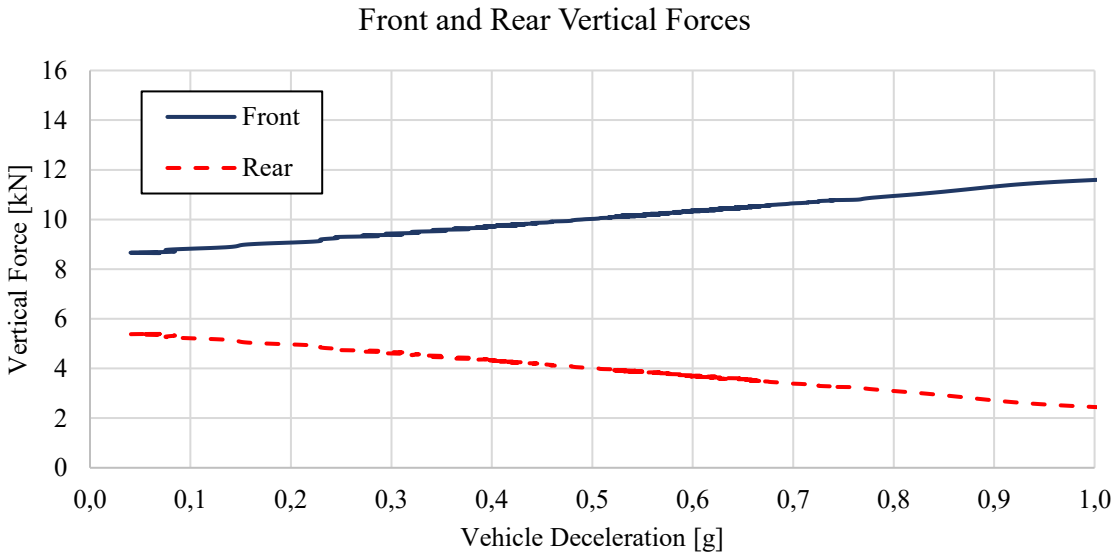

Figure 75. Front and rear axles vertical force as a function of vehicle deceleration.

At this point, the estimated wheel slip ratios and the front and rear vertical forces are the input parameters for the tire model, to estimate the tires friction coefficients and, finally, the longitudinal forces for the front and rear axles.

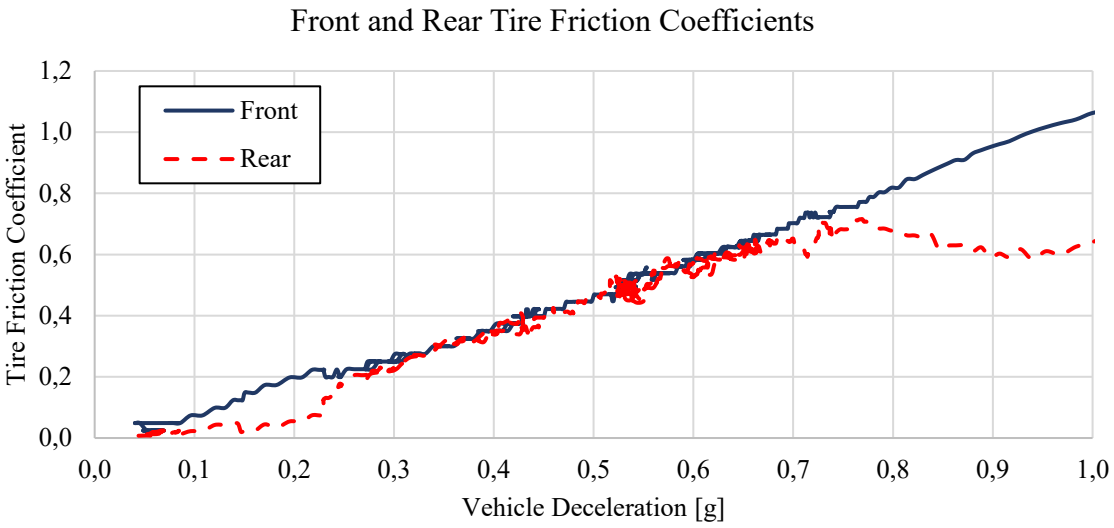

Figure 76. Front and rear tires friction coefficient as a function of vehicle deceleration.

It is possible to note in Figure 76 that, although the slip ratios at the front and rear axles are different, the tires are exploited in a similar manner in the intermediate range of vehicle deceleration. At the extremes, the exploitation is different, but it must be remembered that in the initial and final parts of the maneuver the vehicle deceleration rate of change has been much higher, therefore, the vertical load estimation might have been impaired by the moment of inertia of the vehicle body, which was still rotating to find an equilibrium position due to the sudden acceleration change.

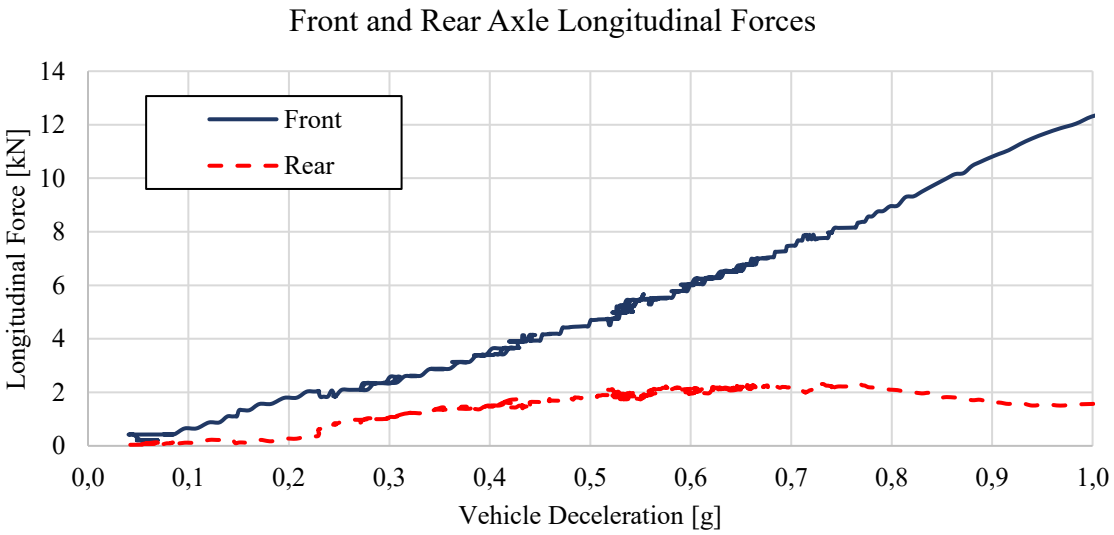

Figure 77. Front and rear axles longitudinal forces as a function of vehicle deceleration.

From the axle longitudinal forces shown in Figure 77 and the wheel radius R_{whl} it is possible to compute the front and rear braking moments τ_f and τ_r for the single wheels:

$$\tau_f = \frac{1}{2} F_{x,f} R_{whl} \tag{5.21}$$

$$\tau_r = \frac{1}{2} F_{x,r} R_{whl} \tag{5.22}$$

Finally, from the brake pressures, the disc geometry, the caliper piston area and the braking torques, it is possible to estimate the friction coefficients of the front and rear brake pads.

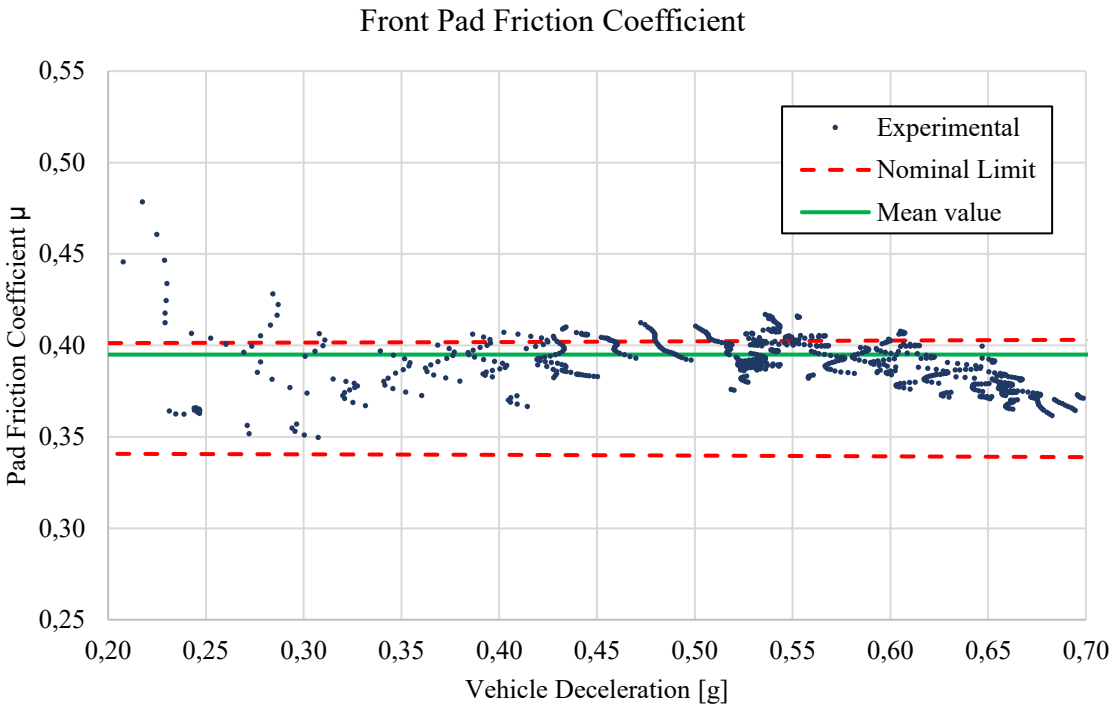

Figure 78. Front brake pads estimated friction coefficient as a function of vehicle deceleration.

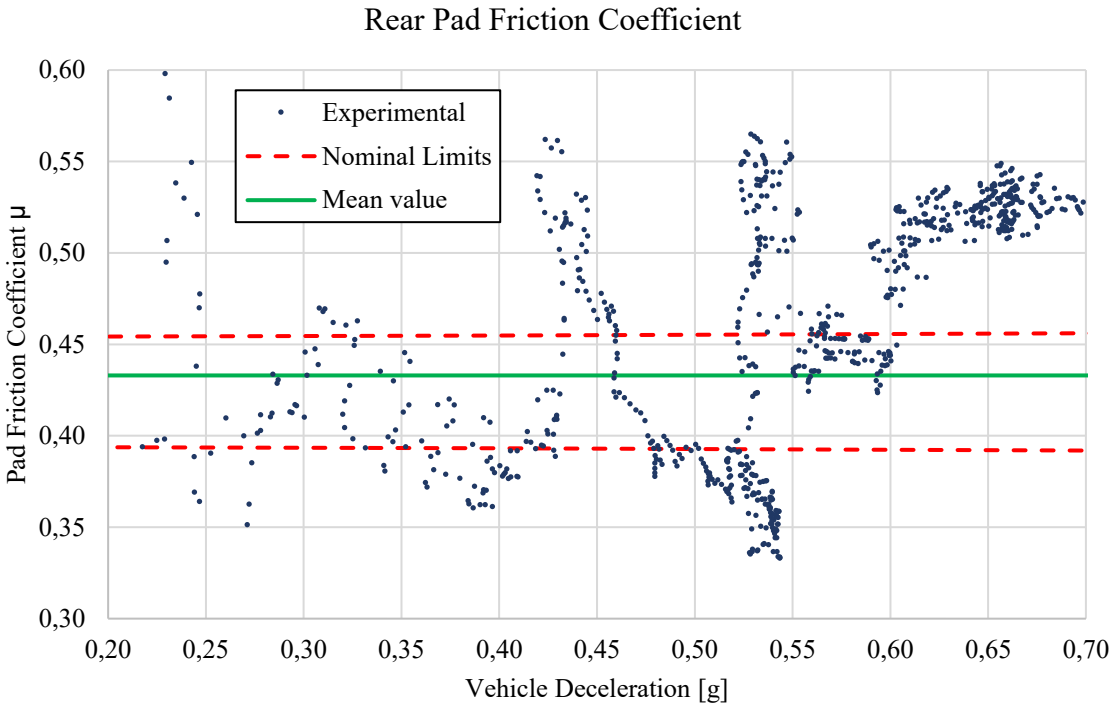

Figure 79 Rear brake pads estimated friction coefficient as a function of vehicle deceleration.

Both front and rear average values shown in Figures Figure 78 and Figure 79 have been computed between 0,3 and 0,6 g of vehicle deceleration, as this is the most linear range in this braking maneuver, where the vertical load estimation at the front and rear axles is more accurate.

The rear friction coefficient is more oscillating with respect to the front one, probably because of the pressure fluctuations given by the EBD intervention. However, both front and rear friction coefficient estimation resulted to be within the tolerance limits given by the brake pad manufacturer.

Averaging the results of the three repetitions of the progressive braking maneuver at 100 °C allowed to obtain a front pad friction coefficient of 0,383 and a rear pad friction coefficient of 0,404, both still within the tolerance limits.

As this estimation strongly depends on the tire model used, it is possible that more accurate results will be achieved using a tire model that matches the tires actually used by the tested vehicle. Although it is generally difficult to obtain from a tire manufacturer a model of their tires, in literature there are methods to obtain the Pacejka coefficient for a longitudinal tire model from ad-hoc braking maneuvers, but such task goes beyond the objectives of this work.

5.5 Model Validation

From the parameters obtained in the previous paragraphs, it is possible to create a simplified model of braking system to simulate a progressive braking maneuver and compare the results obtained with the experimental measurements of the same vehicle.

Recalling the main parameters used, the brake pedal ratio is considered fixed, the brake booster output is defined using four contiguous segments (phase of no output force before the crack point, jump-in phase, boost phase and saturation phase), the TMC is a force-pressure transducer with identical pressure at both circuits, the EBD is simplified as a fixed rear pressure limiter and the front and rear brakes are based on their geometry and on a fixed friction coefficient.

As the model is mainly oriented in the pedal feeling evaluation, the progressive braking maneuver is the most representative for this task, therefore, a comparison between an experimental maneuver and the simulated one will be performed, evaluating the vehicle speed, the rear pressure time evolution and the vehicle deceleration as a function of the pedal force.

As all the experimental maneuvers performed on this vehicle had an irregular application of the brake pedal, with a sudden increase of the vehicle deceleration at the beginning and at the end of the braking maneuver, the same brake pedal force input has been used on the simulation model.

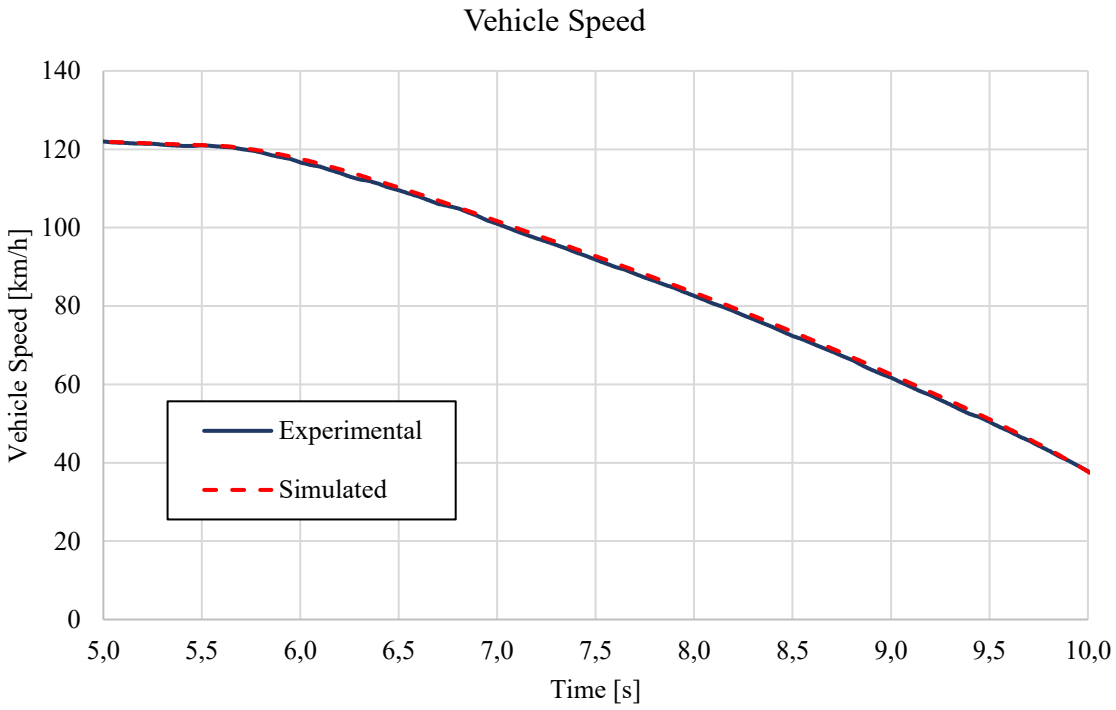

Figure 80. Vehicle speed as a function of time during an experimental progressive braking maneuver and a simulated one.

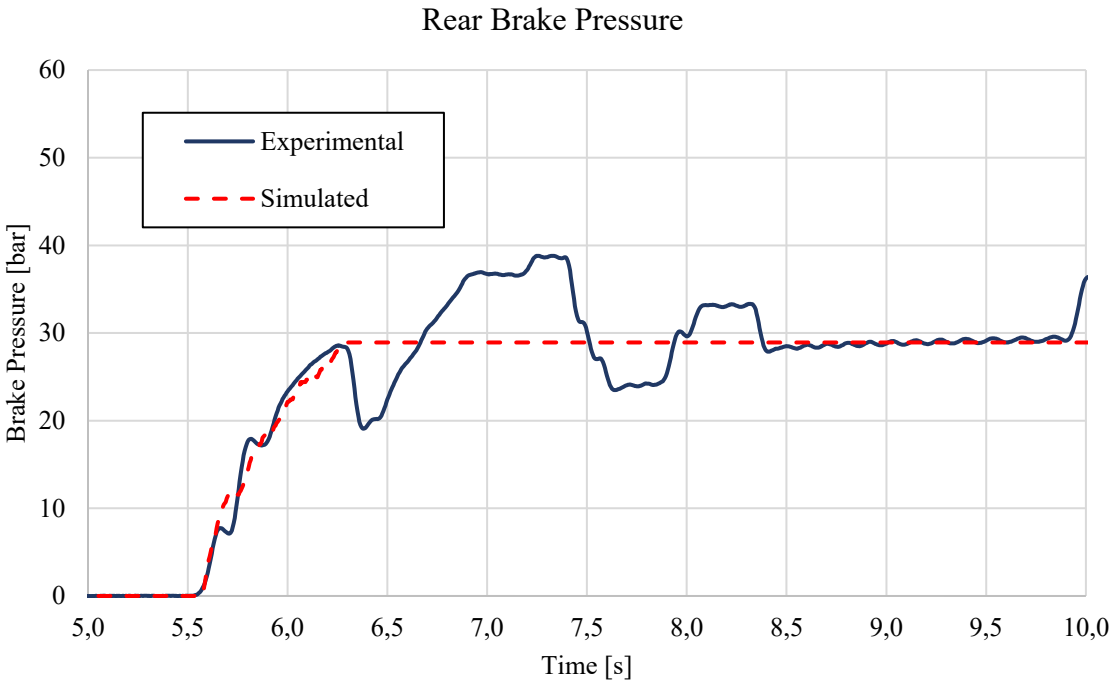

Figure 81. Rear brake pressure as a function of time during an experimental progressive braking maneuver and a simulated one.

In the simulation model, a maximum pressure of 29 bar has been set to replicate the EBD intervention, without simulating all the pressure cycles, as it is shown in Figure 81.

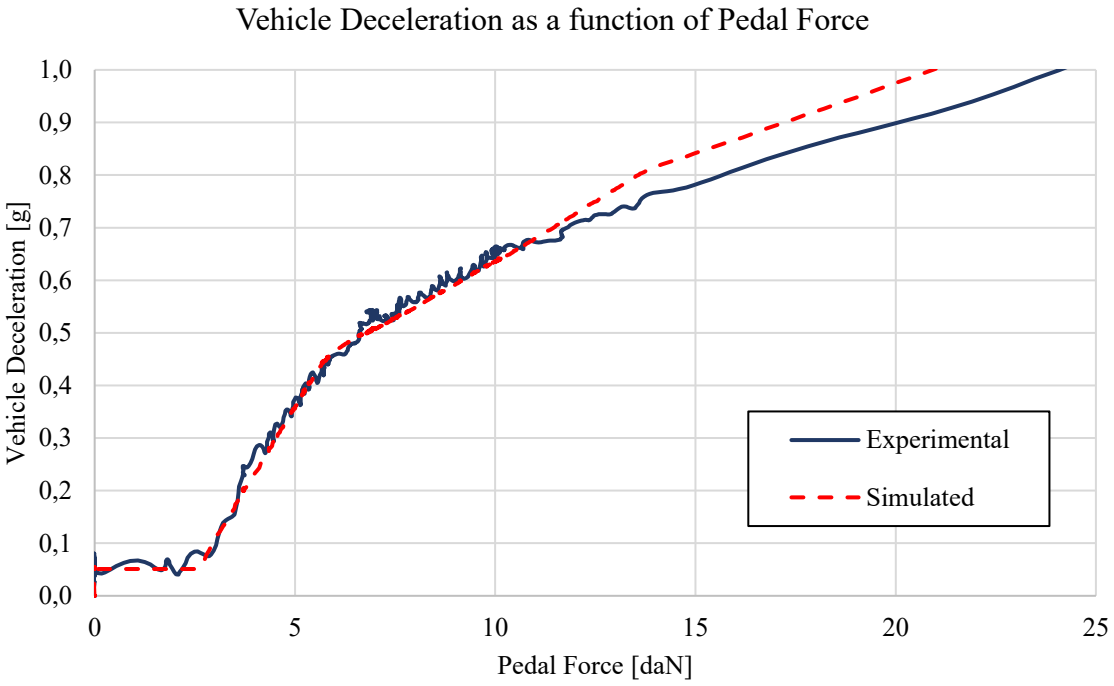

Figure 82. Vehicle deceleration as a function of brake pedal force for an experimental progressive braking maneuver and a simulated one.

It is visible in Figure 82 that the model correctly estimates the vehicle deceleration as a function of the applied pedal force, with a slight deviation from the experimental results at high deceleration levels. Considering that above 0,7 g the vehicle deceleration has suddenly increased in the experimental test, it is possible that such deviation is due to the many dynamic phenomena that occur both in the vehicle body and in the braking system, which have been neglected assuming a slow and constant rate of increase of the vehicle deceleration. As it was unavailable an experimental test with a more linear vehicle deceleration increase, it was not possible to verify the model in more ideal conditions.

Conclusions

The objectives of this thesis were to analyze which components influence the brake pedal feeling and to identify which are the objective parameters related to the pedal feeling that are measurable with the experimental testing of a vehicle. Moreover, it was needed to determine a range of "best feeling" for the identified parameters and to define a model for identifying the main design parameters of a braking system from an experimental test.

In Chapter 2, during the description of each component of the braking system, it has been explained their influence on the brake pedal feeling: the brake pedal, the tandem master cylinder and the drum/disc brakes can be approximated as linear systems which transform the brake pedal force into a braking force with an almost constant gain. The main non-linear component is the brake booster, which gives a fundamental contribution in the tuning of the brake pedal feel, as it allows to modify the applied force without influencing the pedal stroke. Even the friction coefficient of the brake linings contributes to the pedal feeling, but a modification of the material implies a trade-off with its thermal resistance, durability, dust generation and acoustic comfort.

The progressive braking maneuvers allow to correlate with an affordable experimental effort the vehicle deceleration as a function of the brake pedal force and stroke, provided that the maneuver is performed with a smooth variation of the vehicle deceleration in the whole maneuver. The correlation between the experimental tests and the subjective evaluation has shown that the pedal force needed to obtain vehicle decelerations in the range between 0,2 and 0,4 g is the key parameter of influence of the brake pedal feeling and the desired trend is to reduce the effort on the brake pedal, although it is not clear if there is a lower force limit. Increasing the number of tested vehicles could be helpful in better investigating the correlation between subjective feeling and objective measurements. Moreover, it can be stated that the variability of braking performance due to the manufacturing tolerances of the braking system has an influence on the customer evaluation of the pedal feeling, as well as the experience of the driver with previous vehicles: unless the pedal feeling of all the vehicles is harmonized, there will always be a physiological percentage of users unsatisfied of the pedal feeling of their vehicle because it is different with respect to what they were used to.

Since most of the brake application from a customer point of view are performed at low deceleration values, the adoption of a progressive braking maneuver at reduced vehicle speed, such as 50 km/h, aimed to sweep the vehicle deceleration up to 0,4 – 0,5 g, can improve the accuracy of the measurement of the brake pedal feel, reducing the influence of the aerodynamic resistance of the vehicle and, probably, making more evident the blending between conventional braking and regenerative braking for hybrid and electric vehicles.

The model used to determine main design parameters of the braking system from a progressive braking maneuver has shown positive results, although it would be useful to validate the model on more vehicles and to analyze the influence of the tire model on the estimation of the brake pads friction coefficients. If a sufficient number of repetitions is performed and the progressive braking maneuver has a uniform deceleration increase, it might be possible to refine the model to estimate the friction coefficient as a function of the brake pressure, the vehicle speed and the brakes temperature.

If the tire model were unavailable, it is still possible to estimate the front and rear pads friction coefficients at the cost of an increased experimental effort, by performing the progressive braking maneuvers twice, using the only the brakes of one axle at a time.

References

[1] Genta G., Morello L., *The Automotive Chassis*, 2 v., Springer, 2009

[2] Day A., *Braking of Road Vehicles*, United States, Butterworth-Heinemann, 2014

[3] UNECE Regulation No. 13-H – Rev.3 – Braking of passenger cars

[4] Morello L., Rosti Rossini L., Pia G., Tonoli A., *The Automotive Body*, vol. II, Springer, 2011

[5] Pacejka H., *Tyre and Vehicle Dynamics*, 3rd ed., Butterworth-Heinemann, 2012